INFORMATION TO USERS

This dissertation was produced from a microfilm copy of the original document. While the most advanced technological means to photograph and reproduce this document have been used, the quality is heavily dependent upon the quality of the original submitted.

The following explanation of techniques is provided to help you understand markings or patterns which may appear on this reproduction.

1. The sign or "target" for pages apparently lacking from the document photographed is "Missing Page(s)". If it was possible to obtain the missing page(s) or section, they are spliced into the film along with adjacent pages. This may have necessitated cutting thru an image and duplicating adjacent pages to insure you complete continuity.

2. When an image on the film is obliterated with a large round black mark, it is an indication that the photographer suspected that the copy may have moved during exposure and thus cause a blurred image. You will find a good image of the page in the adjacent frame.

3. When a map, drawing or chart, etc., was part of the material being photographed the photographer followed a definite method in "sectioning" the material. It is customary to begin photoing at the upper left hand corner of a large sheet and to continue photoing from left to right in equal sections with a small overlap. If necessary, sectioning is continued again — beginning below the first row and continuing on until complete.

4. The majority of users indicate that the textual content is of greatest value, however, a somewhat higher quality reproduction could be made from "photographs" if essential to the understanding of the dissertation. Silver prints of "photographs" may be ordered at additional charge by writing the Order Department, giving the catalog number, title, author and specific pages you wish reproduced.

University Microfilms

300 North Zeeb Road
Ann Arbor, Michigan 48106

A Xerox Education Company

72-31,328

KILINC, Mustafa Yilmaz, 1942-
MECHANICS OF SOIL EROSION FROM OVERLAND FLOW GENERATED BY SIMULATED RAINFALL.

Colorado State University, Ph.D., 1972
Engineering, civil

University Microfilms, A XEROX Company, Ann Arbor, Michigan

DISSERTATION

MECHANICS OF SOIL EROSION FROM OVERLAND FLOW GENERATED BY SIMULATED RAINFALL

Submitted by

MUSTAFA YILMAZ KILINC

In partial fulfillment of the requirements

for the Degree of Doctor of Philosophy

Colorado State University

Fort Collins, Colorado

May 1972

COLORADO STATE UNIVERSITY

MAY 19 72

WE HEREBY RECOMMEND THAT THE THESIS PREPARED UNDER OUR SUPERVISION

BY MUSTAFA YILMAZ KILINC

ENTITLED MECHANICS OF SOIL EROSION

BE ACCEPTED AS FULFILLING IN PART REQUIREMENTS FOR THE DEGREE OF

DOCTOR OF PHILOSOPHY

Committee on Graduate Work

S. O. Schumm

William D. Striffler

A. C. Miller

Edmund F. Schulz

E. V. Richardson

Adviser

J. W. Leod

Head of Department

PLEASE NOTE:

Some pages may have

indistinct print.

Filmed as received.

University Microfilms, A Xerox Education Company

ABSTRACT OF DISSERTATION

MECHANICS OF SOIL EROSION FROM OVERLAND FLOW GENERATED BY SIMULATED RAINFALL

The mechanics of soil erosion from overland flow generated by simulated rainfall are studied experimentally and analytically. The experiments were conducted in a 4 foot-deep, 5 foot-wide and 16 foot-long flume at the Colorado State University Engineering Research Center. Twenty-four runs were made with bare (without vegetation) sandy soil, using six different slopes (5.7 to 40 percent) and four different rainfall intensities (1.25 to 4.60 inches per hour). Four additional runs were made with 40 percent of soil surface covered by winter wheat. In each run, the sediment yield, mean velocity of flow, water discharge and temperature were measured, and the eroded material was analyzed for grain size distribution.

Flow under rainfall conditions cannot be strictly called laminar, but neither is it turbulent. The Reynolds number $(q_o X/\nu)$ range (0 to 130) was small in these experiments. The flow was influenced by viscosity, and perturbations are damped. Flow subjected to a continuous series of perturbations, however, such as under raindrop impact in this study, appears turbulent and may be called agitated laminar flow. Froude numbers ranged from 0 to 5.4; that is, flow was of the supercritical type.

Momentum and continuity equations for steady, spatially varied overland flow under rainfall were derived, and boundary shear stress, τ_o, was calculated from the momentum equation with a numerical approximation. The stream power was then related to sediment yield as

a transport model. A longitudinal mean local velocity equation for steady spatially varied overland flow in terms of friction slope, rainfall excess, length of run, viscosity, and gravitational acceleration was also derived and tested. Predicted velocities with this equation were comparable to the velocities measured in the experimental runs. Dimensional analysis was performed on all variables, and the data were analyzed by computer, using a nonlinear multiple regression method. Prediction equations were developed from these methods of analysis and models were tested. It was concluded that sediment transport models from dimensional analysis, data analysis and analytical approaches are similar. Velocity, slope and rainfall intensities were found to be the most important variables affecting soil erosion. In sediment transport prediction equations, the slope and Reynolds number (defined as rainfall excess times length of run divided by kinematic viscosity) are dominant parameters.

As expected, soil loss in the experimental flumes was found to decrease in the presence of vegetal cover. However, the decrease in soil loss diminished with increasing rainfall intensities.

Sediment yield from overland flow for laboratory conditions can be predicted by the equations developed in this study. For field conditions, the equations can be used as first approximations of soil loss due to overland flow. The numerical constant of the prediction equations would need to be modified for different soil conditions.

MUSTAFA YILMAZ KILINC
DEPARTMENT OF CIVIL ENGINEERING
COLORADO STATE UNIVERSITY
FORT COLLINS, COLORADO
MAY 1972

ACKNOWLEDGEMENTS

The author wishes to express his appreciation to his major professor Dr. Everett V. Richardson for his assistance and encouragement throughout the course of his graduate program and research. The author also expresses his appreciation for the counsel, comments and review of his dissertation committee members, Prof. E. F. Schulz, Dr. S. A. Schumm, Dr. W. D. Striffler and Dr. A. C. Miller.

This study was made possible by the assistance of Dr. E. V. Richardson, without whose support, aid and encouragement this dissertation would not have been possible, as well as for his helpful suggestions and the many hours he spent reviewing the manuscript.

Special thanks is also due to Dr. A. C. Miller for the time he spent reviewing, correcting and discussing the manuscript. Thanks is also expressed to Dr. D. A. Woolhiser for his comments and suggestions. Thanks are extended to all others who helped me to make this study possible, and special thanks is expressed to my friends Dr. F. H. Chaudhry and Dr. K. Mahmood for their many general discussions, guidance and suggestions relating to this study.

The financial support for this study and the author's graduate program was provided through Dr. E. V. Richardson and the Government of Turkey.

The author would like to thank his wife Zeliha for her assistance in the typing of this manuscript and for her great moral support and patience throughout the course of his academic program at C.S.U.

Finally, thanks is due to Mrs. J. Pence and Mrs. J. Cobb for the final typing of the manuscript, and to Miss S. D. Brown for the preparation of the drawings.

TABLE OF CONTENTS

Chapter		Page
	LIST OF TABLES	xii
	LIST OF FIGURES	xiv
	LIST OF SYMBOLS	xviii
I	INTRODUCTION	1
II	BACKGROUND AND ANALYTICAL CONSIDERATION	8
	2.1 OVERLAND FLOW HYDRAULICS	8
	2.1.1 Background	8
	2.1.2 Theory of Overland Flow	10
	2.2 ANALYTICAL CONSIDERATIONS	17
	2.2.1 Vertical Velocity Profile	18
	2.2.2 Longitudinal Mean Velocity Profile ($\bar{u} = f(x)$)	21
	2.2.3 Mean Velocity Profile of Retarded Overland Flow	23
	2.2.4 Mean Depth of Overland Flow	23
	2.2.5 Friction Slope, S_f, and Friction Factor, f	24
	2.2.6 Average Boundary Shear Stress and Stream Power of Overland Flow	26
	2.3 SOIL EROSION BY WATER	29
	2.3.1 Properties of Erosion	29
	2.3.2 Factors Affecting Erosion	30
	2.3.2.1 Climatic factors	31
	2.3.2.2 Topographic factors	32
	2.3.2.3 Soil factors	33

TABLE OF CONTENTS - (Continued)

Chapter			Page
		2.3.2.4 Vegetative factors: cover and its management	34
		2.3.2.5 Human factors: erosion control measures and soil conservation practices.	35
	2.3.3	Raindrop Erosion (Splash Process)	37
	2.3.4	Overland Flow Erosion	40
2.4		SEDIMENT TRANSPORT MODEL OF OVERLAND FLOW. . . .	41
	2.4.1	Introduction.	41
	2.4.2	Sediment Discharge Models	44
2.5		DIMENSIONAL ANALYSIS	45
	2.5.1	Introduction.	45
	2.5.2	Purpose of Dimensional Analysis	46
	2.5.3	Dimensionless Form of Equations	46
		2.5.3.1 Sediment discharge	46
		2.5.3.1.1 ν , ρ , d_{50} as repeated variables . . .	48
		2.5.3.1.2 ν , ρ , d as repeated variables . . .	48
		2.5.3.1.3 ν , ρ , X as repeated variables . . .	49
		2.5.3.1.4 ν , ρ , u as repeated variables . . .	49
		2.5.3.1.5 u , d , ρ as repeated variables . . .	49
		2.5.3.2 Local velocity	51
III		EQUIPMENT AND EXPERIMENTAL PROCEDURES.	53
3.1		GENERAL DESCRIPTION AND PROCEDURES	53

TABLE OF CONTENTS - (Continued)

Chapter			Page
	3.2	EQUIPMENT AND MATERIALS AND THEIR USAGE.	55
		3.2.1 Flume	56
		3.2.2 Soil.	56
		3.2.3 Carriage and Point-Gage	57
		3.2.4 Collecting Tank	57
		3.2.5 Stage Recorder.	57
		3.2.6 Rainfall Simulator and Control Valves . .	57
	3.3	MEASUREMENTS	59
		3.3.1 Runoff Measurement.	59
		3.3.2 Depth Measurement	60
		3.3.3 Surface-Velocity Measurement.	60
		3.3.4 Sieve Analysis.	61
		3.3.5 Bulk Density.	61
IV	PRESENTATION AND ANALYSIS OF DATA.		63
	4.1	DATA REDUCTION AND TABULATION.	63
		4.1.1 Sediment Concentration.	63
		4.1.2 Water Discharge and Rainfall Excess . . .	66
		4.1.3 Sediment Discharge.	66
		4.1.4 Mean Local Velocity of Overland Flow. . .	69
		4.1.5 Mean Local Depth of Overland Flow	70
		4.1.6 Sediment Size Distribution.	72
		4.1.7 Temperature, Viscosity, Reynolds Number and Froude Number.	74
		4.1.8 Friction Factor, f , and Friction Slope, S_f	76

TABLE OF CONTENTS - (Continued)

Chapter			Page
	4.1.9	Boundary Shear Forces, Critical Tractive Force and Stream Power	77
	4.1.10	Rill Measurements	80
	4.1.11	Summary of Data from Vegetated Surface Runs.	82
4.2		SIMPLE RELATIONSHIPS BETWEEN THE VARIABLES . . .	82
	4.2.1	Sediment Concentration Versus Time. . . .	82
	4.2.2	Sediment Concentration Versus Slope and Intensity	85
	4.2.3	Sediment Discharge Versus Slope and Intensity	85
	4.2.4	Water Discharge Versus Slope and Intensity	85
	4.2.5	Local Mean Velocity and Depth Versus Overland Flow Distance, Slope and Intensity	102
	4.2.6	Friction Factor, f , Versus Reynolds Number, Re	102
	4.2.7	Effect of Vegetation on Erosion and Sediment Discharge.	102
4.3		ANALYSIS OF DATA	102
	4.3.1	Sediment Concentration as a Dependent Variable.	120
	4.3.2	Sediment Discharge as a Dependent Variable.	125
	4.3.3	Averaged Surface Erosion Depths as Dependent Variables	132
	4.3.4	Median Transported Sediment Diameter, d_{50} , and the d_{50}/d_{50_o} Ratio as Dependent Variables	136

TABLE OF CONTENTS - (Continued)

Chapter			Page
		4.3.5 Mean Velocity of Overland Flow as a Dependent Variable	138
		4.3.6 Depth of Flow as Dependent Variable . . .	140
	4.4	RILL ANALYSIS.	141
		4.4.1 Rill/Surface Area Ratio as a Dependent Variable.	142
		4.4.2 Rill Averaged Depth as a Dependent Variable.	144
		4.4.3 Rill Volume, V_R and Rill Volume/Total Erosion Volume Ratio, V_R/V_T , as Dependent Variables	145
V		DISCUSSION OF RESULTS.	147
	5.1	DISCUSSION OF ANALYTICAL RESULTS	147
		5.1.1 Longitudinal Mean Local Velocity Profile	147
		5.1.2 Sediment Transport Equations.	148
	5.2	DISCUSSION OF FIGURES AND SIGNIFICANT RELATED VARIABLES.	148
		5.2.1 Sediment Concentration Versus Time. . . .	149
		5.2.2 Slope and Intensity of Rainfall	149
		5.2.3 Water Discharge	150
		5.2.4 Mean Local Velocity, Depth of Flow Versus Length of Slope	150
		5.2.5 Flow Properties, Reynolds Number and Froude Number	151
		5.2.6 Vegetation Affecting Soil Erosion	152
	5.3	PREDICTION EQUATIONS AND DISCUSSION.	153
		5.3.1 Mean Velocity Prediction of Overland Flow.	157

TABLE OF CONTENTS - (Continued)

Chapter			Page
		5.3.2 Sediment Concentration and Erosion Depth	161
		5.3.3 Sediment Discharge Prediction	166
		5.3.4 Rill Geometry	170
	5.4	FIELD APPLICATION OF RESULT.	170
VI		SUMMARY AND CONCLUSIONS.	173
	6.1	SUMMARY.	173
	6.2	CONCLUSIONS.	174
	6.3	FUTURE STUDY	177
		REFERENCES	179

LIST OF TABLES

Table		Page
2-1	Factors affecting soil erosion due to water (after Baver, 1965, p. 431)	31
4-1	Instantaneous sediment concentration, C_i, for given slope and intensity of rain at given time and the end of flow	64
4-2	Averaged sediment concentration, C_s, water discharge and sediment discharge and rainfall excess for given slope and intensity of rain at the end of overland flow	65
4-3	Infiltration and water discharge for given slope and intensities at given distance	67
4-4	Sediment discharge in terms of different units	68
4-5	Local mean velocity and depth of flow for a given run at a given distance	71
4-6	Sieve analysis of original soil used for the experiment	72
4-7	The d_{84}, d_{50}, d_{16}, and σ of transported sediment, d_b and porosity, P, for a given run (d_{84} = 1.00, d_{50} = .35 or .325 and d_{16} = .1 mm of the original sample)	73
4-8	Experimentally calculated Reynolds number, Re, Froude number, Fr, for a given run, and rainfall excess at a given distance	75
4-9	Friction factor, f, friction slope, S_f, boundary shear, τ_o, and critical tractive force, τ_c, for a given run at a given distance (without rainfall effect using Darcy-Weisbach formula)	78
4-10	Friction factor, f, friction slope, S_f, and boundary shear, τ_o, for a given run at a given distance (with rainfall effect in the indoor laboratory; f is calculated by equation 2-43)	79

LIST OF TABLES - (Continued)

Table		Page
4-11	Boundary shear, τ_o, and stream power for each run at the end of flow (τ_o is calculated by equation 2-55; with rainfall effect in the outdoor laboratory .	81
4-12	Data from rill measurements.	83
4-13	Data from vegetated surface runs	84
4-14	Comparison between vegetation and bare soil.	84
4-15	Correlation matrix of major variables used in stepwise nonlinear regression analysis	119
5-1	Selected prediction equations which are obtained from nonlinear regression analysis and analytical analysis	154
5-2	Predicted mean local velocities of overland flow generated by rainfall at a given distance for each run from analytically obtained equation (equation 2-36).	158
5-3	Predicted mean local velocities of overland flow generated by rainfall at a given distance for each run from regression equation (equation 4-87)	162
5-4	Measured and predicted sediment discharges by equation 4-47 and equation 4-59 respectively	163
5-5	Prediction of rill geometry (equation 4-100 and equation 4-118).	171

LIST OF FIGURES

Figure		Page
2-1	Overland flow on an inclined surface under rainfall and infiltration	13
2-2	Velocity profiles.	18
2-3	Overland flow profile.	21
3-1	General view of the rainfall-runoff facility of CSU. .	54
3-2	The layout of the experiment	54
3-3	Schematic of sprinkler riser for grid system (after Holland, 1969)	58
4-1	Relationship between sediment concentration and time for given rainfall intensities on 5.7 percent slope. .	86
4-2	Relationship between sediment concentration and time for given rainfall intensities on 10 percent slope . .	87
4-3	Relationship between sediment concentration and time for given rainfall intensities on 15 percent slope . .	88
4-4	Relationship between sediment concentration and time for given rainfall intensities on 20 percent slope . .	89
4-5	Relationship between sediment concentration and time for given rainfall intensities on 30 percent slope . .	90
4-6	Relationship between sediment concentration and time for given rainfall intensities on 40 percent slope . .	91
4-7	Relationship between sediment concentration and slope for given rainfall intensities (average concentration values obtained after one hour run).	92
4-8	Relationship between sediment concentration and slope for given rainfall intensities (average concentration values obtained between 0-10 minutes).	93
4-9	Relationship between sediment concentration and slope for given rainfall intensities (average concentration values obtained after first 30 minutes).	94
4-10	Relationship between sediment concentration and slope for given rainfall intensities (average concentration values obtained between 30-60 minutes)	95

LIST OF FIGURES - (Continued)

Figure		Page
4-11	Relationship between sediment concentration and slope for given rainfall intensities (average concentration values obtained between 30-40 minutes)	96
4-12	Relationship between sediment discharge and slope for given rainfall intensities (q_s in lb/hr/ft of width).	97
4-13	Relationship between sediment discharge and slope for given rainfall intensities (q_s in lb/hr/ft of width).	98
4-14	Relationship between sediment discharge and slope for given water discharges (q in cfs/ft of width and q_s in lb/sec/ft of width)	99
4-15	Relationship between sediment discharge and water discharges on given slopes for one hour run.	100
4-16	Relationship between water discharge and slope for given rainfall intensities	101
4-17	Mean local velocity and depth related to slope length for given rainfall intensities on 5.7 percent slope. .	103
4-18	Mean local velocity and depth related to slope length for given rainfall intensities on 10 percent slope . .	104
4-19	Mean local velocity and depth related to slope length for given rainfall intensities on 15 percent slope . .	105
4-20	Mean local velocity and depth related to slope length for given rainfall intensities on 20 percent slope . .	106
4-21	Mean local velocity and depth related to slope length for given rainfall intensities on 30 percent slope . .	107
4-22	Mean local velocity and depth related to slope length for given rainfall intensities on 40 percent slope . .	108
4-23	Relationship between Darcy-Weisbach friction factor, f , and Reynolds number Re for given slopes.	109
4-24	Relationship between Darcy-Weisbach friction factor and distance for given rainfall intensities on 5.7 percent slope.	110

LIST OF FIGURES - (Continued)

Figure		Page
4-25	Relationship between Darcy-Weisbach friction factor and distance for given rainfall intensities on 10 percent slope.	111
4-26	Relationship between Darcy-Weisbach friction factor and distance for given rainfall intensities on 15 percent slope.	112
4-27	Relationship between Darcy-Weisbach friction factor and distance for given rainfall intensities on 20 percent slope.	113
4-28	Relationship between Darcy-Weisbach friction factor and distance for given rainfall intensities on 30 percent slope.	114
4-29	Relationship between Darcy-Weisbach friction factor and distance for given rainfall intensities on 40 percent slope.	115
4-30	Relationship between percentage of erosion decreased by vegetation and rainfall intensity on 40 percent slope (40 percent surface is covered with 3-4 inch high winter wheat)	116
4-31	Relationship between sediment concentration and rainfall intensity (with and without vegetal cover on 40 percent slope)	117
5-1	Predicted velocity versus measured velocity at 3' and 6' ($\bar{u} = (g/3\nu)^{1/3} S_o^{1/3} q_o^{2/3} X^{2/3}$)	159
5-2	Predicted velocity versus measured velocity at 12' and 16' ($\bar{u} = (g/3\nu)^{1/3} S_o^{1/3} q_o^{2/3} X^{2/3}$)	160
5-3	Predicted velocity versus measured velocity at 3' and 6' ($\bar{u} = (1/e^{2.697}) Re^{.627} S_o^{.336}$)	164
5-4	Predicted velocity versus measured velocity at 12' and 16' ($\bar{u} = (1/e^{2.697}) Re^{.627} S_o^{.336}$)	165

LIST OF FIGURES - (Continued)

Figure		Page
5-5	Relationship between measured and predicted sediment discharges (prediction equation: $q_s = (1/e^{11.645}) \, Re^{2.054} \, S_o^{1.46}$)	167
5-6	Relationship between measured and predicted sediment discharges (prediction equation: $q_s = e^{.744} \, ((\tau_o - \tau_c) \, \bar{u})^{1.584}$)	168

LIST OF SYMBOLS

Symbol	Definition	Dimension	Units
A_R	Surface area of rills	L^2	ft^2
A_T	Total area of soil surface	L^2	ft^2
A_i	Area of increment	L^2	ft^2
a	Acceleration of fluid	L/t^2	ft/sec^2
C	Constant for friction relation	--	--
C_i	Instantaneous sediment concentration	F/F	ppm
C_d	Drag coefficient	--	--
C_l	Climatic factor	--	--
C_{lsd}	Constant for slope length, slope degree and raindrop diameter	--	--
C_s	Sediment concentration	F/F	ppm
c.s.	Control surface area	L^2	ft^2
d	Normal depth of flow	L	ft
d_1	Diameter of the transported hemisphere (d_1 = 1.25 dr)	L	in or mm
d_r	Mean diameter of raindrop	L	in or mm
d_{r50}	Median diameter of raindrop	L	in or mm
d_t	Inside diameter of raindrop producer	L	in or mm
d_b	Bulk density of soil	F/L^3	lb/ft^3 or gm/cm^3
d_p	Particle density of soil	F/L^3	lb/ft^3 or gm/cm^3
d_{50}	Median diameter of transported sediment (50% is finer)	L	ft or in

LIST OF SYMBOLS - (Continued)

Symbol	Definition	Dimension	Units
d_{16}	The diameter of the sediment for 16% of the sediment finer than this size	L	ft or in
d_{84}	The diameter of the sediment for 50% of the sediment finer than this size	L	ft or in
D_r	Soil detachment by rainfall	F/L^2	lb/L^2
D_F	Soil detachment by flow	F/L^2	lb/L^2
D_R	Depth of rills	L	ft
du	Differential velocity	L/t	ft/sec
dx	Differential horizontal coordinate	L	ft
dy	Differential vertical coordinate	L	ft
E	Relative amount of soil splashed during 30 min.	F/t	lb/sec
Fr	Froude number	--	--
F	Force	F	lb
f	Darcy-Weisbach friction factor	--	--
f*	Modified friction factor due to raindrop impact	--	--
g	The acceleration of gravity	L/t^2	ft/sec^2
h	Depth of flow	L	ft
h*	Over pressure head due to raindrop impact	L	ft
I (i)	Infiltration rate	L/t	in/hr or ft/sec
i	Subscript i is used for step of increment number	--	--

LIST OF SYMBOLS - (Continued)

Symbol	Definition	Dimension	Units
K	Soil constant	--	--
K_n	Soil and roughness constant for effective force model	--	--
K_m	Soil and roughness constant for effective stream power	--	--
k	Roughness size of surface texture ($K = d_{84}$)	L	ft
K_r	Constant of rainfall	--	--
L	Length	L	ft, in or mm
M	Mass	M	slug
m	Coefficient for effective tractive force model	--	--
n	Coefficient for effective stream power model	--	--
p	Pressure	F/L^2	lb/ft^2
P	Porosity of soil	L^3/L^3	%
P_r	Stream power due to raindrop	FL/tL^2	lb/ft/sec
P_s	Stream power due to flow	FL/tL^2	lb/ft/sec
R^2	Coefficient of determination	--	--
R_c	Critical Reynolds number	--	--
Re	Reynolds number - defined as $q_o X/\nu$	--	--
$Re_{d_{50}}$	Particle Reynolds number	--	--
Re_{q_o}	Rainfall-particle Reynolds number	--	--
Re_x	Reynolds number in terms of distance	--	--

LIST OF SYMBOLS - (Continued)

Symbol	Definition	Dimension	Units
r	Rainfall intensity	L/t	ft/sec or in/hr
Q_s	Dry mass of material in transport	M/tL	slug/sec/ft
q_{si}	Immersed weight of material transported	F/tL	lb/sec/ft
q_s	Sediment discharge	F/tL	lb/sec/ft
r_{30}	Maximum annual 30-min. rainfall	L/t	ft/sec
q_s^*	Dimensionless form of sediment discharge ($q_s^* = C_s$)	F/F	ppm
q_o	Rainfall excess	L/t	ft/sec or in/hr
q	Unit discharge	L^3/tL	cfs/ft
q_x	Unit discharge at X	L^3/tL	cfs/ft
S_o	Bottom slope	L/L	--
S_f	Friction slope	L/L	--
S_f^*	Modified friction slope due to raindrop	--	--
S_{DF}	Soil coefficient for detachment of soil by flow	--	--
S_{TF}	Soil coefficient for transport of soil by flow	--	--
S_{Dr}	Soil coefficient for detachment by rainfall	--	--
S_{Tr}	Soil coefficient for transport by flow	--	--
SEE	Standard error of estimate	--	--
T_r	Transport of soil by rainfall	F/tL	lb/sec/ft
T_F	Transport of soil by flow	F/tL	lb/sec/ft
t	Time coordinate	--	--

LIST OF SYMBOLS - (Continued)

Symbol	Definition	Dimension	Units
$\tan \alpha$	Coefficient of solid friction	--	--
u	Velocity of flow	L/t	ft/sec
$\bar{u}$	Mean local velocity of flow	L/t	ft/sec
u_*	Shear velocity	L/t	ft/sec
u_{max}	Maximum flow velocity	L/t	ft/sec
$\bar{V}$	Vector fluid velocity	L/t	ft/sec
v	Lateral flow velocity of x component	L/t	ft/sec
V_T	Volume of total transported sediment	L^3	ft^3
V_R	Volume of rills	L^3	ft^3
V_x	Terminal velocity of drop at X	L/t	ft/sec
W_T	Total weight of transported sediment	F	lb
V_t	Terminal velocity of raindrop	L/t	ft/sec
X	Length of flow (distance)	L	ft
x	Horizontal space coordinate	L	ft
y	Vertical space coordinate	L	ft
α	Constant of velocity relation for y	--	--
β	Constant of velocity relation for y^2	--	--
β_r	Momentum correction factor for terminal rainfall drop	--	--
ρ	Mass density of water	Ft^2/L^4	$lb/sec^2/ft^4$
ρ_s	Mass density of sediment	Ft^2/L^4	$lb/sec^2/ft^4$

LIST OF SYMBOLS - (Continued)

Symbol	Definition	Dimension	Units
ρ_a	Mass density of air	Ft^2/L^4	$lb/sec^2/ft^4$
θ	Angle of inclination	--	degree
γ	Specific weight of water	F/L^3	lb/ft^3
μ	Dynamic viscosity of fluid	Ft/L^2	$lb/sec/ft^2$
ν	Kinematic viscosity of fluid	L^2/t	ft^2/sec
$\bar{\sigma}$	Surface tension water	F/L	lb/ft
σ	Gradation or size distribution index	--	--
Δ	Finite difference sign	--	--
$\Delta\gamma$	Difference between sediment and water specific weight	F/L^3	lb/ft^3
ΔR^2	Difference or increment or R^2	--	--
τ_o	Average boundary shear stress	F/L^2	lb/ft^2
τ_c	Critical boundary shear stress	F/L^2	lb/ft^2

CHAPTER I

INTRODUCTION

A rapidly expanding population and increasingly greater demands for food have made it essential that man cease exploitation of his natural resources. Soil erosion and sedimentation are of particular importance in the evaluation of water and soil resources. If he continues his abuse of nature in the future as he has in the past, he is almost certain to become extinct.

Paramount among man's ecological concerns are the conservation, development and utilization of soil and water resources. Soil erosion and sedimentation are of particular importance in the evaluation of water and soil resources. History records that many ancient civilizations of the Old World, e.g., Mesopotamia, Anatolia, Egypt, China and Central Asia, declined primarily because their inhabitants could not deal with the problems of erosion, sedimentation and water management. A major reason early settlements of the New World along the shores of Chesapeake Bay fell into decay, it has been ascertained, was that settlers could not handle the problems of sediment deposition in harbors (Task Committee on the Preparation of Sedimentation, 1965).

Soil erosion is the primary cause of problems related to sedimentation, because eroded material is transported to rivers and reservoirs and deposited there. This results in a reduced storage in reservoirs and reduced capacity of rivers to carry flood flows. Moreover, soil erosion, with its concomitant loss of surface soil, means decreasing soil fertility. Sedimentation combines the processes of erosion, entrainment, transportation, deposition and compaction of

sediment. Erosion can be defined as the removal or detachment and transportation of soil particles from their environment by erosive agents such as water, wind, ice, waves and gravity. Erosion may be divided into stream channel erosion and soil erosion. Stream erosion is the removal of stream bed and bank material by water flowing in the stream, whereas soil erosion is defined as sheet, rill and gully erosion of the land surface. This study deals specifically with sheet erosion of the soil by overland flow.

The erosion process in general, and sheet erosion in particular, are comprised of four factors that are categorized in terms of the detaching and transporting capacity of their erosive agents. These include the detaching and transporting capacity of rainfall, and the detaching and transporting capacity of overland flow.

Erosion begins when raindrops first hit the earth's surface and detach soil particles by their impact, or as it is often termed, splash. The detaching capacity of rainfall depends on the raindrop diameter, size distribution, fall velocity and total mass or kinetic energy at impact. The transporting capacity of rainfall depends on available detached particles, rainfall excess and slope of overland surface. Unless the soil surface is covered by vegetation or vegetative residues, raindrops are capable of detaching tremendous quantities of soil as well as transporting some of this detached soil downslope by the splash process. Most eroded particles, however, are moved downslope by overland flow.

Overland flow occurs when the surface storage capacity has been filled and the rainfall intensity exceeds the infiltration rate of the soil. The detaching and transporting capacity of overland flow

depends on surface slope, velocity and depth of flow, that is, the shearing stress or tractive force on the soil boundary. Detachability of soil is related to its physico-chemical properties, especially the cohesiveness of soil particles. The silt plus clay and organic matter content of soil determine the cohesiveness and dispersion of soil components. The smaller the silt plus clay percentage, the higher the dispersion; the smaller the cohesion is, the greater the erosion. The transportability of soil depends on size distribution, diameter and shape of soil grains, availability of detached particles and slope of the surface.

The need to search for the fundamental principles involved in the soil erosion process and to develop criteria and guidelines applicable to field problems is indeed great. The problem of developing a soil loss equation representative of overland flow resulting from rainfall will be investigated. The effects of slope and intensity of rainfall on soil erosion are emphasized in this study.

Within the context of this study, "erosion" will be used to refer only to the removal of soil particles by overland flow resulting from rainfall. Sandy soil was used in this study. Because of the non-cohesiveness of such soils, the soil detaching and transporting capacity of raindrop impact was ignored. The mechanics of soil erosion in relation to rainfall and overland flow hydraulics is an essential and important area of study in the field of sedimentation. Engineers have, over a long period of time, studied stream rather than soil erosion to understand the behavior of sediment transportation by streams. Apart from a few papers, notably Ellison (1947), Meyer and Monke (1965) and Meyer (1971), little comprehensive work has been done

to show the basic mechanics of soil erosion resulting from overland flow generated by rainfall. Yet the importance of the mechanics of soil erosion is critical to man.

The preface of the book, Hydraulics of Sediment Transport by Walter H. Graf (1971), offers the following remarks in connection with the detaching and transporting of soil.

> The understanding and formulation of movement and transportation of solid granular particles in or through liquid bodies represent an important issue within the field of hydraulics, fluvial geomorphology, and others. The problems are complicated, as are many other two-phase and interface problems, and thus have remained often subject to semiempirical or empirical treatment. However, theoretical endeavors do exist, but they are few and are not indisputable, immediate answers, or at least guidelines, are often necessary, and thus a careful examination of existing developments seems justified and timely.

Early research in the field provided empirical equations to be used as a planning tool by conservation technicians. These studies and equations, however, were not designed to meet the present need for a mathematical model to simulate soil erosion as a dynamic process, because they were rather descriptive and qualitative. For example, the approach of Ellison (1947) was to analyze separately each factor and component of erosion by water. Meyer and Wischmeier (1969) followed an idea somewhat similar to Ellison's, but they simulated the process of soil erosion by a mathematical model using various component sub-processes, such as soil detachment by rainfall, transport by rainfall, detachment by runoff and transport by runoff. Meyer and Wischmeier (1969) considered these sub-processes to be separate but interacting phases of the process of soil erosion by water. In their model, the four component sub-processes of the erosion process were evaluated for successive slope length increments. Soil erosion thus could be simulated as a dynamic process, and soil movement could be

described at all locations along a slope at any given time. Meyer (1971) referred to this method as a new approach. He maintained: "The development of a mathematical model for simulating the process of soil erosion by water promises to afford greater precision in soil-loss evaluations on upland areas."

In general, erosion and sedimentation are problems for geologists, fluvial geomorphologists, pedologists, agronomists and hydraulic engineers. Most geologists have attempted to study sedimentation in relation to a parent material and soil characteristics with a large time scale; consequently, much of their work has little immediate practical application. Agriculturists and pedologists have given primary attention to soil properties in relation to erosion, with little effort to relate erosion to the hydraulics of the system. Most of their research has been conducted in order to find empirical relations and to study erosion qualitatively. Hydraulic engineers, in general, have had almost no interest in and made no attempt to study soil erosion because they already had a sufficiently complex problem with stream erosion. While studies of soil erosion have suffered in almost every related field, an interdisciplinary approach would lend the comprehensiveness that the problem needs. One of the objectives of this study is to enlist the cooperation of geologists, agronomists, watershed managers, pedologists and engineers in the hope that they might find the investigation of this problem of soil erosion a worthy endeavor.

Although certain similarities exist between soil erosion and stream erosion mechanics, there is a need to study and analyze each process separately. The complexity of the problem prevents formulating the

mechanics of erosion by a theoretical approach. The approach followed in this study was, therefore, semi-analytical and empirical, based on experimental results obtained from an outdoor physical model under given and limited controlled variables.

The research was conducted at Colorado State University's rainfall-runoff facility under simulated rainfall upon a sandy soil in a plywood flume. Land slopes up to 40 percent and rainfall intensities up to 4.6 inches per hour were investigated. Since the phenomenon of erosion is so complex, a study of a simulated model where factors can be controlled and altered is advantageous. In this research, discharge, velocity, depth of flow and sediment rate were measured for each slope and intensity of rainfall.

Analysis of the experimental data led to the formulation of a soil loss prediction equation for a single short-duration storm. The qualitative effect of reducing soil erosion by planting a grass cover (winter wheat) was also investigated. The results of the experimentation show that it is possible to obtain a soil loss prediction equation or sediment discharge equation that can be applied in the field, for a given slope and rainfall intensity under known soil characteristics. The statistical results of this study and theoretical reasoning are similar.

In this dissertation, Chapter II is devoted to the background, theoretical aspect of the problem and dimensional analysis of possible variables that are important to the problem. Chapter III describes the experimental procedures, material and equipment used for the experiment and collection of data. In Chapter IV, the data are presented in tables and figures, and the statistical analysis of

data with results are shown. In Chapter V, results are compared and discussed. In Chapter VI, the study is summarized, conclusions are listed and recommendations for future research are given.

The uniqueness of this research lies in its study of effect of slope on erosion using grades of up to 40 percent; up to now no study has been conducted reaching 40 percent slope. The purpose of selecting such a steep slope is to study the region on the upland areas of a watershed.

To reiterate, the specific purpose of this experiment is to study the development of soil loss prediction equations for practical use under a given slope, intensity of rainfall and soil characteristics, as well as the qualitative effect of vegetative cover (winter wheat) on erosion. By means of this soil loss prediction equation the expected soil loss may be calculated and soil conservation practices improved.

CHAPTER II

BACKGROUND AND ANALYTICAL CONSIDERATION

This chapter first traces the analytic background of overland flow, including a derivation of the momentum and continuity equations with special reference to present studies. Overland flow is then considered in simplified form and a model is proposed for longitudinal mean velocity variation. A dimensional analysis on the important variables of sediment transport is also performed to interpret the various phenomena taking place in the form of dimensionless parameters.

2.1 OVERLAND FLOW HYDRAULICS

2.1.1 Background

Overland flow is that part of the surface runoff which flows in a thin sheet over the land surface toward stream channels. Overland flow formulation and solution has long been of great interest to hydrologists and hydraulic engineers. Hydrologists have sought a more sophisticated method of predicting the runoff from overland and to determine the rainfall-runoff relationships. They are also interested in calculating the water surface profile of overland flow, especially under the action of rainfall.

There are many problems involved in using an entirely hydraulic procedure for predicting overland flow. Overland flow is primarily unsteady and spatially varied because of its dependence on rainfall supply and its depletion by infiltration, neither of which is constant with time or location. Flow depths, too, may vary from below to above

critical depth, depending on the rate of flow and nature of surface, and may be laminar, turbulent, or both. Some conditions under which flow may become unstable with the formation of roll waves and raindrop impact on the sheet of flowing water also provide additional complications in overland flow (Robertson, et al., 1964).

Different aspects of overland flow have been studied for various purposes by a number of researchers, namely Hinds (1926), Favre (1933), Horton (1938), Ree (1939), Horner (1942), Izzard and Augustine (1943), Izzard (1944), Keulegan (1944), Parson (1949), Woo (1956), Behlke (1957), Liggett (1959), Yu and McNown (1963), Morgali (1963), Robertson, et al., (1964), Henderson and Wooding (1964), Wooding (1965), Chen and Hansen (1966), Grace and Eagleson (1965, 1966), Woolhiser and Liggett (1967), Chen and Chow (1968), Woolhiser (1969), Chow (1969), Yoon and Wenzel (1971), Kisisel (1971) and Li (1972). Concepts related to the conservation of mass and momentum, or energy, were used by all these researchers to derive the dynamic equation of overland flow.

The problem is not only to derive the governing equations of overland flow, but also to solve the equations for velocity and depth with respect to time and space coordinates. One of the major problems in solving the equations is to express the friction function under rainfall impact. For the case of kinematic-wave approximation, S_o, slope of surface is assumed equal to S_f, friction slope. Because of the complexity of the problem, analytical solutions are not possible without appropriate simplifications; hence, the method of characteristics and the finite-difference method have been widely used. Even the numerical solutions of equations require certain simplifications and

assumptions before they can be put into the form of numerical analysis. Woolhiser and Liggett (1967, p. 754) described the problem as follows:

> ...there is no general analytic solution to this system of equations. Analytic solutions have been restricted to limited regions of the solution domain or to special cases where suitable simplifications could be made. Numerical and graphical solutions have been obtianed for some special cases. Unfortunately, graphical techniques are prohibitively slow, and many of the finite difference schemes have exhibited convergence problems.

Overland flow analysis and equations may be used not only for rainfall-runoff relations, routing problems and flow profile calculations, but also for problems of erosion and sediment transport over mobile land bed under rainfall and infiltration action. Utilizing the existing derivations, solutions and ideas, the same kind of equations may be used for overland flow erosion. Velocity and depth profiles over the land as a function of distance and time can be used to evaluate the erosion process.

Using the tractive force approach and relating these overland flow characteristics, the rate of sediment transport over land surface can be evaluated. Tractive force and stream power can also be evaluated by examining the length of overland flow in relation to erosion as determined by the overland flow equation and its analysis.

2.1.2 Theory of Overland Flow

The fundamental laws governing overland flow are the principles of the conservation of mass and momentum, or energy. The momentum approach to overland flow is utilized if the boundary shear stress is significant. Based on these principles, two equations can be developed, an equation of continuity based on the principle of the conservation of mass, and an equation of momentum based on the principle of the

conservation of momentum. The flow can be treated as an incompressible viscous fluid. Flow variables include velocity and depth of flow. They are functions of space coordinates as well as time if flow is unsteady, but in case of steady flow they are only functions of space coordinates. Further assumptions are unidirectional and two-dimensional flow under constant intensity of rain and infiltration.

In the literature, overland flow equations are known as shallow water equations. The continuity and momentum equations for shallow flow are given as follows. The continuity equation is

$$\frac{\partial h}{\partial t} + \frac{\partial(\bar{u}h)}{\partial x} = q_o \qquad \text{or} \qquad \frac{\partial h}{\partial t} + \bar{u}\frac{\partial h}{\partial x} + h\frac{\partial \bar{u}}{\partial x} = q_o \ , \tag{2-1}$$

and the momentum equation is

$$\frac{\partial \bar{u}}{\partial t} + \bar{u}\frac{\partial \bar{u}}{\partial x} + g\frac{\partial h}{\partial x} = g\,(S_o - S_f) - \frac{q_o}{h}(\bar{u} - v) \ , \tag{2-2}$$

in which

q_o = inflow rate or rainfall excess (L/t) [1/],

g = the acceleration of gravity (L/t^2) ,

S_o = the bottom slope (L/L) ,

S_f = the friction slope (L/L) , defined by an appropriate relation such as Darcy-Weisbach, Chezy or Manning's Equation,

$\bar{u}$ = mean local velocity component in x direction (L/t) ,

h = depth of flow (L) ,

v = the x component of the velocity of the lateral inflow (L/t) , and

---

[1/] In this thesis, L is length, t is time, F is force, and M is mass.

x and t = space and time coordinates, respectively.

These two nonlinear partial differential equations for gradually varied unsteady flow were first derived by and have for some time been called the "de St. Venant Equations," after the late 19th century French mathematician. There is no general analytical solution for these shallow water equations unless certain simplifications and assumptions are made for special cases. Usually the method of characteristics and the finite difference method are used to solve this system of equations.

The method of deriving equations of motion for overland flow has become an art rather than a science. There is no single and standard method of obtaining equations, and different methods and approaches to obtain these equations have been tried in the past. Although approaches are different for each investigator, all equations are comparable, and the principles are the same, except that their coordinate systems, symbols, assumptions, definitions and evaluation of terms in general form may differ according to the investigator's area of interest.

The following derivation of the momentum and continuity equations for overland flow under rainfall is made for a control volume of the fixed Cartesian Coordinate System (Fig. 2-1); the derivation gives results similar to those presented by Chen and Chow (1968). It is assumed there are steady, spatially varied flow; unidirectional, two-dimensional, uniform, constant infiltration and rainfall intensity; and momentum and velocity correction coefficients of unity. From Newton's Second Law of Motion ($\bar{F} = M\bar{a}$, where $\bar{F}$ is a vector force, $\bar{a}$ is a vector acceleration, $-$ is vector sign, and M is mass) at

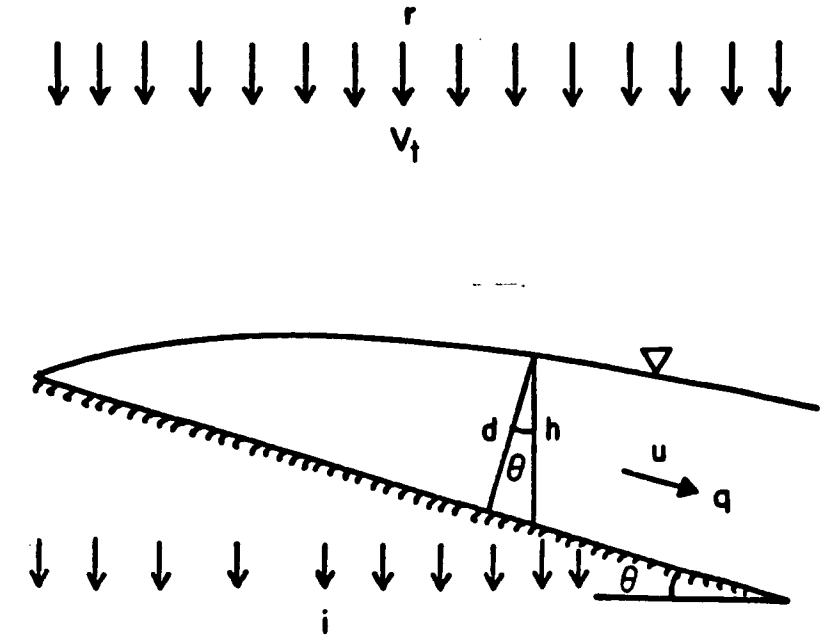

a. Overland Flow Profile

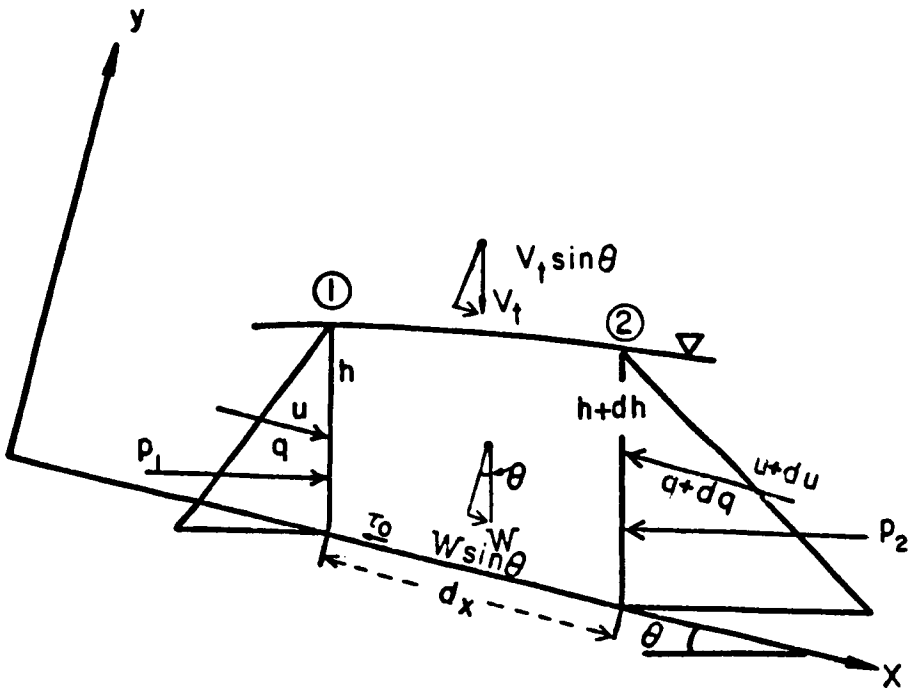

b. Two-Dimensional Cartesian Coordinate System and Control Volume of Overland Flow Segment

Fig. 2-1. Overland flow on an inclined surface under rainfall and infiltration.

equilibrium condition, the summation of the forces acting on the control volume in the direction of flow must equal the change in momentum flux within the control volume. All forces are taken in x direction.

Momentum flux at section one is

$$\rho\bar{u}^2h \quad \text{or} \quad \rho q\bar{u} ,$$

in which

ρ = mass density of water (Ft^2/L^4) , and

q = unit discharge (L^3/tL).

Momentum flux at section two is

$$\rho(\bar{u} + d\bar{u}^2)\ (h + dh) , \quad \text{or} \quad \rho(q + dq)\ (\bar{u} + d\bar{u}) ,$$

and addition of momentum by rainfall in x direction on control volume is

$$\rho r V_t \sin\theta\ dx ,$$

in which

r = rainfall intensity (L/t) ,

V_t = terminal velocity of raindrop (L/t) ,

θ = an angle of inclination (degrees), and

dx = the distance increment (L).

The net change of momentum flux on control volume in direction of x with the dx increment is

$$\rho(q + dq)\ (\bar{u} + d\bar{u}) - \rho q\bar{u} - \rho r V_t \sin\theta\ dx.$$

After simplifying, and ignoring the second order differentials,

$$dM = \rho\bar{u}dq + \rho q d\bar{u} - \rho r V_t \sin\theta \, dx \,, \tag{2-3}$$

in which dM represents the net change of momentum flux (F).

The forces acting on the control volume are pressure, gravity and drag. Although pressure distribution is assumed hydrostatic, the over pressure head, h^*, due to raindrop impact, is also included in pressure force evaluation. Over pressure head, h^*, was first defined by Chen (1962) and later by Grace and Eagleson (1965) as:

$$h^* = \frac{\beta_r \, r V_t \cos^2\theta}{g} \,, \tag{2-4}$$

in which

β_r = the momentum correction factor for the terminal drops (β_r is assumed unity here), and

h^* = the over pressure head due to raindrop impact (L).

The pressure force in x direction at section one is

$$\tfrac{1}{2} \rho g (h \cos\theta + h^*)^2 .$$

The pressure force at section two is

$$\tfrac{1}{2} \rho g [(h + dh) \cos\theta + h^*]^2 .$$

The net pressure on the control volume, after simplifying and ignoring all small terms, is

$$(\rho g \cos^2\theta \, h dh + \rho g h^* dh) .$$

The gravity force is simply a weight component of the control volume in the x direction that can be expressed as

$$\rho g h \sin\theta \, dx \quad .$$

The shear force (drag on the bottom) is

$$\tau_o dx \ ,$$

in which τ_o represents the average boundary shear stress (F/L^2). Equating the change of momentum to the summation of all forces in the x direction (as positive) will yield:

$$\rho\bar{u}dq + \rho q d\bar{u} - \rho r V_t \sin\theta \, dx = \rho g h \sin\theta \, dx$$

$$- \rho g \cos^2\theta \, h dh - \rho g h^* dh - \tau_o dx \quad . \tag{2-5}$$

Dividing this equation by dx ,

$$\rho \left(\bar{u}\frac{dq}{dx} + q\frac{d\bar{u}}{dx}\right) - \rho r V_t \sin\theta = \rho g h \sin\theta$$

$$- \rho g \left(\cos^2\theta \, h \frac{dh}{dx} + h^* \frac{dh}{dx}\right) - \tau_o \quad . \tag{2-6}$$

Rearranging,

$$\rho \frac{d(\bar{u}q)}{dx} - \rho r V_t \sin\theta = \rho g h \sin\theta$$

$$- \rho g \frac{dh}{dx}\left(h \cos^2\theta + h^*\right) - \tau_o \quad . \tag{2-7}$$

The final form of the momentum equation then becomes

$$\rho \frac{d(\bar{u}^2 h)}{dx} - \rho r V_t \sin\theta = \rho g h \sin\theta$$

$$- \rho g \frac{d}{dx}\left(\tfrac{1}{2} h^2 \cos^2\theta + h h^*\right) - \tau_o \quad . \tag{2-8}$$

For incompressible steady flow, the continuity equation in the vector integral form is

$$\iint_{c.s.} \bar{V} \cdot d\bar{A} = 0 \ , \tag{2-9}$$

in which

$\bar{V}$ = the vector fluid velocity,

$d\bar{A}$ = the vector differential area on the control surface, ($|dA|\ \bar{n}$) , and

c.s.= the control surface.

After summing, the inflows through c.s. are equal to outflow through c.s. which yields

$$\bar{u}h + (r - i)\, dx = (\bar{u} + d\bar{u})\ (h + dh) \ , \tag{2-10}$$

in which i = the infiltration rate (L/t).

Simplifying and rearranging this equation, it can be reduced to

$$\bar{u} \frac{dh}{dx} + h \frac{d\bar{u}}{dx} = r - i \quad . \tag{2-11}$$

By further rearranging, and substituting $q_o = r - i$, the continuity equation is

$$\frac{d(\bar{u}h)}{dx} = q_o \qquad \text{or} \qquad \frac{d(q)}{dx} = q_o \quad . \tag{2-12}$$

2.2 ANALYTICAL CONSIDERATIONS

In this section, mathematical models describing velocity profiles are derived by using certain assumptions for steady spatially varied overland flow, with and without the raindrop impact on the profile. Recent studies by Yoon and Wenzel (1971) and Kisisel (1971) show that raindrop impact retards the surface velocity of the flow and increases resistance to flow. At the present state of knowledge, there is no

theoretical way of expressing this velocity profile and friction factor or friction slope. In the following analysis, an attempt is made to express velocity, depth, and boundary shear in terms of rainfall excess, distance and slope.

2.2.1 Vertical Velocity Profile

By assuming no raindrop impact and that laminar flow has similar velocity profiles along the overland distance, the velocity profile of overland flow in the vertical direction can be considered to be a second-degree curve of the form presented in Fig. 2-2a.

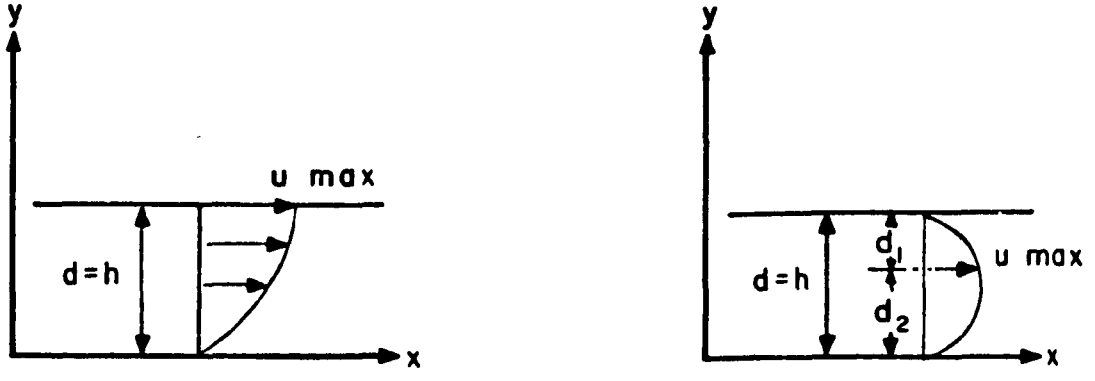

a. Velocity profile without raindrop impact.

b. Velocity profile with raindrop impact.

Fig. 2-2. Velocity profiles.

The velocity profile model is

$$u = \alpha y + \beta y^2 , \qquad (2\text{-}13)$$

in which α and β = constants.

The constants of Eq. (2-13) can be determined by employing the boundary and initial conditions (B.C., I.C.), which are:

$$u = 0 \quad \text{when} \quad y = 0$$

$$u = u_{max} \quad \text{when} \quad y = h \qquad \text{B.C.}$$

and

$$\frac{du}{dy} = 0 \quad \text{when} \quad y = h \qquad \text{I.C.}$$

Applying these conditions, Eq. (2-13) leads to results:

$$0 = 0 + 0$$

$$u_{max} = \alpha h + \beta h^2 \tag{2-14}$$

$$\frac{du}{dy} = \alpha + 2\beta y \rightarrow 0 = \alpha + 2\beta h \quad . \tag{2-15}$$

Solving for α and β yields

$$\alpha = \frac{2u_{max}}{h} \tag{2-16}$$

and

$$\beta = -\frac{u_{max}}{h^2} \quad . \tag{2-17}$$

Substituting these values into Eq. (2-13) yields the vertical velocity profile for laminar overland flow, which is

$$u = \frac{2u_{max}}{h}\, y - \frac{u_{max}}{h^2}\, y^2 \quad . \tag{2-18}$$

Unit discharge and mean velocity can be determined as follows:

$$q = \bar{u}h = \int_0^h u\,dy. \tag{2-19}$$

Substituting the equation for u, we get

$$q = \int_0^h \left(\frac{2u_{max}}{h} y - \frac{u_{max}}{h^2} y^2 \right) dy \qquad (2\text{-}20)$$

and then by differentiating

$$q = \int_0^h \left(\frac{2u_{max}}{2h} y^2 - \frac{u_{max}}{3h^2} y^3 \right) , \qquad (2\text{-}21)$$

we can obtain

$$q = u_{max} h - \frac{u_{max} h}{3} = u_{max} h \left(1 - \frac{1}{3}\right) = \frac{2}{3} u_{max} h \quad . \qquad (2\text{-}22)$$

Through equating we get

$$q = \frac{2}{3} u_{max} h = \bar{u} h \quad . \qquad (2\text{-}23)$$

Solving for $\bar{u}$ yields

$$\bar{u} = \frac{2}{3} u_{max} \quad . \qquad (2\text{-}24)$$

This relation can also be obtained by any calculus using parabolic curve properties. For further analysis, differentiation of u is required, and is as follows:

$$\frac{du}{dy} = \frac{2u_{max}}{h} - \frac{2u_{max}}{h^2} y \qquad (2\text{-}25)$$

when $y = 0$

$$\frac{du}{dy} = \frac{2u_{max}}{h} \qquad \text{or} \qquad \frac{du}{dy} = \frac{3\bar{u}}{h} \quad . \qquad (2\text{-}26)$$

2.2.2 Longitudinal Mean Velocity Profile ($\bar{u} = f(x)$)

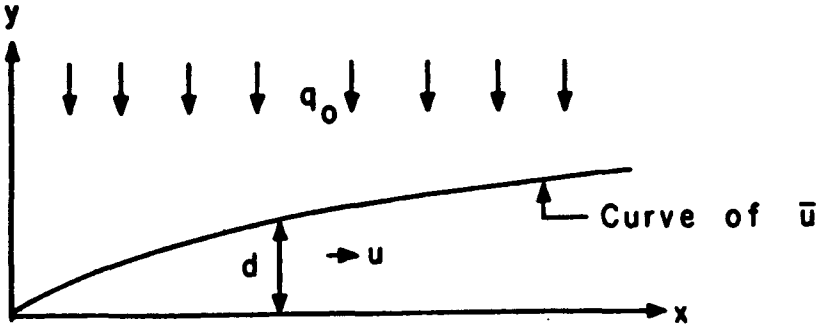

Fig. 2-3. Overland flow profile.

Mean velocity profile (Fig. 2-3) as a function of overland flow distance, X , can be obtained by assuming

$$\tau_o = \gamma \, d \, S_f \, , \tag{2-27}$$

and

$$\gamma \, d \, S_f = \mu \left(\frac{du}{dy} \right) \Big|_{y = 0} \, , \tag{2-28}$$

in which

γ = the specific weight of water (F/L^3) ,

μ = the dynamic viscosity of water $(F - t/L^2)$, and

d = the normal depth of flow (L).

The right side of the equation is the Newtonian definition of shear stress, the the left side of the equation comes from the boundary shear stress relation for steady uniform flow. When $y = 0$, $\frac{du}{dy} = \frac{3\bar{u}}{h}$; substituting these values of $\frac{du}{dy}$ into Eq. (2-28) yields

$$\gamma \, d \, S_f = \mu \, \frac{3\bar{u}}{h} \, . \tag{2-29}$$

Assuming $h = d$ and substituting $\mu = \rho\nu$ and $\gamma = \rho g$, the equation becomes

$$\rho\, g\, d\, S_f = \rho\nu \frac{3\bar{u}}{d} \quad , \tag{2-30}$$

in which ν = the kinematic viscosity of water (L^2/t).

Solving for $\bar{u}$ from the above equation gives:

$$\bar{u} = \frac{g\, S_f d^2}{3\nu} \quad . \tag{2-31}$$

If the continuity equation is applied,

$$q = q_o X = \bar{u} d \quad , \tag{2-32}$$

where X = the length of surface (distance) (L).

Solving for d from the above relation yields,

$$d = \frac{q_o X}{\bar{u}} \quad . \tag{2-33}$$

Substituting this relation into Eq. (2-31) gives

$$\bar{u} = \frac{g\, S_f}{3\nu} \left(\frac{q_o X}{\bar{u}}\right)^2 \quad . \tag{2-34}$$

Rearranging the terms,

$$\bar{u}^3 = \frac{g\, S_f}{3\nu}\, q_o^{\,2}\, X^2 \quad , \tag{2-35}$$

and taking the cube root gives the mean velocity profile of overland flow as a function of distance, friction slope, rainfall excess, and known constants. The final relation is

$$\bar{u} = \left(\frac{g}{3\nu}\right)^{1/3} S_f^{\,1/3}\, q_o^{\,2/3}\, X^{2/3} \tag{2-36}$$

or

$$\bar{u} = \left(\frac{g}{3\nu}\right)^{1/3} S_f^{1/3} q^{2/3} \quad . \tag{2-37}$$

To solve this equation, S_f must be evaluated. For a short segment of overland, and ignoring raindrop impact on shallow flow, S_f may be assumed equal to S_o.

2.2.3 Mean Velocity Profile of Retarded Overland Flow

If similar analysis is conducted for the velocity profile, where the surface velocity is retarded by rainfall drops, assuming $d_1 = h/3$ and $d_2 = 2h/3$ in Fig. 2-2b, the mean velocity profile of overland flow will be (where d_1 is the affected depth of flow and d_2 is the unaffected depth of flow in feet),

$$\bar{u} = \left(\frac{g}{4\nu}\right)^{1/3} S_f^{1/3} q_o^{2/3} X^{2/3} \quad . \tag{2-38}$$

The only difference between Eq. (2-36) and Eq. (2-23) is the presence of (4) instead of (3). This equation gives somewhat mean velocity, but mean depth will be a little greater.

2.2.4 Mean Depth of Overland Flow

Utilizing continuity, and Eqs. (2-33 and 2-36) the mean depth of flow can be obtained for unretarded flow as follows:

$$d = \frac{q_o X}{\left(\frac{g}{3\nu}\right)^{1/3} S_f^{1/3} q_o^{1/3} X^{1/3}} \tag{2-39}$$

Simplifying yields:

$$d = \left(\frac{3\nu}{g}\right)^{1/3} S_f^{-(1/3)} q_o^{1/3} X^{1/3} \quad . \tag{2-40}$$

2.2.5 Friction Slope, S_f, and Friction Factor, f

Solving Eq. (2-31) for S_f in terms of depth and velocity of flow and using Darcy-Weisbach relation and uniform flow friction slope assumption yields

$$S_f = \frac{3\nu\bar{u}}{gd^2} \tag{2-41}$$

and the friction factor, f, will be:

$$f = \frac{8gd^3S_f}{q^2} = \frac{3gdS_f}{\bar{u}^2} \quad , \tag{2-42}$$

where f is the Darcy-Weisbach friction coefficient.

Recent studies by Li (1972), Kisisel (1971) and Yoon and Wenzel (1971) show that raindrop impact on flow increases the friction factor and, as a result, friction slope, S_f, and boundary shear, τ_o. Li (1972) measured boundary shear, τ_o, under simulated rainfall in the CSU hydraulics laboratory and calculated friction factors, f, for given rainfall intensities and slope. He obtained the following empirical relation from nonlinear regression analysis:

$$f = \frac{27.162\ r^{.407} + 24}{Re} \tag{2-43}$$

where Re is the Reynolds number.

The above relationship is for smooth bed; if this equation is to be used for our case, the constant, 24, should be changed. The friction slope under raindrop impact will be different from the friction slope of uniform flow assumption. The modified friction slope, S_f^*, due to raindrop impact was given by Chen and Chow (1968) as follows:

$$S_f^* = \frac{h^*}{h \cos \theta} \frac{\partial h}{\partial x} \cos \theta + S_f \quad . \tag{2-44}$$

where S_f^* is the modified friction slope due to raindrop (L/L). Using the Darcy-Weisbach formula, friction slope, S_f, in terms of f, $\bar{u}$ and d, is,

$$S_f = \frac{f}{8g} \frac{\bar{u}^2}{h \cos \theta} \quad , \tag{2-45}$$

The modified friction slope due to raindrop impact in terms of modified friction factor becomes

$$S_f^* = \frac{f^*}{8g} \frac{\bar{u}^2}{h \cos \theta} \quad , \tag{2-46}$$

where f^* = modified friction coefficient due to raindrop impact. Equating Eqs. (2-44) and (2-46) and solving for f^* will yield

$$f^* = \frac{h^*}{\bar{u}^2} \frac{\partial h}{\partial x} \cos \theta + \frac{f}{8g} \tag{2-47}$$

For laminar uniform flow, the friction factor, f, is given as:

$$f = \frac{C}{Re} \quad , \tag{2-48}$$

where C = constant (As a special case, $C = 24$ for overland flow and Reynolds number is in the form of $Re = \frac{\bar{u}h \cos \theta}{\nu} = \frac{q}{\nu} = \frac{q_o X}{\nu}$).

The following relationships of friction factors are given by Chen and Chow (1968). For turbulent flow on smooth surfaces, the friction factor is

$$\frac{1}{\sqrt{f}} = 2 \log_{10} Re \sqrt{f} + 0.404 \quad . \tag{2-49}$$

For turbulent flow on rough surfaces, the friction factor is

$$\frac{1}{\sqrt{f}} = 2 \log_{10} \frac{2h \cos \theta}{k} + 1.74 \quad , \tag{2-50}$$

where k is the roughness size of the surface texture. It may be used as $k = d_{84}$, where d_{84} is diameter of sediment of which 84 percent is finer than this diameter. Chen and Chow (1968) commented that, although it may be assumed that the lower critical Reynolds number for flow without rainfall is 500 and with rainfall is 200, such an assumption is rather arbitrary and open to question. They expressed the critical Reynolds number, Re, explicitly in terms of relative roughness by equating two equations (2-48) and (2-50) for f :

$$R_c = C \left(2 \log_{10} \frac{2h \cos \theta}{k} + 1.74\right)^2 \tag{2-51}$$

where R_c = critical Reynolds number.

According to Eq. (2-51), the Reynolds number of the present study falls in the laminar flow category.

2.2.6 Average Boundary Shear Stress and Stream Power of Overland Flow

Substituting Eq. (2-40) into Eq. (2-27) gives the boundary shear as:

$$\tau_o = (3g^2 \rho^3 \nu)^{1/3} S_f^{2/3} q_o^{1/3} X^{1/3} \tag{2-52}$$

The product of Eqs. (2-36) and (2-52) yields the following relation for stream power:

$$P_s = \tau_o \bar{u} = \rho g S_f q_o X = \gamma S_f q \quad , \tag{2-53}$$

where P_s = the stream power of flow (F/L-t).

In sediment transport, evaluation of boundary shear, τ_o, and stream power, P_s, are very important. Since analytical solution for τ_o or P_s is impossible because friction slope, S_f, and friction factor, f, are unknown, and since sediment transport is closely related to τ_o or P_s, these should be evaluated either experimentally or numerically or both. Calculation of S_f or f can be done only for uniform flow; hence there is no way of finding f and S_f analytically for spatially varied flow, except through simplifications and restrictive assumptions. Moreover, raindrop impact complicates the problem further.

Shear stress, τ_o, can be measured directly in flumes without sediment transport, but it can not be measured in overland flow with sediment transport. In this study, τ_o will be approximated by solving the momentum equation (2-8) numerically. Solving for τ_o, Eq. (2-8) yields,

$$\tau_o = \rho g h \sin\theta - \rho g \frac{d}{dx}\left[\tfrac{1}{2} h^2 \cos^2\theta + hh^*\right] - \rho \frac{d(\bar{u}^2 h)}{dx} + \rho r V_t \sin\theta \quad . \tag{2-54}$$

Substituting the value of h^*, $\frac{d(\bar{u}h)}{dx} = q_o$, $q = q_o X$, $h = q_o X/\bar{u}$ and $\frac{dh}{dx} = \frac{d(q_o X/\bar{u})}{dx}$ into Eq. (2-54) will yield the final form of τ_o as follows:

$$\tau_o = \frac{\gamma q}{\bar{u}} \sin\theta + \rho r V_t \sin\theta - \frac{\gamma q}{\bar{u}^2} \cos^2\theta - \frac{\rho r V_t \cos^2\theta}{\bar{u}} + \frac{\gamma X q}{\bar{u}^3} \frac{d\bar{u}}{dx} \cos\theta + \frac{\rho X r V_t \cos^2\theta}{\bar{u}^2} \frac{d\bar{u}}{dx} - \rho \bar{u} q_o - \rho q \frac{d\bar{u}}{dx} \tag{2-55}$$

Equation (2-55) can be solved by numerical approximation using $\frac{d\bar{u}}{dx}$ obtained from the graph or for short increment with the following relationship:

$$\frac{d\bar{u}}{dx} \cong \frac{\Delta\bar{u}}{\Delta x} \cong \frac{\bar{u}_{i-1} - \bar{u}_i}{x_{i-1} - x_i} \tag{2-56}$$

in which i = the increment or step number.

To solve Eq. (2-55), necessary calculations were made as follows. Experimental values of $\bar{u}$ were plotted versus x and best polynomial curve fit was done with computer analysis of data. From these curves $\frac{\Delta\bar{u}}{\Delta x}$ were obtained for $\Delta x = 1$ foot. Terminal velocity of raindrop, required in Eq. (2-55), was calculated by using the equation derived by Chow and Harbaugh (1965), namely:

$$V_t = (4\gamma\, d_r^3 \,/\, 3\rho_a\, C_d\, d_1^2\,)^{\frac{1}{2}} \quad , \tag{2-57}$$

where

d_r = the mean diameter of raindrop (L) (d_r is obtained from Holland's (1969) publication about CSU rainfall-runoff facility),

ρ_a = the mass density of air (ft^2/L^4) , (assumed 0.0024 $lb/sec^2/ft^4$)

C_d = the drag coefficient of air (0.4 for hemisphere),

d_1 = the diameter of the transformed hemisphere which is geometrically equal to 1.25 d_r (L).

V_t was found as equal to 16.5 feet per second for the present study. The remaining terms needed in Eq. (2-55) are obtained from experimental data. Substituting the values of the terms into Eq. (2-55), τ_o was

calculated for each run at the end of flow, and will be presented in Chapter IV. With this method the values of τ_o included effect of raindrop impact on friction factor, f, and friction slope, S_f, without determining them.

2.3 SOIL EROSION BY WATER

2.3.1 Properties of Erosion

Ellison, who defined soil erosion as "a process of detachment and transportation of soil materials by erosive agents" (1947), is one of the first investigators who studied soil erosion processes quite comprehensively. His ideas, definitions and approaches are still valid, although current analyses are much more mathematical. Ellison suggested dividing the soil erosion process into four processes, detachment of soil by runoff and transport of soil by runoff, and studying them independently. His categorization was applied by Meyer and Monke (1965) and Meyer (1971).

Although water erosion may be divided into rainfall and runoff erosion, the overall erosion usually occurs as a result of the combined effect of raindrop impact (splash) first and subsequent runoff (overland flow). Water erosion may be broken down into three stages, sheet, rill and gully. The first stage, "sheet erosion," was defined by the Soil Conservation Society of America in 1952 as "removal of a fairly uniform layer of soil or material from the land surface by the action of rainfall and runoff." The second stage, the rill or micro channel stage, begins after runoff occurs, because if removal of soil is caused by raindrop splash only, it will be uniform. If this were not the

case, after runoff began, channelization would soon commence and erosion would no longer be uniform. If runoff does not stop during the "rill erosion" stage, the runoff itself would create more micro-channels and would deepen them. The third stage would occur when gullies start to form after concentration and channelization of runoff is increased. The appearance of gullies with their small drainage areas in field would be different from main drainage-way gullies, which develop in non-cultivated areas.

2.3.2 Factors Affecting Erosion

The basic factors affecting soil erosion are climate, topography, soil, vegetation and erosion control measures and conservation practices, the human factor. One of the most common expressions for the five soil erosion factors was given in Baver's Soil Physics, 1965:

$$\text{Erosion} = \emptyset\ (C_1, T, V, S, H)$$

in which

C_1 = the climatic factors,

T = the topographic factors,

V = the vegetative factors,

S = the soil factors, and

H = the human factor.

Baver (1965) also shows these relationships schematically in Table 2-1. Any of these five main factors can assume values which, even taken alone, may create a rainfall erosion problem. Two of the most important influences on erosion are slope and rainfall. The effect of these

factors are more pronounced on bare soil then on a vegetated soil. In the following discussion, each group of factors will be described and explained.

TABLE 2-1. FACTORS AFFECTING SOIL EROSION DUE TO WATER (AFTER BAVER, 1965, p. 431)

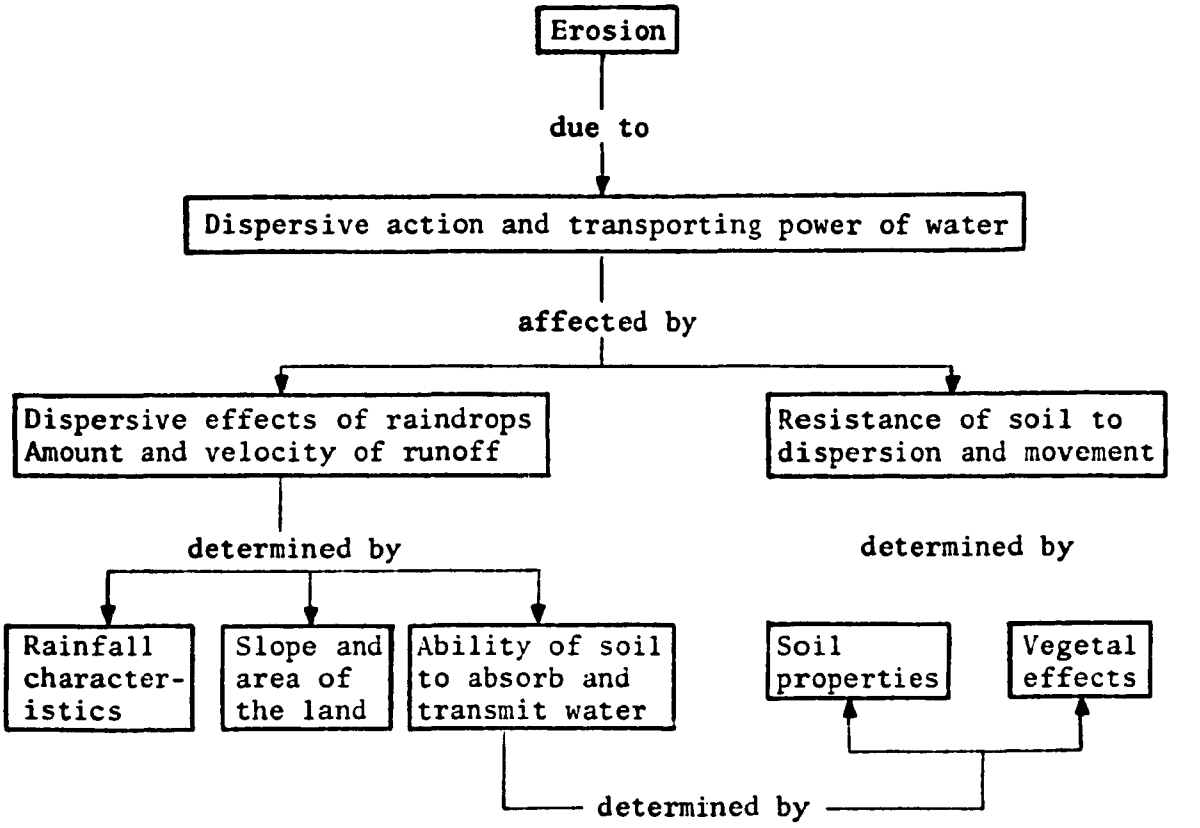

2.3.2.1 Climatic factors

Rainfall, which generates runoff and erosion, is obviously the most important factor among the other major climatic factors of wind, temperature and snow. Because wind erosion is an entirely different topic, it will not be included here. The effect of temperature on erosion and runoff is a result of variability of soil moisture,

compactness and permeability in turns of freezing and thawing, and change of viscosity, which affects suspension.

Wischmeier (1959) found that the rainstorm parameter most highly correlated with soil loss from fallow ground was a product term, kinetic energy of the storm times maximum 30-minute intensity. This product is called "rainfall-erosion index." The rainfall-erosion index is defined as 72 to 97 percent of the variation in individual-storm erosion from tilled continuous fallow ground on each of six widely scattered soils (Smith and Wischmeier, 1962). Rainfall energy is a function of the combination of drop velocities and rainfall amount, so that the maximum 30-minute intensity is an indication of the excess rainfall available for runoff.

2.3.2.2 Topographic factors

Erosion on bare soil becomes a problem wherever the topography becomes even slightly rolling. Conversely, on extremely flat lands, there is no erosion problem. Thus, slope is the main feature of topography which is concerned in erosion study. As a matter of fact, on slopes of less than 10 percent, the amount of erosion approximately doubles as slope increases twofold. As concluded by Zingg (1940), total soil loss varied with the 1.6 power of slope length and the 0.6 power loss per unit area. The uniformity of slope is important in determining and establishing suitable erosion control practices.

Much work has been done under both field and simulated rainfall conditions to evaluate the effect of slope (magnitude and length) on erosion, but little has been done to evaluate the curvature of slope. The effect of degree of slope on soil loss was studied under sprinklers

by Duley and Hays (1932), Neal (1938), Borst and Woodburn (1940) and Zingg (1940). They offered proof that soil loss increased with each unit increase in percent of slope. A silty clay loam gave greater erosion on the flatter slopes than did a sandy soil, while the same loam gave less erosion on steeper slopes than did a sandy soil. Under artificial rainfall, Borst and Woodburn (1940) found soil loss proportional to $S_o^{1.30}$, in which S_o is the percentage of slope. Neal (1938) found soil loss proportional to $S_o^{.7}\, r^{1.2}$, in which r represents intensity of rain in inches per hour.

2.3.2.3 Soil factors

The major soil factors which affect soil erosion and runoff are texture, structure, permeability, compactness and infiltration capacity of soil profile. Erodibility, detachability and transportability of soil determine the rate and amount of soil erosion. On the other hand, under the same hydraulic conditions, under the same climatic, topographic and vegetative factors, different types of soil will have the potential for different erodibility and soil loss.

Soil scientists and conservationists have long been interested in obtaining an index of the erodibility of soils by measuring some physical properties of soil. One of the first attempts was made by Middleton (1930), who measured the several physical properties of the soils from the various experimental stations and made correlation analyses between these properties and the erosion measured in the field. He suggested the "dispersion ratio" and "erosion ratio" as erosion indices to relate erosion to the physical characteristics of soil. The dispersion ratio can be obtained by dividing the amount of silt plus

clay by the total quantity of silt plus clay that was present. The silt plus clay is easily obtained by shaking the soil in pure water, which will cause the soil to be suspended. The erosion ratio is simply equal to dispersion ratio divided by the colloid-moisture equivalent ratio.[1/] Some soils erode more readily than others. The greater the dispersion and erosion ratio of soil, the more easily it can be dispersed and eroded. A colloid-moisture equivalent ratio was used to express the relative permeability of the soil. Water permeability was considered to increase with this ratio. On the assumption that erosion should increase directly with the dispersion ratio and inversely with the colloid-moisture equivalent ratio, the erosion ratio was obtained. Based on these criteria, soils are divided according to erodibility and nonerodibility. If the dispersion ratio is greater than ten and the erosion ratio is greater than fifteen, the soil is erodible; if the dispersion ratio is less than ten and the erosion ratio is less than fifteen, the soil is nonerodible.

2.3.2.4 Vegetative factors: cover and its management

The greatest protection against soil erosion is plant cover. Cover and its management affect both the infiltration rate and the susceptibility of soil to erosion. The use of crop pattern and rotation is the tool for controlling erosion without harming the

---

1/ The colloid-moisture equivalent ratio is obtained as follows: colloid percentage of soil, i.e., particles finer than .001 mm diameter, divided by moisture equivalent, which was defined by Briggs and McLane (1907) as the percentage of water retained by a sample of soil one centimeter deep which has been saturated with water and drained under a centrifugal force of 1000 times gravity for 30 minutes.

productivity of land. The most effective cover is a well-managed, dense sod. Erosion occurs easily on a field of poorly managed and poorly cultivated crops.

Baver (1965) divided the major effects of vegetation on runoff and erosion into five categories: interception of rainfall by the vegetative cover; decrease in the velocity of runoff and the cutting action of water; root effects in increasing granulation and porosity; biological activities associated with vegetative growth and their influence on soil porosity; and the transpiration of water leading to subsequent drying out of the soil.

The most important effects of vegetative cover on erosion are absorption (dissipation) of raindrop impact or kinetic energy and reduction of overland flow velocity and tractive force. Ree (1949) studied the hydraulic characteristics of vegetation for vegetated waterways and divided the effects of vegetation on flow into: resistance to flow, vegetal protection against erosion, and change of velocity distribution. Because vegetation and mulches increase the hydraulic roughness and decrease the effective slope steepness, they reduce the runoff velocity and, as a result, erosion.

2.3.2.5 Human factors: erosion control measures and soil conservation practices

Since human beings disturb the soil, manipulate the vegetation, and change the natural sequence of evolution, all erosion control and conservation practices may be considered human factors. Both the major cause of erosion and the major deterrent to erosion are human beings.

All soil erosion control measures and practices have a *curative* and a *protective* function. Curative measures prevent the erosion

problem; protective measures reduce or regulate the erosion loss after it starts. Curative and protective erosion control measures may be applied by the use of technical structural designs, vegetative deterrents, and legislative or administrative deterrents.

Technical practices are structural in nature, and engineering measures which are designed to reduce runoff and erosion are not usually curative but preventive and regulative. Contour tillage, diversion, waterways, ponds and reservoirs, check dams and gully control structures may be included under technical erosion control practices.

The use of grass-lined waterways is the basic conservation practice commonly utilized by farmers. One of the oldest and best mechanical erosion control practices is terracing. Terraces are constructed to reduce erosion by shortening the length and degree of slope. The mechanical structures are designed for the purpose of grading and gully control, water storage, flood prevention, sediment storage, water level control, drainage and irrigation and streambank protection.

Vegetative practices are curative measures designed to stop runoff and erosion from the very beginning in order to insure the soil stability. Strip cropping, rotation, residue management, stubble mulch farming, grass seeding, tree planting, etc., are considered vegetative erosion control practices.

It should be noted that legislative and administrative erosion control measures are the most effective means of initiating, financing and determining the success of technical and vegetative measures. Zoning, rotational grazing, taxing and fining are included under administrative and legislative practices.

2.3.3 Raindrop Erosion (Splash Process)

The major erosive agents are raindrops and flowing surface water or overland flow. The difference between surface flow erosion and raindrop splash erosion is that the runoff tends to channelize and usually makes rills and gullies, whereas splash erosion tends to remove soil particles from the surface as a uniform sheet layer. Splash erosion has been considered the initial phase of the water erosion process (Ellison, 1944). Soil erosion by splash is a function of drop size, drop velocity and rainfall intensity, expressed by Ellison (1945) as:

$$E = K V_t^{4.33} d_r^{1.07} r^{0.65} \quad , \tag{2-58}$$

in which

E = the relative amount of soil splashed in grams during a 30-minute period,

K = a constant of soil,

V_t = velocity of raindrops in feet per second,

d_r = diameter of raindrops in millimeters, and

r = inches depth of rainfall per hour.

Musgrave (1947) suggested the annual soil loss prediction equation as a first approximation in the following mathematical relation for sheet erosion.

$$E = K S_o^{1.35} L_s^{0.35} r_{30}^{1.75} \quad , \tag{2-59}$$

in which

E = erosion loss in tons per acre,

S_o = slope in percent,

L_s = length of slope in feet, and

r_{30} = the maximum annual 30-minute rainfall in inches per hour.

It is usually impossible to observe shallow surface flow acting alone in detaching thin sheets or layers of soil from the broad surface of a field. The reason that sheet erosion is not easily observed in the field is that the effects of irregularities of the surface, together with the effects of other roughness in the soil's structural properties, cause minor rills (micro channels) to form. Once these rills are formed, they continue deepening and end as gullies. The significant erosion caused by the flowing surface water will occur within these channels. Rolling, lifting, and abrading of soil particles in scour erosion are the three main processes of soil detachment.

The study of rainfall momentum and energy in relation to erosion requires knowledge of the determining factors: raindrop mass, size, size distribution, shape, velocity and direction (Smith and Wischmeier, 1960). Neal and Baver (1937) attempted to measure momentum of rainfall directly by the use of torsion balances, but due to wind shielding and adhering water drops, this research was not successful. Laws and Parsons (1943) first investigated the diameter of drop and size distribution in natural rain with respect to erosion. They measured drop size by the flour method, using a calibration curve. Median drop size, d_{r50}, usually describes the drop size distribution. Median refers to the midpoint of the total volume. Laws and Parson (1943) described the relationship of median drop size to intensity by the equation,

$$d_{r50} = 2.23\ r^{0.182} \quad . \qquad (2\text{-}60)$$

The fall velocity of raindrops was studied by Laws to assist in understanding the action of rain in the eroding of soil (Laws, 1941), using photographic equipment to measure drop velocity. In natural rain, air turbulence can either increase or decrease drop velocity. The magnitude of air turbulence during rainfall and the effects of drop velocity have not been studied. Wind also has an appreciable effect on drop velocity. The kinetic energy of rainfall is important in erosion studies, since erosion is a work process, and much of the energy required to accomplish this work is derived from the falling raindrops.

The raindrop impact-splash process shows high detachment but low transport capacity, while sheet and microchannel flow evidences low detachment capacity and high transport capacity. Little (1940) concluded that the erosivity of flow was a function of turbulence and, therefore, a function of velocity squared per unit of flow depth.

Chow and Harbaugh (1965) designed a rainfall simulator for laboratory study, and they derived theoretical relationships to obtain drop size and terminal velocity. These equations include rainfall drop size:

$$d_r = 2.4\ (\bar{\sigma}\, d_t)^{1/3} \quad (d_r \text{ is expressed in inches}) \quad , \qquad (2\text{-}61)$$

in which

$\bar{\sigma}$ = the surface tension of water in contact with air (F/L) (Average value is 5×10^{-3} lb/ft),

d_t = the inside diameter of the producer tube in inches (L).

$$d_r = 61.0\ (\bar{\sigma}\ d_t)^{1/3} \quad (d_r \text{ is expressed in millimeters}) \quad . \quad (2\text{-}62)$$

Drop terminal velocity in feet per second was given before as Eq. (2-57):

$$V_t = (4\ \gamma\ d_r^{\ 3}/3\ \rho_a\ C_d\ d_1^{\ 2})^{1/2} \quad ,$$

Drop velocity at given distance for a known terminal velocity,

$$V_x = V_t[1 - \exp(-2gX/V_t^{\ 2})]^{1/2} \quad , \quad (2\text{-}63)$$

where V_x = terminal velocity of drop at X distance (L/t).

2.3.4 Overland Flow Erosion

The transportability of a soil particle in the flowing overland flow will depend largely on its size, distribution, density shape, and compactness. The transporting capacity of surface flow will depend on the velocity of surface flow or velocity head, $u^2/2g$; the depth of flow; the capacity of the flow to suspend soil materials, as this factor will limit the soil content of the flow; slope; and roughness (irregularities) of the soil surface.

The mechanics of soil erosion by rainfall and overland flow was studied experimentally by Meyer and Monke (1964). They performed a multiple regression analysis on the data. The resulting equation which best fits runoff erosion was:

$$E = C_{lsd}\ L_s^{\ 1.9}\ S_o^{\ 3.5}\ d_r^{\ 0.5} \quad , \quad (2\text{-}64)$$

in which C_{lsd} = constant for L_s , S_o and d_r .

Meyer and Wischmeier (1969) simulated the process of soil erosion by water in a mathematical soil-erosion model. They assumed that the velocity of flow in small upland rills is approximately proportional to $S_o^{1/3} q^{1/3} / n^{2/3}$, the tractive force is proportional to u^2, and the carrying capacity of flowing water is proportional to u^5. Any change in S_o, q, and n may greatly affect the erosion rates. The resistance of a soil to the erosive forces of rainfall and runoff depends on the properties of the soil, such as particle size, shape, density, cohesiveness, and aggregate strength plus the soil macro-structure (cloddiness) that affects detachability from the soil mass and transportability by runoff.

2.4 SEDIMENT TRANSPORT MODEL OF OVERLAND FLOW

2.4.1 Introduction

The concept of stream erosion and sediment transportation equations may be modified and used in land erosion. Moreover, the mechanics of stream channel erosion and land erosion are complimentary. From the hydraulic standpoint, understanding the mechanism of stream channel erosion is a necessity and is a great aid in understanding land erosion.

Some early sediment transport equations were given by different investigators, such as Du Boys (1879), Schoklitsch (1935), MacDougall (1934), Kalinske (1947), Meyer-Peter and Muller (1948), Einstein (1950), Laursen (1958), Colby (1964), and Bagnold (1966). They generally related the sediment discharge (bedload) to the tractive forces, stream power, slope, flow rate, roughness and particle properties. Any bedload transport equation for alluvial channels using tractive force or stream

power methods may be modified for overland flow and used as a transport equation for land erosion.

Huff and Kruger (1967) adapted Bagnold's equation (1966) for overland flow under rainfall. The transport equation for sheet flow is:

$$q_{si} = e_g \frac{(P_s + P_r - P_c)}{\tan \alpha} \quad \text{(for the immersed weight of material transported),} \quad (2\text{-}65)$$

or

$$Q_s = \left(\frac{\rho_s}{\rho_s - \rho} \right) q_s \quad \text{(for dry mass of material in transport),} \quad (2\text{-}66)$$

in which

Q_s = dry mass of material in transport $(M/L^2\text{-}t)$,

$\tan \alpha$ = the coefficient of solid friction,

ρ_s = density of soil particles (Ft^2/L^4) ,

P_r = stream power due to rainfall $(F/L\text{-}t)$,

P_c = critical stream power to initiate the motion, and

e_g = the efficiency of transfer of stress from liquid to solids.

The value of P_s is given by:

$$P_s = \rho \, g \, S_o \, q \quad , \quad (2\text{-}67)$$

and the power input to the flow from rainfall is:

$$P_r = K_r \, r \, (1 - e^{-0.481(r)^{1/4}})^2 \quad , \quad (2\text{-}68)$$

in which

K_r = a constant, and

r = rainfall intensity in mm per hour.

Smerdon and Beasley (1961) presented a plot of critical tractive force as a function of dispersion ratio; in this case, the value of critical tractive power can be obtained using the relationships between tractive force and streampower. Equation (2-65) may be used with some modifications for land erosion.

In simulation of soil erosion Meyer and Wischmeier (1969) broke the erosion process down into four component sub-processes: soil detachment by rainfall, transport by rainfall, detachment by runoff, and transport by runoff. These were considered separate but interacting phases of the soil erosion process by water. Meyer and Wischmeier used the following mathematical models to evaluate each component subprocesses.

(1) Soil detachment by rainfall, D_r :

$$D_r = S_{Dr} A_i r^2 , \qquad (2\text{-}69)$$

(2) Transport by rainfall, T_r :

$$T_r = S_{Tr} S_o r , \qquad (2\text{-}70)$$

(3) Detachment by runoff, D_F :

$$D_F = S_{DF} A_i q^{2/3} S_o^{2/3} , \qquad (2\text{-}71)$$

(4) Soil transport by runoff, T_F :

$$T_F = S_{TF} q^{5/3} S_o^{5/3} , \qquad (2\text{-}72)$$

in which A_i = the area of the increment, and

S_{Dr} , S_{Tr} , S_{DF} and S_{TF} = the soil coefficients.

2.4.2 Sediment Discharge Models

The following models can be used for sediment discharge resulting from overland flow:

$$q_s = K_n (\tau_o - \tau_c)^n \tag{2-73}$$

and

$$q_s = K_m ((\tau_o - \tau_c) \bar{u})^m \quad , \tag{2-74}$$

in which

q_s = sediment discharge (F/tL) ,

K_n and K_m = constants representing soil and roughness properties, and

n and m = coefficients to be found experimentally.

Equation (2-73), which uses the tractive force concept, is one of the earliest models for sediment transport by stream flow.

Equation (2-74) is similiar to Eq. (2-65) which uses the stream power concept. In Eq. (2-65), stream powers resultant from flow and rainfall are separated. If τ_o is calculated for overland flow generated by rainfall, rainfall effect will be taken into account. It is not necessary, therefore, to calculate separately stream powers resulting from flow and rainfall. In this study, calculated τ_o combines both effects. These two models will be tested with experimental data, and predicted values of sediment discharge will be compared with measured values in Chapter V.

2.5 DIMENSIONAL ANALYSIS

2.5.1 Introduction

Langhaar (1967) defined dimensional analysis as a treatment of the general forms of equations that describe natural phenomena. Dimensional analysis has been used in all fields of engineering, especially in fluid mechanics and hydraulics. Usually natural phenomena are complex, and large number of variables are involved. Dimensional analysis, therefore, reduces and groups variables so that trivial variables can be eliminated or ignored. It can easily identify the significant variables involved in any problem. The relationship between an independent and dependent variable also can be obtained by dimensional analysis. Too, dimensional analysis contributes to analytical, and mathematical analysis of a problem relative to a given general mathematical model. Langhaar (1967) in the preface of his book noted that:

> The application of dimensional analysis to any particular phenomenon is based on the assumption that certain variables, which are named, are the independent variables of the problem, and that all variables, other than these and the dependent variable, are redundant or irrelevant. This initial step - the naming of the variables - often requires a philosophic insight into natural phenomena...The second step in the dimensional analysis of a problem is the formation of a complete set of dimensionless products of variables.

If meaningful dimensionless groups are not obtained, the dividing or multiplying of dimensionless groups together elicits meaningful groups. These dimensionless groups can be related to each other linearly or non-linearly. The exponents of a dimensionless product are a solution of a certain set of homogeneous linear algebraic equations.

2.5.2 Purpose of Dimensional Analysis

The purpose of dimensional analysis is to deduce information about a phenomenon from the single premise, which is that the phenomenon can be described by a dimensionally correct equation among certain variables. A reduction of the number of variables in a problem greatly amplifies the information that is obtained from a few experiments (Langhaar, 1967). The main purpose of dimensional analysis in this study is to reduce the large number of variables involved in erosion and sediment problems to a few dimensionless groups and to obtain a relation between erosion and the independent variables.

2.5.3 Dimensionless Form of Equations

2.5.3.1 Sediment discharge

The sediment discharge by means of overland flow is a function of the hydraulic properties of flow, the physical properties of soil and surface characteristics. In this analysis, sediment transport as a result of erosion under simulated rainfall is assumed to be related to the following variables.

$$q_s = (C_s, u, i, r, q_o, d, d_{50}, X, S_o, d_b, \mu, \nu, g, \rho, \rho_s, \Delta\gamma, \overline{\sigma}) \quad (2\text{-}75)$$

in which

d_b = the bulk density of soil (F/L^3) ,

$\Delta\gamma$ = the difference between sediment and water specific weight (F/L^3) , and

d_{50} = the median diameter of transported sediment (L).

Elimination of some of the variables is possible since some are closely related to others, one may explain another, and some of them have relatively less effect on sediment discharge. For example, $\mu = \rho \nu$; therefore μ is unnecessary. In the equation, $\gamma = \rho g$, and since, Eq. (2-75) has ρ_s and ρ , $\Delta\gamma$ can be eliminated. Bulk density, d_b , is related to porosity in percent by $P = (1 - d_b/dp)\ 100$, in which d_p represents particle density equal to 2.65 gm/cm^3. The advantage of retaining porosity is its dimensionlessness.

Nordin and Richardson (1971) defined sediment concentration as the ratio by weight or volume of the sediment discharge to the total discharge of the water-sediment mixture. Therefore, if u and d are used in Eq. (2-71), C_s will be eliminated because the dimensionless form of sediment discharge will be sediment concentration. All the independent variables related to sediment discharge, consequently, will have the same correlation as sediment concentration.

After eliminating the variables which are dependent, Eq. (2-75) reduces to:

$$q_s = \emptyset\ (u,\ q_o,\ d,\ d_{50},\ X,\ \nu,\ g,\ \rho,\ \rho_s,\ S_o,\ P)\ , \qquad (2\text{-}76)$$

in which P = porosity of soil in percent.

Dimensionless groups of variables are dependent on the selection of repeated variables. By changing repetitious variables each time, different groupings can be obtained. Selection of these repeated variables will be based on representation of flow, geometry, and sediment characteristics in consideration of the physical phenomenon

of sediment transport. In the following analysis, different sets of variables will be selected as repeated variables and the results of the dimensionless form of equations will be shown.

2.5.3.1.1 ν , ρ , d_{50} as repeated variables

When ν , ρ and d_{50} are selected as repeating variables, Eq. (2-76) will be expressed as,

$$\frac{q_s d_{50}^3}{\rho \nu^3} = \phi\left(\frac{ud_{50}}{\nu}, \frac{q_o d_{50}}{\nu}, \frac{d}{d_{50}}, \frac{X}{d_{50}}, \frac{gd_{50}^3}{\nu^2}, \frac{\rho_s}{\rho}, S_o, P\right). \quad (2\text{-}77)$$

If this equation is expressed in terms of known, common dimensionless numbers, and meaningless groups are eliminated, then Eq. (2-77) reduces to:

$$q_s^* = \phi\left(Re_{d_{50}}, Re_{q_o}, \frac{d}{d_{50}}, S_o, P\right), \quad (2\text{-}78)$$

in which

q_s^* = a dimensionless form of sediment discharge,

$Re_{d_{50}}$ = the particle Reynolds number,

Re_{q_o} = rainfall-particle Reynolds number, and

d/d_{50} = roughness properties.

2.5.3.1.2 ν , ρ , d as repeated variables

If ν , ρ , and d are repeated and some of the variables are eliminated and rearranged, the following equation is obtained:

$$q_s^* = \phi\left(Re, Re_{q_o}, \text{roughness}, S_o, P\right), \quad (2\text{-}79)$$

in which Re is the Reynolds number most common in hydraulics.

2.5.3.1.3 ν , ρ , X as repeated variables

When ν , ρ and X are repeated, a similar relationship will be obtained as in the previous equations; however, the Reynolds number will assume a different form:

$$q_s^* = \emptyset \left(\frac{uX}{\nu} , \frac{q_o X}{\nu} , \frac{d}{X} , \frac{d_{50}}{X} , \frac{gX^3}{\nu^2} , \frac{\rho_s}{\rho} , S_o, P \right) \quad . \qquad (2\text{-}80)$$

After eliminating unimportant variables and rearranging terms,

$$q_s^* = \left(Re_X, Re_{q_o}, \text{roughness}, S_o, P \right) \quad , \qquad (2\text{-}81)$$

in which Re_X is the Reynolds number in terms of distance.

2.5.3.1.4 ν , ρ , u as repeated variables

Repeating ν , ρ , and u will give the dimensionless relation,

$$q_s^* = \emptyset \left(\frac{q_o}{u} , \frac{ud}{\nu} , \frac{ud_{50}}{\nu} , \frac{uX}{\nu} , \frac{g\nu}{u^3} , \frac{\rho_s}{\rho} , S_o, P \right) \quad . \qquad (2\text{-}82)$$

Rearranging and eliminating insignificant groups from this equation gives:

$$q_s^* = \emptyset \left(Re, Re_{d_{50}}, Re_X, \frac{q_o}{u} , S_o, P \right) \quad . \qquad (2\text{-}83)$$

Three different forms of the Reynolds number are obtained in Eq. (2-83).

2.5.3.1.5 u , d , ρ as repeated variables

Finally, if u , d , and ρ are used as repeated variables, Eq. (2-75) will take the form of the dimensionless relation,

$$\frac{q_s}{\rho u^3} = \emptyset \left(\frac{q_o}{u} , \frac{d_{50}}{d} , \frac{X}{d} , S_o, P, \frac{ud}{\nu} , \frac{u}{\sqrt{dg}} , \frac{\rho_s}{\rho} \right) \; ; \qquad (2\text{-}84)$$

that is,

$$q_s^* = \emptyset \text{ (Re, Fr, } S_o\text{, P, roughness)} \quad . \tag{2-85}$$

The appearance of the Froude number, Fr , in the equation means that the dimensionless groups can be multiplied or divided by one another to obtain new dimensionless groupings. For instance, if the first group of the dimensionless form of sediment discharge is multiplied by the square of the Froude number, the sediment concentration will be:

$$\frac{q_s}{\rho u^3} \times \frac{u^2}{dg} = \frac{q_s}{gud} = C_s \quad . \tag{2-86}$$

Rewriting the above equations gives

$$\frac{q_s}{\rho gud} = \emptyset \left(\frac{ud}{\nu} , \frac{u}{\sqrt{ug}} , \frac{q_o}{u} , \frac{d_{50}}{d} , \frac{X}{d} , S_o, P, \frac{\rho_s}{\rho} \right) \quad . \tag{2-87}$$

This means that

$$C_s = \emptyset \text{ (Re, Fr, } S_o\text{, P, roughness)} \quad . \tag{2-88}$$

In Eq. (2-88), sediment concentration becomes a function of the Reynolds number, Fround number, slope, porosity and roughness of surface.

It will be easily seen from the dimensionless relationships of sediment discharge, as in Eqs. (2-78, 2-79, 2-83, and 2-85), that most of the dimensionless groups are repeated in a slightly different form, especially the Reynolds number. Equation (2-88) can be considered as the final form of a dimensional analysis.

In conclusion, if further simplification and elimination of variables is accomplished, a more compact form of the dimensionless

relation of sediment discharge to sediment concentration will be obtained. The Froude number, Fr , can be eliminated from Eq. (2-88) because of the constant effect of gravity. After eliminating groups and rearranging parameters, Eq. (2-88) assumes the form,

$$C_s = \phi \left(Re,\ S_o,\ P,\ \frac{d_{50}}{d} \right) \quad . \tag{2-89}$$

Sediment discharge and concentration have the same physical significance. In relating the variables or parameters, the Reynolds number, Re , slope and roughness are the most important parameters affecting sediment discharge and concentration.

2.5.3.2 Local velocity

The local velocity of overland flow is a function of rainfall, slope, gravity and surface characteristics. The following variables were assumed to be a function of velocity,

$$u = \phi\ (q_o,\ d,\ d_{50},\ X,\ S_o,\ \nu,\ g,\ P) \quad , \tag{2-90}$$

in which ν , g , and d have been designated repeated variables. For dimensional analysis, Eq. (2-90) can be represented in the dimensionless relationship,

$$\frac{u}{\sqrt{dg}} = \phi \left(\frac{q_o d}{\nu} ,\ \frac{d_{50}}{d} ,\ \frac{X}{d} ,\ S_o,\ P \right) \quad . \tag{2-91}$$

If the dimensionless groups are replaced with known common numbers, Eq. (2-91) is

$$Fr = \phi \left(Re,\ S_o,\ P,\ \frac{d_{50}}{d} ,\ \frac{X}{d} \right) \quad . \tag{2-92}$$

The dimensionless form of velocity gives a relationship similar to the relation given by the sediment discharge or sediment concentration. The same parameters, such as the Reynolds number, slope and roughness, appeared in Eq. (2-89) and Eq. (2-92). If Eq. (2-92) is rearranged, more meaningful results can be obtained. For example, the first group Froude number, Fr , can be divided by slope, S_o , and the result will be, $\frac{u}{\sqrt{dgS_o}}$. This is simply $\frac{u}{\sqrt{\tau_o/\rho}} = \frac{u}{u_*}$, in which u is velocity and u_* is shear velocity. Eliminating X/d and rearranging Eq. (2-92), the relation, $u/u_* = \emptyset$ (Re, S_o, P, d_{50}/d) can be found. By squaring the first term,

$$\frac{u^2}{(\tau_o/\rho)} = \emptyset \quad \text{Re, } S_o, \text{ P, } \frac{d_{50}}{d} \tag{2-93}$$

in which P and d_{50}/d represent porosity and roughness of surface.

Using the $\tau_o = f \rho u^2/8$ relation (ABS p. 336), in which f is the Darcy-Weisbach resistance coefficient, f will be:

$$f = \frac{8(\tau_o/\rho)}{u^2}, \quad \text{or} \quad \frac{8}{f} = \frac{u^2}{(\tau_o/\rho)} .$$

Substituting 8/f for $u^2/(\tau_o/\rho)$ in Eq. (2-93), the result will be:

$\frac{8}{f} = \emptyset$ (Re, S_o, roughness), or the general dimensionless form of the friction factor can be written as:

$$\frac{1}{f} = 8\ \emptyset \text{ (Re, } S_o, \text{ roughness)}. \tag{2-94}$$

Equation (2-94) is the general form for the reciprocal of f ; the Darcy-Weisbach friction factors, as a function of the Reynolds number; the slope, and the surface roughness characteristics.

CHAPTER III

EQUIPMENT AND EXPERIMENTAL PROCEDURES

In this chapter, the experimental set-up and procedures are explained. Equipment and material used in research are described briefly. Procedure of data collection and measurement of variables are discussed.

3.1 GENERAL DESCRIPTION AND PROCEDURES

The experiment for this study was conducted at the rainfall-runoff facilities of the model watershed adjacent to the Engineering Research Center (ERC) of Colorado State University (CSU). (Detailed information about this facility can be obtained from Holland, 1969.) The one-acre CSU model watershed is located southeast of the Engineering Research Center (ERC), Foothills Campus.

A 4' x 5' x 16' flume filled with disturbed sandy soil with a given surface slope was exposed to simulated rainfall. Rainfall was produced by using commercial sprinklers on 10' risers spaced on a 10' x 17.5' rectangular grid.

A general view of the rainfall-runoff facility, the location of the experiment flume and other elements of the set-up are shown in Fig. 3-1. The layout of the experiment is shown in Fig. 3-2.

Runoff was recorded continuously in a collection tank with a stage-recorder. The discharge was sampled every five to ten minutes during a run for sediment concentration and sediment discharge. No special equipment was used to sample discharge. Bottles were simply held by hand under the outflow, and the entire runoff was sampled.

Fig. 3-1. A general view of the rainfall-runoff facility of CSU.

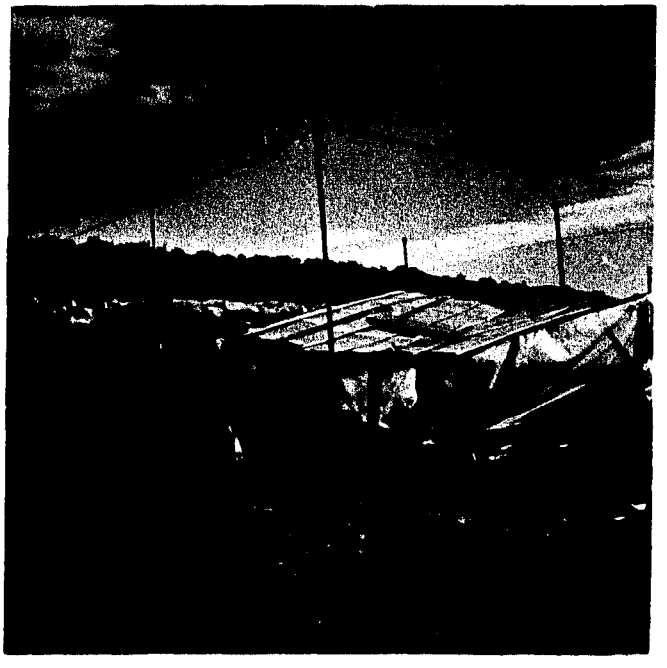

Fig. 3-2. The layout of the experiment.

After drying sediment discharge samples, weight of sediment was divided by weight of evaporated water and the ratio was multiplied by one million, so that sediment concentration was obtained in parts per million. Sediment concentrations were averaged for each run.

The average surface velocity was measured with respect to distance by means of a dye injection. Before each run, bulk density soil samples were taken from the surface. Water temperature was measured for each run. The depth of flow with respect to overland distance was measured using a point gage mounted on a movable carriage atop the flume. After each run, depth, surface area and volume of rills were measured.

The major controlled variables were intensity of rainfall and slope of soil surface. Intensity was controlled automatically using the facility's control valves for desired intensities. Before each run, the surface was leveled, smoothed and soil compactness brought back to its original state. Desired slopes of 5.7, 10, 15, 20, 30 and 40 percent were obtained by using level-gage, shovel and point-gage attached to a carriage. Infiltration and erodibility of surface were kept constant at all times. Four different rainfall intensities were used with each slope. Six slopes were selected, giving a total of 24 runs with a bare soil. In addition four runs were made with the vegetated surface.

3.2 EQUIPMENT AND MATERIALS AND THEIR USAGE

All materials and equipment used for this experiment are listed and their properties are given below. Their relationship to this study will be explained briefly.

3.2.1 Flume

The 4 foot high, 5 foot wide and 15 foot long plywood flume was constructed and installed in the rainfall-runoff facility between two rows of rainfall risers. The flume was centered along the rows in such a way that it would get uniform rainfall from the risers on both sides. The flume had an outlet four feet wide on the west side, discharging into a collection tank with a wooden channel inclining toward the west end.

3.2.2 Soil

The flume was filled with sandy soil which was compacted. The texture of the soil was about 90 percent sand and 10 percent silt and clay. The soil sample had a non-uniform size distribution with d_{50} = .35 millimeter, and with:

$$\sigma = \frac{1}{2}\left(\frac{d_{84}}{d_{50}} + \frac{d_{50}}{d_{16}}\right) = \frac{1}{2}\left(\frac{1.0^{mm}}{.35^{m}} + \frac{.35^{m}}{.10^{m}}\right) = 3.2 \qquad (3\text{-}1)$$

in which

d_{16} = the diameter of the sediment recorded for 16 percent of the samples having a diameter finer than this size,

d_{50} = the median diameter of the sediment recorded for 50 percent of the samples having a diameter finer than this size,

d_{84} = the diameter of the sediment recorded for 84 percent of the samples having a diameter finer than this size, and

σ = the gradation or size distribution index in which one and less represents uniform soil; if gradation is greater than one, soil is nonuniform.

Before each run, bulk density samples were taken for compactness indication and porosity calculation.

3.2.3 Carriage and Point-Gage

A four-wheeled carriage was installed at the top of the flume. The carriage was leveled horizontally and was able to move up and down. A point-gage capable of reading to the nearest tenth of a foot with vernier was attached to the carriage vertically and could be moved horizontally on the main carriage. The main purpose of the carriage and point-gage were to measure depth of overland flow with respect to time and distance.

3.2.4 Collecting Tank

To collect and store the total discharges, a tank six feet in diameter and three feet high was installed at the end of the box. The tank was calibrated for depth versus volume of water.

3.2.5 Stage Recorder

A floating-type stage recorder was attached to record water level continuously with respect to time. An eight-hour chart, having a mechanical clock drive, with a scale of five inches per foot and one division per five minutes, was used.

3.2.6 Rainfall Simulator and Control Valves

Rainfall was simulated by a sprinkler riser shown in Fig. 3-3. The ten foot high risers were placed ten feet apart. The sprinkler head was mounted on top of the riser. A seven foot section of 3/4-inch steel pipe joined the sprinkler to the tire pressure tap. Each nozzle was fitted with a control valve, and a series of valves was connected

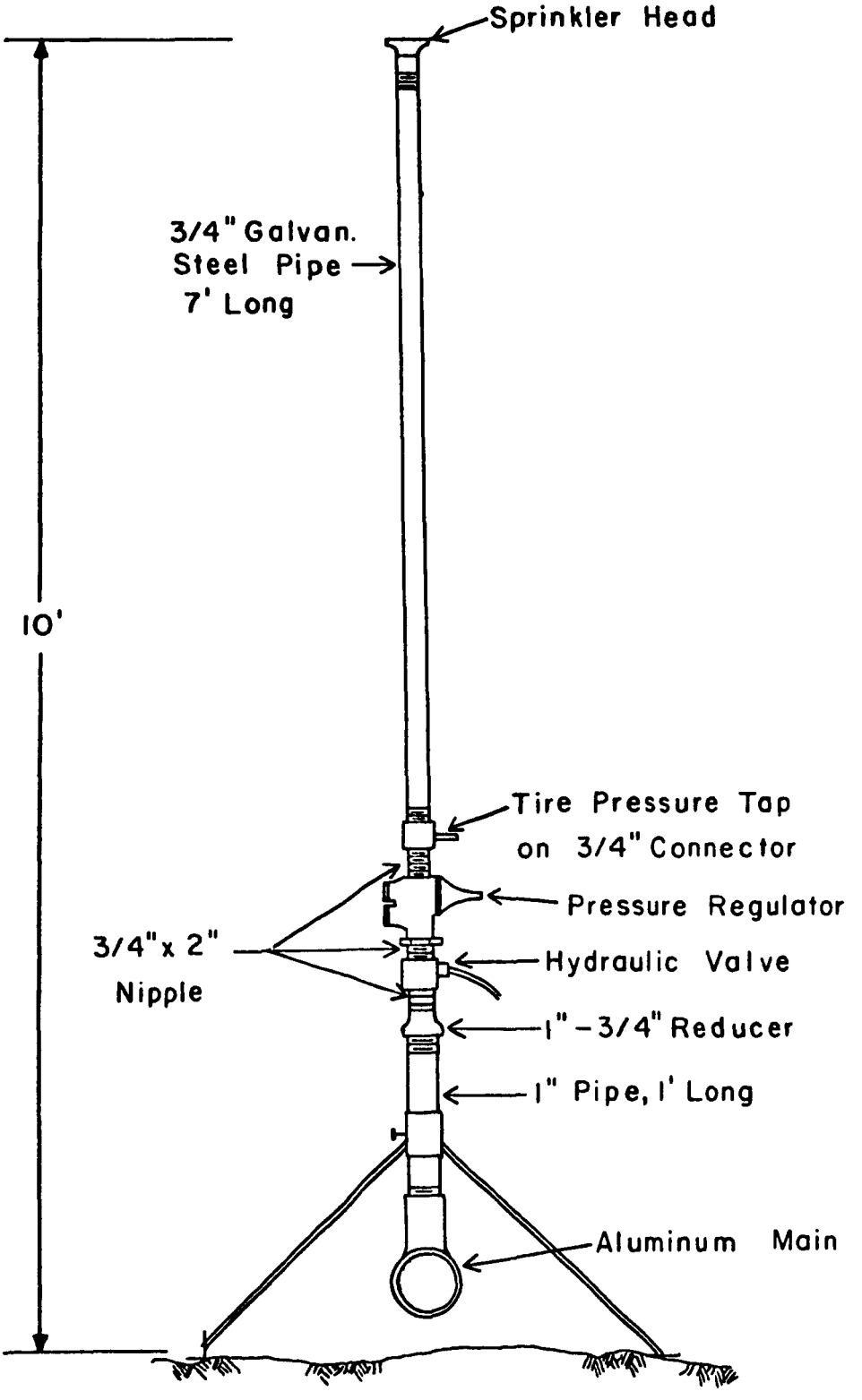

Fig. 3-3. Schematic of sprinkler riser for grid system (after Holland, 1969).

to one pressure manifold to provide simultaneous operation of a set of sprinklers (Holland, 1969). Figure 3-3 shows the elements of the sprinkler riser.

Four independent control valves were fixed to manipulate the pressure system of the sprinkler riser on the upstream part of the flume so that rainfall production would operate independently of the main control center. Using specific valves, desired intensities of rainfall were obtained: 1.25, 2.25, 3.65 and 4.60 inches per hour. These separate pressure-controlling valves enabled the experiment to operate independently.

3.3 MEASUREMENTS

All measurements explained here were made when flow reached steady state, which means no change with respect to time. Before every run, soil was saturated by water so that infiltration was constant.

3.3.1 Runoff Measurement

Total runoff was recorded continuously by the recorder attached to the collector tank. Runoff passing overland as a result of rainfall excess was discharged toward the collector tank through the outlet and channel. Chart recordings were converted into volume per time (cfs) by using the calibration curves. Records showed that discharge was constant, i.e., discharge inreased by distance linearly. To calculate unit discharge at any X distance, the relation

$$q_x = q_o X \tag{3-2}$$

was used, in which

q_x = unit discharge at X distance in cfs/ft of width,

q_o = rainfall excess in ft/sec, and

X = the distance from the beginning of flow in ft.

3.3.2 Depth Measurement

A three-foot point-gage for measuring depth of flow at different sections over the land surface during rainfall was intended for usage; however, point-gage measurements were not successful or reliable due to rainfall impact depressions and to the movable bed.

3.3.3 Surface-Velocity Measurement

Overland flow velocity was measured by dye injection into the surface flow both for the left and right halves of the flume. A liquid dye (Rhodomine WT) and food color were injected over the ground surface at the upper end of the flume. As the dyed water started to flow, one observer watched the dye trace, while another kept a stop watch and note pad. When the dye front passed each successive four-foot down-slope distance, the first observer signaled the second observer, who recorded the time. Increments of time provided the average velocity over each four-foot reach of slope. As the dye trace faded, it was reinforced with a new slug of dye. The leading edge of the dye trace was used in timing its movement. These measurements were repeated every 10 to 15 minutes, three to four times during every one-hour run. All values were averaged to obtain average point velocity at every four foot station along the 16' overland flow for each run. These values were assumed as mean velocities at that point.

3.3.4 Sieve Analysis

All oven-dried sediment samples were analyzed for size distribution by sieve analysis. Samples of each run were separated into two to five time groups and sieved eight times to separate the sediment sample into nine diameter groups. The following diameters of sieves were used in the sieve analysis, 2000, 1000, 701, 500, 354, 250, 125 and 53 microns. The percentage by weight of each diameter was calculated. The percentage of sediment retained by the given diameter sieve revealed that much sediment was coarser than the diameter and the remaining percentage of sediment finer than this diameter group.

3.3.5 Bulk Density

Bulk density soil samples were dried in the oven and weighed. Bulk volume of samples was determined from the sampling cup. The weight of the sample was divided by bulk volume, and bulk density was obtained. Porosity of soil can be found from bulk density relative to the equation:

$$\text{Bulk density, } d_b \text{ , } = \frac{\text{weight of oven-dried soil}}{\text{undisturbed (bulk) volume of soil}} \text{ ,}$$

and

$$\text{Porosity (\%)} = \left(1 - \frac{d_b}{d_p}\right) \times 100, \qquad (3\text{-}3)$$

in which

d_b = the bulk density (F/L^3), and

d_p = the particle density (F/L^3).

Porosity and bulk density are compactness indicators of soil surface.

Besides determining porosity and bulk density temperature of flow, water was measured for each run in order to obtain viscosity. For every run, rill depth and length were measured, and the number of rills were counted. Pictures were also taken before, during and after each run.

CHAPTER IV

PRESENTATION AND ANALYSIS OF DATA

As discussed in the previous chapter, data collected for each experiment (run) included slope, rainfall intensity, sediment discharge samples, flow discharge records, surface flow velocity, rill geometry and water temperature. A run is defined as the experiment conducted with fixed slope and rainfall intensity. From these experimental data, the following secondary data were calculated: sediment concentration, sediment discharge, water discharge, infiltration, rainfall excess, bulk density, mean local velocity of flow, mean depth of flow, sediment size distribution, friction factor, friction slope, tractive force, critical tractive force, stream power, Reynolds number, Froude number, rill mean depth, rill surface area and rill volume.

Data were reduced and summarized for each run. From these data simple plots on Cartesian coordinates were made. The results of all experimental data collection, calculation, tabulation and plotting are summarized in the form of tables and figures in this chapter. Moreover, statistical analyses of the data using the computer are explained, and results are shown with brief discussion.

4.1 DATA REDUCTION AND TABULATION

4.1.1 Sediment Concentration

Sediment concentrations of samples that were collected every five to ten minutes during each run are given in Table 4-1. The average concentration for each run is given in Table 4-2.

TABLE 4-1. INSTANTANEOUS SEDIMENT CONCENTRATION, C_i, FOR GIVEN SLOPE AND INTENSITY OF RAIN AT GIVEN TIME AND THE END OF FLOW

Rainfall Intensity	Slope 5.7%		10%		15%		20%		30%		40%	
	Time (minute)	ppm (C_s)	Time	ppm (C_s)	Time	ppm (C_s)	Time	ppm (C_s)	Time	ppm (C_s)	Time	ppm (C_s)
1.25 inch per hour	5	5840	2	11870	5	25295	3	25375	5	33169	5	36210
	10	6025	5	19137	10	24065	15	28306	10	38752	15	47405
	17	6119	10	12088	22	24079	22	29273	15	35268	20	42995
	24	5150	22	13517	31	25219	30	28356	20	37288	25	49613
	30	5000	31	14499	18	26888	37	28077	30	38563	30	42328
	40	5210	48	14970	60	25119	45	29136	40	37426	35	42375
	50	5125	60	15300			53	30895	50	40676	40	42764
	60	5018					60	28454	60	48655	50	45494
											60	42159
2.25 inch per hour	3	6000	3	23957	1	50972	2	88651	1	97153	1	134116
	12	6220	5	30259	10	51119	5	106800	2	126927	3	167507
	25	6830	15	32381	20	55523	10	104384	5	135994	5	157669
	35	7017	25	33852	30	57600	17	106164	10	202485	10	194965
	48	6623	38	33132	40	55021	25	116938	15	198095	15	206622
	60	6807	48	34253	50	60359	32	118252	20	206266	20	226616
			60	36191	60	66332	40	114127	25	191298	25	239299
							45	100217	30	202177	30	245598
							50	97086	35	18 8253	35	242672
							55	99577	40	186375	40	230562
							60	90607	45	169631	45	223164
									60	168272	60	222230
3.65 inch per hour	2	8150	1	35862	2	61422	2	162472	1	191585	1	301335
	5	7757	12	43942	5	97612	5	167874	3	247223	2	309511
	12	8098	24	43386	7	90252	10	178098	6	244670	5	314449
	24	8333	36	43251	15	77000	15	169071	11	208079	8	326792
	36	7949	48	45217	23	77150	20	150010	15	204913	12	334913
	48	7847	60	48158	30	77273	25	149112	19	226705	15	326795
	60	8242			37	80526	30	140350	23	216512	20	311586
					45	80228	40	139216	27	218890	25	317103
					52	79218	50	138016	30	213970	30	307475
					60	75253	60	138217	40	213867	40	305912
									50	213574	50	304118
									60	213214	60	305000
4.60 inch per hour	1	12826	1	53353	1	112783	1	217804	1	243286	1	311831
	12	14690	10	50353	3	109328	4	219790	3	290012	2	343521
	24	14315	20	52883	5	110579	8	211510	5	287342	3	368421
	36	14416	30	54444	10	115858	12	236201	7	280649	5	374000
	48	14818	40	53016	15	110726	17	198516	10	264346	8	387975
	60	15000	50	52238	20	109058	22	194961	15	259592	10	348421
			60	53866	25	106299	27	190272	20	245116	15	355395
					30	109590	30	190098	25	240386	20	344557
					35	108422	40	189217	30	238516	25	354565
					40	105567	50	191000	40	238000	30	369807
					45	107670	60	190516	50	238124	40	358716
					50	109000			60	237980	50	354896
					55	107700					60	354218
					60	107712						

TABLE 4-2. AVERAGED SEDIMENT CONCENTRATION, C_s , WATER DISCHARGE AND SEDIMENT DISCHARGE AND RAINFALL EXCESS FOR GIVEN SLOPE AND INTENSITY OF RAIN AT THE END OF OVERLAND FLOW

Run No.	Slope (%)	Intensity of rain (in/hr)	C_s (ppm)	q (cfs/ft of width)	q_s (lb/sec/ft of width)	q_o (ft/sec)
I	5.7	1.25	5436	.000279	.000096	.0000174375
II	5.7	2.25	6583	.0007171	.00030	.0000448187
III	5.7	3.65	8054	.001274	.00646	.000079625
IV	5.7	4.60	14344	.0016295	.001482	.0001018437
V	10.0	1.25	14483	.000316	.000294	.00001975
VI	10.0	2.25	32004	.000727	.001508	.0000454375
VII	10.0	3.65	43300	.001289	.00372	.0000805625
VIII	10.0	4.60	52279	.0016556	.00588	.000103475
IX	15.0	1.25	24434	.000332	.00548	.00002075
X	15.0	2.25	57418	.0007398	.002974	.0000462375
XI	15.0	3.65	79895	.0013023	.007138	.0000813938
XII	15.0	4.60	109234	.001683	.01288	.0001051875
XIII	20.0	1.25	28493	.000349	.000644	.0000218125
XIV	20.0	2.25	103891	.000741	.005686	.0000463125
XV	20.0	3.65	154167	.001306	.014904	.000081625
XVI	20.0	4.60	202717	.001696	.02666	.0001060
XVII	30.0	1.25	37975	.0003588	.000922	.000022425
XVIII	30.0	2.25	172744	.000745	.01015	.0000465625
XIX	30.0	3.65	217769	.001329	.022648	.0000830625
XX	30.0	4.60	255279	.001700	.03752	.00010625
XXI	40.0	1.25	44149	.0003659	.00134	.0000228687
XXII	40.0	2.25	207585	.000748	.013096	.00004675
XXIII	40.0	3.65	313749	.001335	.03700	.0000834575
XXIV	40.0	4.60	355885	.001702	.06508	.00010637

4.1.2 Water Discharge and Rainfall Excess

Total discharge was recorded as the stage of flow versus time. It was then converted into volume versus time by using the calibration curves prepared before each run. Water discharge from the sediment discharge was separated. Because sediment concentration was sampled, sediment discharge was easily differentiated from water discharge. Sediment discharge and water discharge were calculated and are tabulated for each run (Table 4-2). Water discharge data were constant with respect to time. Thus, after a brief initial time the flow and erosion rates were steady, but spatially varied. In other words, because of uniform constant rainfall and runoff, water discharge must change with distance. It was assumed that water discharge increased with distance linearly. Thus, $q = q_o X$ and the rainfall excess becomes $q_o = dq/dx = q/X$. Rainfall excesses, q_o, are tabulated for each run in Table 4-2. The unit discharge at any distance, X, can be calculated by the relation $q_x = q_o X$. Rainfall intensity minus rainfall excess gives the infiltration, and the results are summarized in Table 4-3. Because intensity of rain and rainfall excess are constant, infiltration was constant for each run. As shown in Table 4-3, water discharge (runoff) was calculated for given distances, i.e., at 3, 6, 12 and 16 feet, as cubic feet per second per foot of width, for given slope and intensity of rainfall.

4.1.3 Sediment Discharge

After calculating sediment discharge from water discharge, the data were converted into several units for each run and tabulated for given slopes and intensities in Table 4-4. Sediment discharge was

TABLE 4-3. INFILTRATION AND WATER DISCHARGE FOR GIVEN SLOPE AND INTENSITIES AT GIVEN DISTANCE

Run No.	Slope (%)	Intensity (ft/sec)	Infiltration, i (ft/sec)	q (cfs/ft) @ 3'	q (cfs/ft) @ 6'	q (cfs/ft) @ 12'	q (cfs/ft) @ 16'
I	5.7	.00002893	.0000114925	.00005230	.00010460	.00020925	.0002790
II	5.7	.0000520833	.0000072646	.000135	.000270	.000540	.0007171
III	5.7	.0000844907	.0000048657	.0002393	.0004785	.000957	.001274
IV	5.7	.0001064815	.0000046378	.000306	.000612	.001224	.0016295
V	10.0	.00002893	.00000918	.0000597	.0001194	.0002388	.000316
VI	10.0	.0000520833	.0000066458	.0001365	.000273	.000546	.000727
VII	10.0	.0000844907	.0000039282	.00024169	.0004834	.00096675	.001289
VIII	10.0	.0001064815	.0000030065	.0003104	.00062085	.0012417	.0016556
IX	15.0	.00002893	.00000818	.0000623	.0001246	.000249	.000332
X	15.0	.000052083	.0000058458	.0001387	.00027743	.00055415	.0007398
XI	15.0	.0000844907	.0000030969	.000244	.000488	.000977	.0013023
XII	15.0	.0001064815	.000001294	.00031556	.000631	.00126225	.001683
XIII	20.0	.00002893	.0000071175	.0000654	.0001308	.0002616	.000349
XIV	20.0	.0000520833	.0000057708	.0001389	.00027787	.00055575	.000741
XV	20.0	.0000844907	.0000028657	.00024488	.00048975	.0009795	.001306
XVI	20.0	.0001064815	.000004815	.000318	.000636	.001272	.001696
XVII	30.0	.00002893	.000006505	.0000672	.000134	.0002688	.0003588
XVIII	30.0	.0000520833	.0000055208	.0001398	.0002796	.0005592	.000745
XIX	30.0	.0000844907	.0000014282	.0002492	.0004984	.00099675	.001329
XX	30.0	.0001064815	.0000002315	.00031875	.0006375	.001275	.001700
XXI	40.0	.00002893	.0000060613	.0000686	.000137	.0002744	.0003659
XXII	40.0	.0000520833	.0000053333	.0001403	.0002805	.000561	.000748
XXIII	40.0	.0000844907	.0000010332	.0002503	.0005006	.001001	.001335
XXIV	40.0	.0001064815	.0000001065	.0003191	.000638	.0012765	.001702

TABLE 4-4. SEDIMENT DISCHARGE IN TERMS OF DIFFERENT UNITS

Run No.	q_s (lb/sec/ft of width)	q_s (lb/hr)	q_s (lb/hr/ft of width)	q_s (ton/hr/acre)	Erosion (in/hr)	Erosion (ft/hr)
I	.000096	1.728	.3456	.0435	.0028205	.0002350427
II	.00030	5.400	1.080	.1423	.0092307696	.0007692308
III	.000646	11.628	2.3256	.29163	.018923077	.001576923
IV	.001482	26.676	5.3352	.6615	.042923077	.003576923
V	.000294	5.292	1.0584	.1309	.0084923076	.0007076923
VI	.001508	27.144	5.4288	.6757	.0438461544	.0036538462
VII	.00372	66.960	13.392	1.780	.1153846152	.0096153846
VIII	.00588	105.84	21.168	2.845	.1846153848	.0153846154
IX	.000548	9.864	1.9728	.249	.0161538456	.0013461538
X	.002974	53.53	10.7060	1.316	.0853846152	.0071153846
XI	.007138	128.484	25.6968	3.200	.2076923076	.0173076923
XII	.01288	231.840	46.3680	5.760	.3738461544	.0311538462
XIII	.000644	11.592	2.3184	.292	.018923077	.0015769231
XIV	.005686	102.348	20.4696	2.51	.1629487176	.0135790598
XV	.014904	268.272	53.6544	6.544	.4246153848	.0353846154
XVI	.02666	479.88	95.976	11.810	.7661538456	.0638461538
XVII	.000922	16.596	3.3192	.3983	.0258461544	.0021538462
XVIII	.01015	182.70	36.5400	4.41	.2861538456	.0238461538
XIX	.022648	407.664	81.5328	9.766	.633717949	.052809829
XX	.03752	675.36	135.072	16.175	1.04953846	.0874615395
XXI	.001134	20.412	4.0824	.4766	.030923077	.002576923
XXII	.013096	235.728	47.1456	5.477	.355384615	.0296153846
XXIII	.03700	666.000	133.200	15.650	1.015384615	.0846153846
XXIV	.06508	1171.44	234.288	27.25	1.767948718	.1473290598

was expressed in pounds per second per foot of width, pounds per hour, and tons per acre per day for each run. The data were also converted into inches of surface soil per hour for each run. Sediment discharge and erosion rate may not change linearly with respect to distance because of the nonlinear change of velocity and boundary shear with respect to distance. The sediment discharge data represent total sediment removed uniformly from the 16-foot long experiment flume.

4.1.4 Mean Local Velocity of Overland Flow

Velocities of overland flow were measured by means of dye. When the colored flow passed prescribed stations, the time of travel was recorded. Point velocities for every three-foot station were calculated using this data. As an example, let t_1 represent time of travel from zero to three feet and t_2 represent time of travel from three to six feet. Relating distance to time as follows gives

$$\frac{x_2 - x_1}{t_2 - t_1} = \frac{6 - 3}{t_2 - t_1} = \bar{u}_1 \quad , \qquad (4\text{-}1)$$

in which $\bar{u}_1$ represents the average velocity between three feet to six feet and this is defined as the point velocity at a three-foot distance, as shown in the following sketch. Point velocities at 3, 6, 12 and 16 feet were calculated using this method, and profiles were obtained from this data.

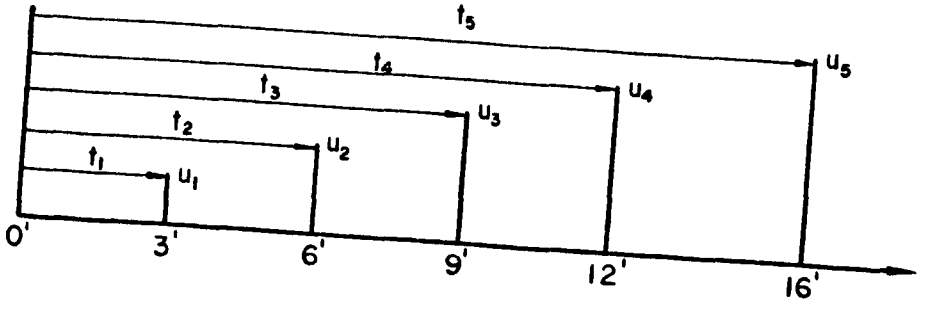

Since depth of flow was very shallow and the dye was thoroughly mixed with water, the measured point velocities were assumed to represent mean overland flow velocities at given distances. The result of velocity calculations are shown in Table 4-5. Mean point velocities for given slopes, intensities and distances were the main source of statistical analysis.

4.1.5 Mean Local Depth of Overland Flow

The measurement of depth was the most difficult problem in the overland flow experiment. There is no exact method yet in practice to measure depth of overland flow, especially with a movable bed, under simulated rainfall. The U. S. Geological Survey uses a point gage or hook gage attached to a carriage to measure depth of overland flow under rainfall in the laboratory and in the field (Emmett, 1970). In this experiment several methods were considered, such as, manometers mounted on the sides of the box to measure piezometric head, a simple ruler placed in the flow, electric capacitance and a chemical staff gage, but ultimately a point gage with carriage, such as those used by Geological Survey, was used. The point gage flow depth measurement had appreciably scattered and was not considered reliable. For this reason, the mean depth of flow with respect to distance was calculated from unit discharge and mean point velocity data. Since unit discharge changed linearly with respect to distance for steady flow, unit discharge at any X distance was calculated by $q_x = q_o X$. Depth of flow at any X distance was calculated by $d_x = q_x/u_x$. The results of these calculations are listed in Table 4-5.

TABLE 4-5. LOCAL MEAN VELOCITY AND DEPTH OF FLOW FOR A GIVEN RUN AT A GIVEN DISTANCE

	Velocities, measured (ft/sec)				Depth, calculated (ft) on the basis of continuity			
Run No.	$\bar{u}$ at 3'	$\bar{u}$ at 6'	$\bar{u}$ at 12'	$\bar{u}$ at 16'	d at 3'	d at 6'	d at 12'	d at 16'
I	.05224	.0768	.1314	.17602	.001001	.001362	.00159	.001585047
II	.08620	.1367	.2172	.29820	.001566	.001975	.002486	.0024047619
III	.12636	.1875	.2842	.41981	.001894	.002552	.003367	.0030347
IV	.14862	.21618	.3476	.50321	.002059	.002831	.003521	.0032382
V	.06849	.099038	.17315	.22004	.000872	.0012056	.001379	.0014361
VI	.1267	.2066	.3203	.37083	.0010772	.0013214	.001705	.00196047
VII	.19006	.30219	.48049	.52252	.001272	.0016	.002012	.00246689
VIII	.2302	.3572	.5781	.61291	.0013484	.001738	.002148	.0027012
IX	.081167	.11732	.2052	.27404	.0007676	.001062	.001213	.0012115
X	.15016	.23875	.37962	.42323	.000924	.001162	.0014597	.00174798
XI	.22524	.35813	.5694	.63473	.001083	.001363	.001716	.002051738
XII	.27155	.42767	.6976	.74872	.001162	.001475	.001810	.00224784
XIII	.09238	.14688	.2335	.32034	.000708	.0008905	.0011203	.00108947
XIV	.1709	.27105	.42988	.47193	.000813	.001025	.0012928	.001570148
XV	.2564	.40665	.64495	.71794	.000955	.001204	.001519	.00181909
XVI	.3067	.49024	.79293	.82652	.001037	.0012973	.00160417	.002051977
XVII	.10772	.17084	.27096	.36484	.000624	.000784	.000992	.00098344
XVIII	.19928	.31606	.50127	.56472	.0007015	.0008846	.0011156	.0013192379
XIX	.2989	.47406	.75185	.84204	.0008337	.001051	.001326	.0015783098
XX	.3562	.57253	.91267	.94373	.0008948	.0011135	.001397	.001801363
XXI	.12012	.1905	.30215	.40398	.000571	.0007192	.000908	.00090574
XXII	.2222	.3524	.5526	.62442	.000631	.000796	.0010152	.0011979
XXIII	.34209	.5386	.8584	.92119	.0007317	.000929	.001166	.0014492
XXIV	.41667	.6625	1.008	1.0523	.0007658	.000963	.0012664	.00161741

4.1.6 Sediment Size Distribution

The results of sieve analyses for the original soil samples used are shown in Table 4-6. In Table 4-7 the d_{84}, d_{50}, d_{16} and σ of the transported sediment, the porosity and bulk density of the soil for each run are given. Both the porosity in percent and bulk density in pounds per cubic feet, were found constant for each run. The range of σ was 2.5-4.5 (Table 4-7). This indicates that the transported sediment was nonuniform in size, having diameters of varying sizes. The σ of the original soil was

$$\sigma = \frac{1}{2}\left(\frac{1.00}{.350} + \frac{.350}{.1}\right) = 3.2,$$ indicating a nonuniform size distribution.

TABLE 4-6. SIEVE ANALYSIS OF ORIGINAL SOIL USED FOR THE EXPERIMENT

Sieve diameter in micron	Net weight of sed.	Percentage of total	Percentage finer
2000	6.9	1.26	98.74
1000	80.0	14.56	84.18
701	56.0	10.19	73.99
500	49.8	9.1	64.89
354	54.3	9.88	55.01
250	62.5	11.38	43.63
125	94.0	17.11	26.52
53	81.3	14.80	11.72
53	64.5	11.74	

TABLE 4-7. THE d_{84} , d_{50} , d_{16} , AND σ OF TRANSPORTED SEDIMENT, d_b AND POROSITY, P , FOR A GIVEN RUN (d_{84} = 1.00, d_{50} = .35 or .325 AND d_{16} = .1 MM OF THE ORIGINAL SAMPLE)

Run No.	d_{84} (mm)	d_{50} (mm)	d_{16} (mm)	d_b Bulk density (lb/ft^3)	P Porosity (%)	σ (Dimensionless)
I	1.30	.49	.080	93.6	43	4.39
II	1.25	.50	.200	93.6	43	2.50
III	1.30	.49	.200	93.6	43	2.56
IV	1.20	.48	.150	93.6	43	2.85
V	1.00	.40	.100	93.6	43	3.25
VI	1.20	.40	.100	93.6	43	3.50
VII	1.20	.40	.130	93.6	43	3.04
VIII	1.25	.40	.130	93.6	43	3.10
IX	.90	.36	.130	93.6	43	2.63
X	1.00	.40	.150	93.6	43	2.58
XI	1.00	.40	.100	93.6	43	3.25
XII	1.00	.30	.100	93.6	43	3.17
XIII	.80	.30	.075	93.6	43	3.33
XIV	.90	.31	.100	93.6	43	3.00
XV	1.00	.30	.100	93.6	43	3.17
XVI	1.10	.25	.100	93.6	43	3.45
XVII	.65	.30	.060	93.6	43	3.39
XVIII	1.00	.30	.060	93.6	43	4.16
XIX	.80	.30	.055	93.6	43	4.06
XX	1.00	.30	.053	93.6	43	4.49
XXI	.65	.27	.040	93.6	43	4.58
XXII	.85	.27	.053	93.6	43	4.12
XXIII	.95	.27	.065	93.6	43	3.84
XXIV	1.00	.27	.053	93.6	43	4.40

As seen in Table 4-6, only about 1-1/2 percent of the sediment had a diameter larger than 2 millimeters and about 12 percent had a diameter finer than .053 millimeters, that is, silt plus clay range. Sieve analysis of transported sediment also showed that approximately 1-2 percent of the sediment had a diameter larger than 2 millimeters and 5-16 percent was finer than .053 millimeters.

4.1.7 Temperature, Viscosity, Reynolds Number and Froude Number

Temperature of flow for each run was measured, and corresponding kinematic viscosities were recorded in Table 4-8. Utilizing the steady-linear relationship of unit discharge and distance, the Reynolds and Froude numbers were calculated at given distance for each run using the following relations,

$$Re = \frac{qx}{\nu} \quad , \tag{4-2}$$

$$Fr = \frac{u}{\sqrt{gd}} \quad . \tag{4-3}$$

Calculated values of the Reynolds number and the Froude number are listed in Table 4-8. The critical Reynolds number, Rc , was calculated for only the last run using the data collected at the end of the flume to determine if flow was laminar or turbulent, using the criteria given in Chapter II ($Rc = C\ (2 \log_{10} \frac{2R}{k} + 1.74)^2$, Equation 2-51). The reason for calculating only the Rc of last run, i.e., maximum Rc , was because it was sufficient for finding the range of Rc . Sample calculation of Rc for last run is,

$$Rc = 24\ (2 \log \frac{.72}{.50} + 1.74)^2 = 24 \times 4.2 = 101.8 \quad .$$

TABLE 4-8. EXPERIMENTALLY CALCULATED REYNOLDS NUMBER, Re , FROUDE NUMBER, Fr , FOR A GIVEN RUN AND RAINFALL EXCESS AT A GIVEN DISTANCE

Run No.	Rainfall excess, q_o , $(ft/sec)^o$	Temp. (F^0)	Kin. Vis. $\nu \times 10^5$ (ft^2/sec)	Re @ 3'	Re @ 6'	Re @ 12'	Re @ 16'	Fr @ 6'	Fr @ 12'	Fr @ 16'
I	.0000174375	57.0	1.282	4.08	8.16	16.32	21.76	.581	.853	.779
II	.0000448187	48.2	1.430	9.44	18.88	37.76	50.15	1.077	1.286	1.071
III	.000079625	48.2	1.430	16.734	33.46	66.92	89.09	1.190	1.453	1.342
IV	.0001018437	50	1.410	21.7	43.40	86.81	115.57	1.401	1.598	1.558
V	.00001975	52.8	1.390	4.295	8.59	17.18	22.73	.735	1.052	1.023
VI	.0000454375	52.8	1.390	9.82	19.64	39.28	52.30	1.184	1.445	1.475
VII	.0000805625	52.8	1.390	17.39	34.78	69.55	92.73	1.568	1.888	1.853
VIII	.000103475	52.8	1.390	22.33	44.665	89.33	119.11	1.769	2.061	2.078
IX	.00002075	57	1.282	4.860	9.719	19.423	25.90	1.060	1.083	1.387
X	.0000462375	48.2	1.430	9.700	19.40	38.75	51.73	1.444	1.668	1.783
XI	.0000813938	55	1.312	18.600	37.195	74.466	99.26	2.160	2.513	2.469
XII	.0001051875	57	1.282	24.615	49.22	98.459	131.28	2.305	2.770	2.782
XIII	.0000218125	61	1.220	5.361	10.72	21.44	28.606	1.378	1.626	1.710
XIV	.0000463125	52.8	1.390	9.99	19.99	39.982	53.31	1.739	2.082	2.098
XV	.000081625	59	1.240	19.75	39.50	79.00	105.32	2.296	2.587	2.966
XVI	.00010600	57	1.282	24.805	49.61	99.22	132.29	2.435	3.098	3.215
XVII	.000022425	61	1.220	5.508	10.98	22.03	29.41	1.624	1.709	2.050
XVIII	.0000465625	57	1.282	10.90	21.81	43.03	58.11	2.370	2.612	2.739
XIX	.0000830625	61	1.220	20.43	40.85	91.70	108.93	3.176	3.545	3.735
XX	.000106250	57	1.282	24.863	49.73	99.454	132.61	3.517	3.916	3.918
XXI	.0000228687	61	1.220	5.65	11.23	22.49	29.94	2.400	3.207	2.365
XXII	.00004675	57	1.282	10.94	21.88	43.76	58.35	3.445	4.424	3.179
XXIII	.000083475	60.8	1.222	20.483	40.966	81.915	109.25	4.217	5.134	4.264
XXIV	.000106375	57	1.282	24.891	49.766	99.571	132.76	5.016	5.447	4.611

Thus, the range of Rc is 0 to 101.8 (Rc = 0; no flow), that is, laminar flow range. Note that the Froude number of flow for almost all points is greater than one; therefore, it may be called supercritical agitated laminar flow.

4.1.8 Friction Factor, f , and Friction Slope, S_f

Utilizing the Darcy-Weisbach definition of friction coefficient,

$$f = 8 \frac{\tau_o}{\rho u^2} \quad , \tag{4-4}$$

and expressing gravity, depth and velocity of flow in terms of friction slope, the equation reduces to:

$$f = \frac{8\rho g d S_f}{\rho u^2} = \frac{8 g d S_f}{u^2} = \frac{8 g q S_f}{u^3} \quad . \tag{4-5}$$

From this equation, S_f can be solved for

$$S_f = f \frac{u^2}{8gd} \quad . \tag{4-6}$$

If f or S_f is known, calculation of each of them on the basis of the other is easy. In the case of uniform flow, if $S_o = S_f$, then f will be:

$$f = \frac{g d S_o}{u^2} \quad , \tag{4-7}$$

and S_o will be:

$$S_o = f \frac{\bar{u}^2}{8gh} \quad . \tag{4-8}$$

To calculate friction slope we may use the relation obtained in Chapter II:

$$S_f = \frac{3\nu}{g} \frac{\bar{u}}{d^2} = \frac{3\nu q}{gd^3} \quad . \tag{4-9}$$

Assuming no rainfall effect, S_f was calculated at various distances for each run using Eq. (4-9) (Table 4-9). The determined values of S_f were then used to calculate the friction factors assuming no rainfall effect. The calculated f is shown in Table 4-9.

The values in Table 4-9 were calculated without consideration of rainfall impact. Equation (2-43), obtained by Li (1972), was used for evaluating S_f which included rainfall impact effect.

In this study it was necessary to change the constant (24). In Table 4-10 the values of f were calculated by using the previously stated equation with a constant of 34 (Yoon and Wenzel, 1971). After friction factor calculation, friction slope, S_f, was calculated (Table 4-10).

4.1.9 Boundary Shear Forces, Critical Tractive Force and Stream Power

Using the following definition of boundary-shear force, τ_o, the tractive force per area of boundary is calculated,

$$\tau_o = \gamma d \, S_f \quad . \tag{4-10}$$

Since γ, unit weight of water, d, depth of flow and S_f, friction slope are known, τ_o can be calculated by Eq. (4-10). In previous

TABLE 4-9. FRICTION FACTOR, f , FRICTION SLOPE, S_f , BOUNDARY SHEAR, τ_o , AND CRITICAL TRACTIVE FORCE, τ_c , FOR A GIVEN RUN AT A GIVEN DISTANCE (WITHOUT RAINFALL EFFECT USING DARCY-WEISBACH FORMULA)

Run No.	S_f @ 3'	S_f @ 6'	S_f @ 12'	S_f @ 16'	f @ 3'	f @ 6'	f @ 12'	f @ 16'	τ_o @ 16'	τ_c @ 0'-16'
I	.062275	.04945	.06206	.08622	6.10	3.86	1.54	.833	.007361	.0061
II	.0468	.046685	.04583	.06981	2.88	1.443	.7195	.3633	.00814	.0062
III	.0469	.03835	.0334	.0652	1.406	.86017	.494	.19005	.00875	.0061
IV	.0460	.0354	.03683	.0641	1.081	.7022	.3378	.14577	.0093	.0060
V	.095476	.07224	.09655	.11386	4.549	3.008	1.1256	.72113	.00874	.0057
VI	.115544	.12525	.1165	.10292	1.988	.9171	.49233	.4190	.01444	.0057
VII	.133498	.13418	.134927	.10326	1.143	.56869	.28286	.27718	.0196	.0057
VIII	.14415	.13464	.14266	.10039	.8587	.45967	.21689	.23115	.02235	.0057
IX	.16446	.12422	.166576	.2234	5.10	3.379	1.2615	.7052	.013214	.0051
X	.23436	.23559	.237387	.18446	2.354	1.171	.58186	.4683	.02503	.0057
XI	.234717	.235655	.23636	.18605	1.2263	.61047	.3040	.2898	.02928	.0057
XII	.240187	.234786	.2543	.18417	.9255	.47365	.21845	.22632	.03247	.0048
XIII	.20945	.21059	.21146	.31003	5.022	2.499	1.244	.6359	.01638	.0047
XIV	.3348	.33409	.3331	.2527	2.25	1.1285	.56586	.5594	.03145	.0048
XV	.32478	.32409	.32292	.2612	1.1526	.57767	.2897	.26867	.03548	.0047
XVI	.340617	.34795	.368034	.2459	.9258	.4533	.21426	.24052	.0423	.0040
XVII	.31433	.31593	.312976	.46507	4.8485	2.422	1.2182	.61417	.02151	.0047
XVIII	.42857	.4275	.42624	.36164	1.8656	.9353	.4689	.4149	.03413	.0047
XIX	.513595	.512584	.51072	.41818	1.1779	.59031	.2961	.2713	.049073	.0047
XX	.5314	.551577	.55857	.36994	.9084	.4375	.21601	.2446	.05662	.0047
XXI	.38988	.38979	.38787	.57732	4.445	2.2258	1.1171	.5627	.0245	.00415
XXII	.74578	.741	.71434	.6081	2.3045	1.1558	.5995	.5282	.052985	.00415
XXIII	.787075	.7687	.77765	.57418	1.1709	.5997	.29634	.3009	.0663	.00415
XXIV	.86852	.8732	.7683	.50584	.8567	.4262	.2421	.27576	.07756	.00415

TABLE 4-10. FRICTION FACTOR, f , FRICTION SLOPE, S_f , AND BOUNDARY SHEAR, τ_o , FOR A GIVEN RUN AT A GIVEN DISTANCE (WITH RAINFALL EFFECT IN THE INDOOR LABORATORY; f IS CALCULATED BY EQUATION 2-43)

Run No.	f @ 3'	f @ 6'	f @ 12'	f @ 16'	S_f @ 3'	S_f @ 6'	S_f @ 12'	S_f @ 16'	τ_o @ 16'
I	15.815	7.9075	3.954	2.965	.1674	.1329	.1668	.225	.022253
II	7.6613	3.8306	1.915	1.442	.141117	.140699	.14107	.20699	.031060
III	4.793	2.397	1.1986	0.9004	.15685	.128187	.11162	.2029	.03842
IV	3.8959	1.9479	.924	0.7315	.16224	.12483	.1231	.22208	.044869
V	15.02	7.512	3.756	2.84	.31366	.23725	.317	.371698	.033309
VI	7.365	3.682	1.84	1.383	.42603	.11617	.42979	.376587	.046069
VII	4.613	2.306	1.153	.865	.50855	.5109	.5136	.37164	.057208
VIII	3.786	1.893	.9464	.7098	.5776	.5395	.57161	.3832	.06459
IX	13.277	6.639	3.322	2.491	.44236	.3340	.44766	.59942	.045315
X	7.456	3.728	1.866	1.398	.7063	.70992	.71516	.556132	.06066
XI	4.313	2.156	1.077	.808	.7843	.78757	.78993	.61592	.078855
XII	3.435	1.718	.8586	.644	.8462	.826995	.89615	.62347	.087451
XIII	12.036	6.019	3.01	2.256	.5632	.56607	.56867	.8249	.056079
XIV	6.459	3.618	1.809	1.356	.67218	1.0067	1.0038	.74667	.0731566
XV	4.061	2.031	1.015	.762	1.08523	1.08288	1.079	.838168	.095142
XVI	3.408	1.704	.852	.639	1.200	1.2255	1.2963	.8258	.105742
XVII	11.715	5.877	2.93	2.194	.34567	.8493	.8418	1.15278	.070742
XVIII	6.635	3.316	1.681	1.245	1.45813	1.45365	1.4698	1.1683	.096178
XIX	3.926	1.964	.875	.736	1.63322	1.59873	1.44804	1.28353	.12641
XX	3.40	1.7	.850	.637	1.8715	1.9427	1.96745	1.22261	.1374275
XXI	11.42	5.75	2.87	2.155	1.12025	1.12632	1.1202	1.50736	.0851933
XXII	6.611	3.305	1.653	1.239	2.0081	2.00163	1.93018	1.56552	.117021
XXIII	3.916	1.958	.979	.734	2.43133	2.3735	2.40169	1.66842	.1508805
XXIV	3.396	1.699	.849	.637	2.98876	3.00603	2.64431	1.692983	.1708666

sections, because two kinds of S_f were calculated, two kinds of τ_o corresponding S_f were calculated, too. Calculated τ_o is shown in Tables 4-9 and 4-10 for a given slope and rainfall intensity for each run. The critical tractive force, τ_c, was calculated using d_{50} and Shields relation, and then listed in Table 4-9 for each run. The third way of calculating τ_o is numerical approximation of the momentum equation by measured data (as explained in Chapter II, p. 25). Equation (2-55) was solved for τ_o. The tractive force τ_o is calculated directly without S_f or f, at the end of flow for each run. These values of τ_o are shown in Table 4-11. The values of τ_o which also include rainfall effects (Table 4-11), are less than τ_o calculated by Li's (1972) equation but more than the τ_o calculated by the Uniform Flow Assumptions. The differences between the values of Table 4-10 and 4-11 come from variance in boundaries, depth of flow and rainfall simulators in the two experiments. After τ_o was calculated effective tractive force $(\tau_o - \tau_c)$, and effective stream powers $(\tau_o - \tau_c)\bar{u}$, were then determined (Table 4-11).

4.1.10 Rill Measurements

At the end of each run, dimensions of rills were measured and also photographed. Assuming trapezoidal shape for the short segment of rills, length, depth, bottom width and surface width of rills were measured and recorded. From the measurements, the volume of rills V_R was calculated at the end for each run. Since bulk density of soil is known, total erosion at the end of each run was converted to bulk volume of sediment:

TABLE 4-11. BOUNDARY SHEAR, τ_o, AND STREAM POWER FOR EACH RUN AT THE END OF FLOW (τ_o IS CALCULATED BY EQUATION 2-55; WITH RAINFALL EFFECT IN THE OUTDOOR LABORATORY)

Run No.	$\frac{\Delta\bar{u}}{\Delta x} = \frac{d\bar{u}}{dx}$ @ 16'	τ_o (lb/ft^2) @ 16'	$\tau_o - \tau_c$ (lb/ft^2) @ 16'	$(\tau_o - \tau_c)\,\bar{u}$ (lb/ft-sec) @ 16'
I	.0111	.010724	.004624	.00081392
II	.0190	.01845	.01225	.00365295
III	.027	.0240686	.0179686	.0075434
IV	.033	.031583	.025583	.0128736
V	.0142	.022212	.016512	.0036333
VI	.025	.038316	.032616	.012095
VII	.036	.045837	.040137	.020972
VIII	.043	.050945	.045245	.027731
IX	.0180	.025163	.0200632	.005498
X	.0294	.04481	.03911	.0165525
XI	.0460	.051295	.045595	.0289405
XII	.0570	.0619066	.0571066	.0427568
XIII	.0220	.033846	.029146	.00933663
XIV	.0340	.050406	.045606	.0215228
XV	.0550	.05768	.05298	.0380365
XVI	.0660	.067906	.063906	.0528196
XVII	.0262	.04107	.03707	.0135246
XVIII	.0430	.053696	.048996	.027669
XIX	.0680	.06095	.05625	.047365
XX	.0770	.06722	.06252	.059002
XXI	.0310	.049101	.044951	.018160
XXII	.0510	.060544	.056394	.0352135
XXIII	.0800	.068225	.064075	.059025
XXIV	.095	.0762806	.0721306	.075903

$$V_T = \frac{W_T}{d_b} \quad , \qquad (4\text{-}11)$$

in which

V_T = volume of total transported sediment (L^3) ,

W_T = weight of total transported sediment (F) .

All the measurements and calculations were put into dimensionless form as simple ratios, so they would be free of units and could easily be compared with other researchers' results or applied elsewhere. The calculated ratios were: rill volume/volume of total transported sediment volume, rill surface area/total area exposed, and width/depth of rill. The results of all calculations are listed in Table 4-12.

4.1.11 Summary of Data from Vegetated Surface Runs

The affect of vegetation on erosion is shown in the set of data (Table 4-13) which were obtained from runs over 40 percent of the vegetated surface. In Table 4-14 the comparison between runs from vegetated surface and runs from bare surface under the same slope and intensities is shown.

4.2 SIMPLE RELATIONSHIPS BETWEEN THE VARIABLES

4.2.1 Sediment Concentration Versus Time

Simple relationships between time and sediment concentration were plotted for each slope for given intensities of rainfall using data in Table 4-1. These relations are shown in Figs. 4-1 to 4-6. The figures show that sediment concentration was steady although there was some oscillation for the first five to ten minute period of each run. Statistical analysis of data showed that changes in relation to time

TABLE 4-12. DATA FROM RILL MEASUREMENTS

Run No.	V_T (ft^3/hr)	V_R (ft^3/hr)	A_R (mean) (ft^2/hr)	V_R/V_T (per hr)	A_R/A_T[1/] or W_R (A_T = 80 ft^2) (per hr)	V_R/ft of width (ft^3/ft/hr)	A_R/ft of width (ft^2/ft/hr)	D_R (mean) (ft/hr/ft of width)
I	.0185	.001889	14.8	.1021	.185	.0003778	2.96	.0001276
II	.0577	.0007974	18.16	.1382	.227	.001595	3.632	.00043915
III	.124	.028185	25.28	.2273	.316	.005637	5.056	.001114913
IV	.285	.07644	28.24	.2682	.353	.015288	5.648	.0027067
V	.0565	.006865	15.68	.1215	.196	.001373	3.136	.00043782
VI	.290	.04634	18.88	.1598	.236	.009268	3.776	.00245445
VII	.715	.1678	25.76	.2347	.322	.03356	5.152	.006514
VIII	1.131	.33715	28.56	.2981	.357	.067431	5.712	.0011905
IX	.1054	.0147	16.72	.1396	.209	.00294	3.344	.0008792
X	.572	.105	20.08	.1834	.251	.0210	4.016	.0052291
XI	1.373	.3692	26.40	.2689	.330	.07384	5.28	.013985
XII	2.477	.8040	29.44	.3246	.368	.1608	5.888	.02731
XIII	.124	.02192	18.88	.1768	.236	.004384	3.776	.001161
XIV	1.094	.23762	21.68	.2172	.271	.047524	4.336	.01096
XV	2.866	.8363	27.28	.2918	.341	.16726	5.456	.0306562
XVI	5.127	1.844	30.32	.3596	.379	.3688	6.064	.0508179
XVII	.177	.0386	21.44	.2182	.268	.00772	4.288	.00180037
XVIII	1.952	.5034	24.32	.2579	.304	.10068	4.864	.020699
XIX	4.355	1.516	29.68	.3482	.371	.31032	5.936	.05227763
XX	7.215	2.952	33.04	.4091	.413	.5904	6.608	.08934625
XXI	.218	.0523	23.20	.2398	.290	.01046	4.64	.0022543
XXII	2.5185	.8104	28.16	.3218	.352	.16208	5.632	.02877841
XXIII	7.1154	2.983	33.60	.4192	.420	.5966	6.720	.08878
XXIV	12.5154	6.115	37.20	.4886	.465	1.2230	7.440	.1643817

[1/] Magnitude of A_R/A_T is equal to W_R which is the mean rill width in ft/hr/ft of width.

TABLE 4-13. DATA FROM VEGETATED SURFACE RUNS

Slope (%)	Rainfall Intensity (in/hr)	C_s (ppm)	q_s (lb/sec/ft)	q (cfs)	q (cfs/ft)	q_o (ft/sec)	Temp (C°)	$\nu \times 10^5$ (L^2/t)	Re (q/ν)
40	1.25	9399.3	.000094	.00080	.0016	.00001	18	1.39	11.15
40	2.25	83464.98	.003148	.00306	.000601	.000038	18	1.39	42.0
40	3.65	165815.6	.00829	.0040	.00080	.000050	18	1.39	57.2
40	4.60	2237600.5	.02236	.0080	.0016	.00010	18	1.39	11.5

TABLE 4-14. COMPARISON BETWEEN VEGETATION AND BARE SOIL

Slope (%)	Rainfall Intensity (in/hr)	C_s, vegetated soil (ppm)	C_s, bare soil (ppm)	Difference ΔC_s	Erosion decreased (%)
40	1.25	9399.30	44149	34749.7	78.71
40	2.25	83464.98	207585	124120	59.79
40	3.65	165815.6	313749	147933.4	47.15
40	4.60	223760.5	355885	132124.5	37.126

are not significant. Sediment concentration and discharge, thus, are steady and do not change with time.

4.2.2 Sediment Concentration Versus Slope and Intensity

The relation between slope, averaged sediment concentration and rainfall intensity for a rainfall duration of one hour, is given in Fig. (4-7). The same type of plotting was done in Figs. (4-8, 4-9 and 4-10) by separating the concentration for the first zero to ten minutes, the first thirty minutes, and the last thirty minutes for given conditions of the runs. Figure (4-11) shows averaged, C_s , between thirty to forty minutes versus intensity and slope. Figures (4-7) through (4-11) show similarly shaped curves in which there is no change with time.

4.2.3 Sediment Discharge Versus Slope and Intensity

Converting sediment discharge into different units such as lb/hr, lb/hr/ft of width or lb/sec/ft of width and plot versus slope and intensities as seen in Figs. (4-12, 4-13, and 4-14) yields curves similar to those in Fig. (4-11). Sediment discharge versus water discharge was also plotted for a given slope, as seen in Fig. (4-15). It shows a shape almost similar to the rest of the figures.

4.2.4 Water Discharge Versus Slope and Intensity

Total discharge for one hour was plotted versus slope for each rainfall intensity in Fig. (4-16). This figure indicates that there was only a slight increase in discharge with slopes for a given intensity.

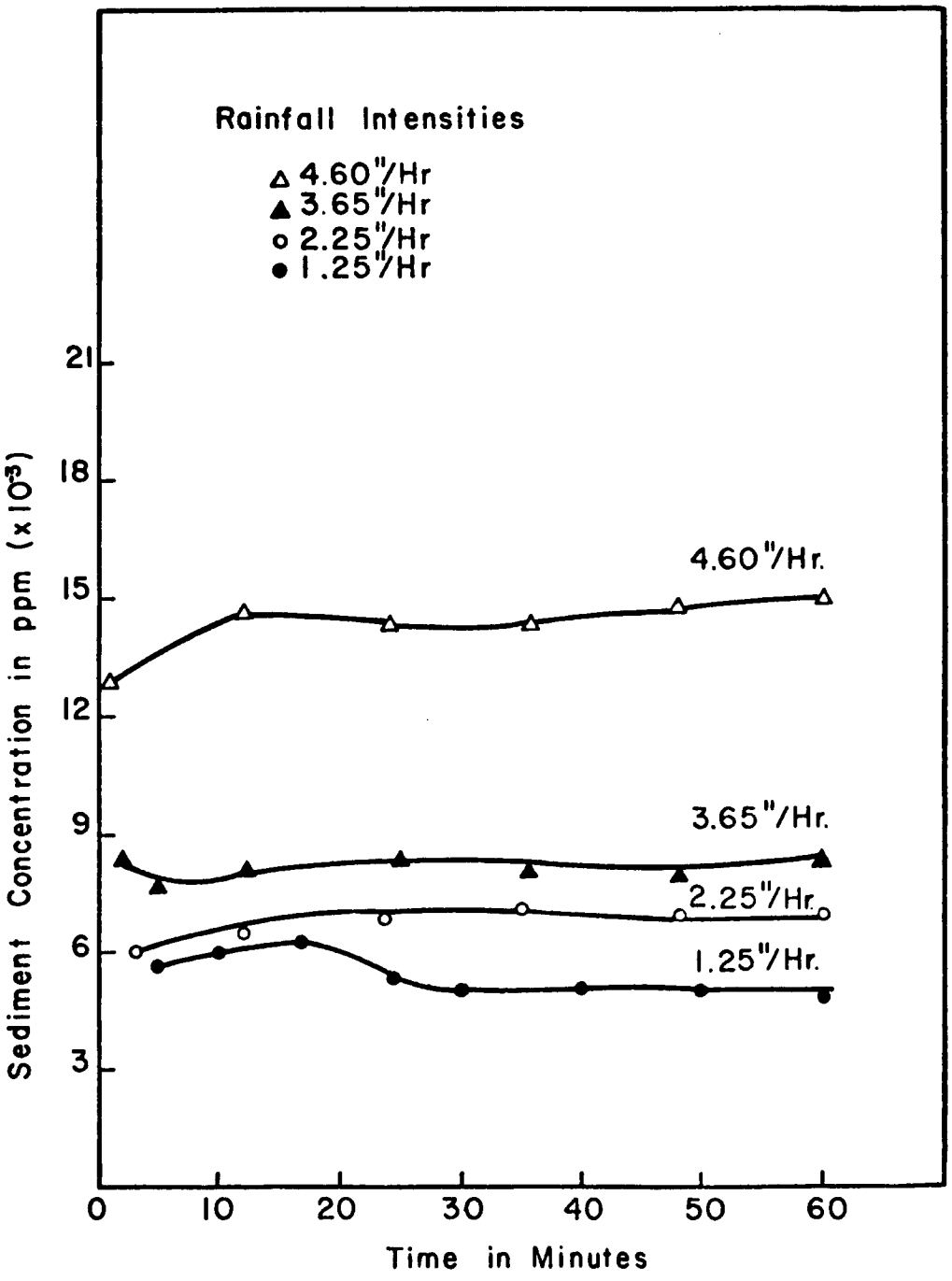

Fig. 4-1. Relationship between sediment concentration and time for given rainfall intensities on 5.7 percent slope.

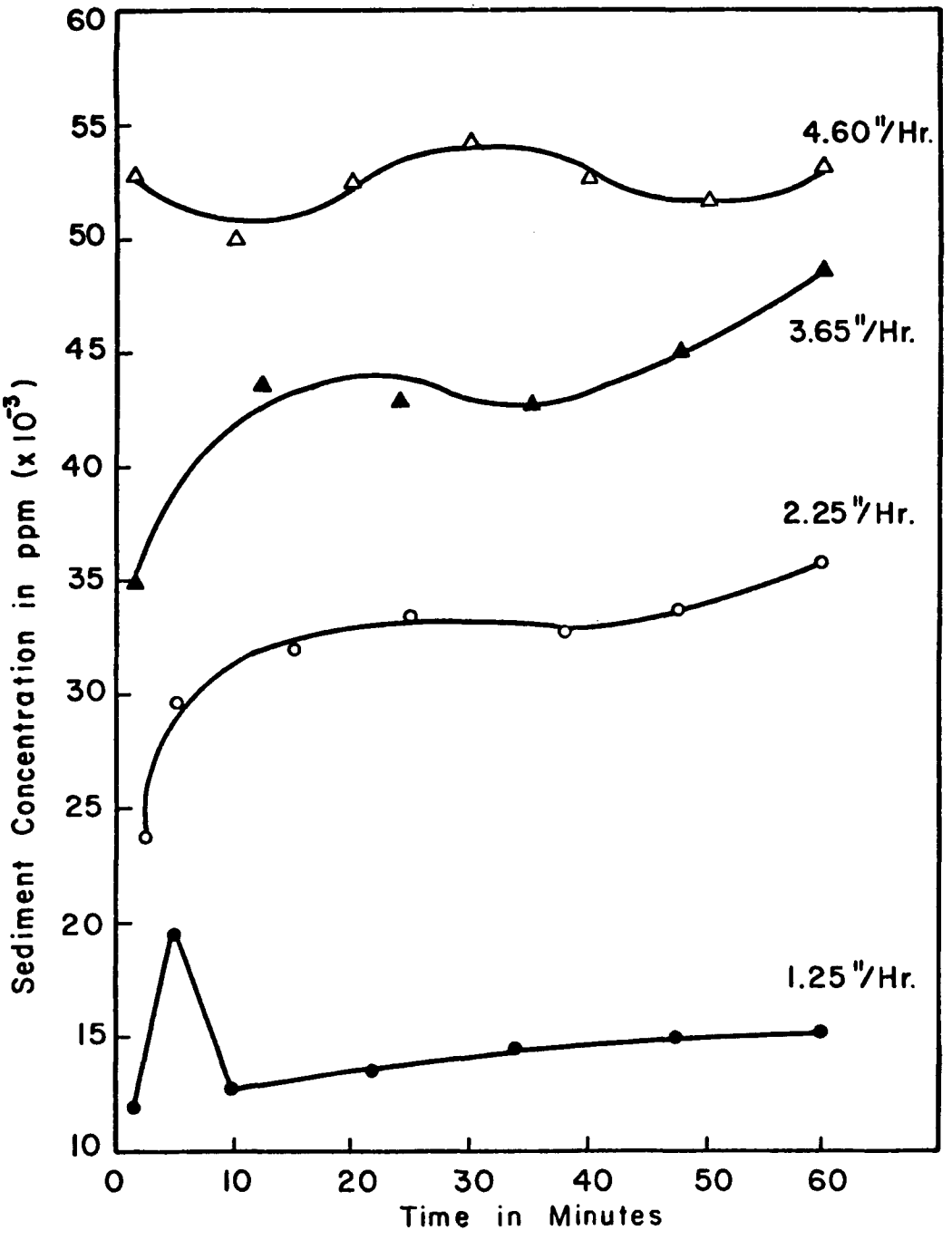

Fig. 4-2. Relationship between sediment concentration and time for given rainfall intensities on 10 percent slope.

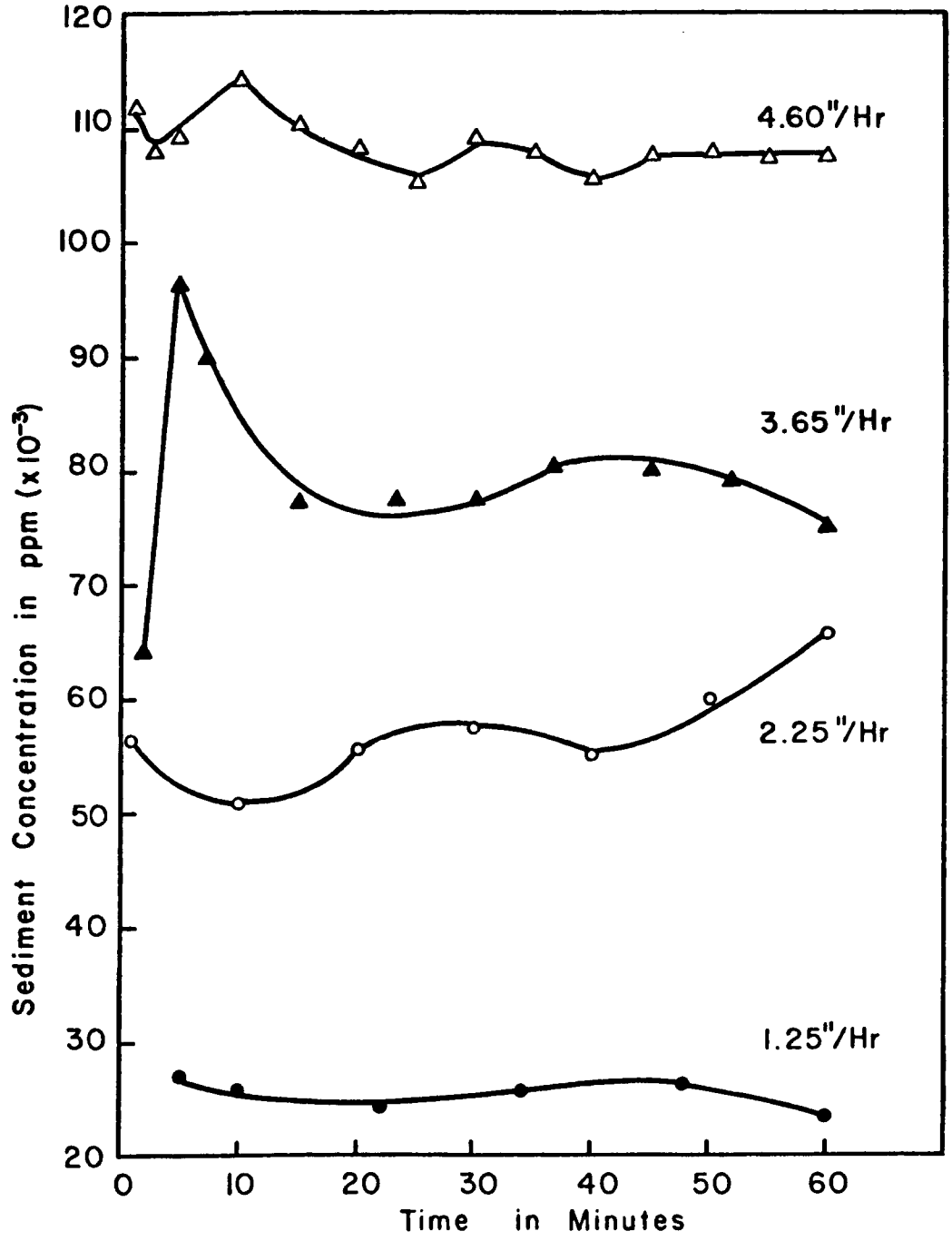

Fig. 4-3. Relationship between sediment concentration and time for given rainfall intensities on 15 percent slope.

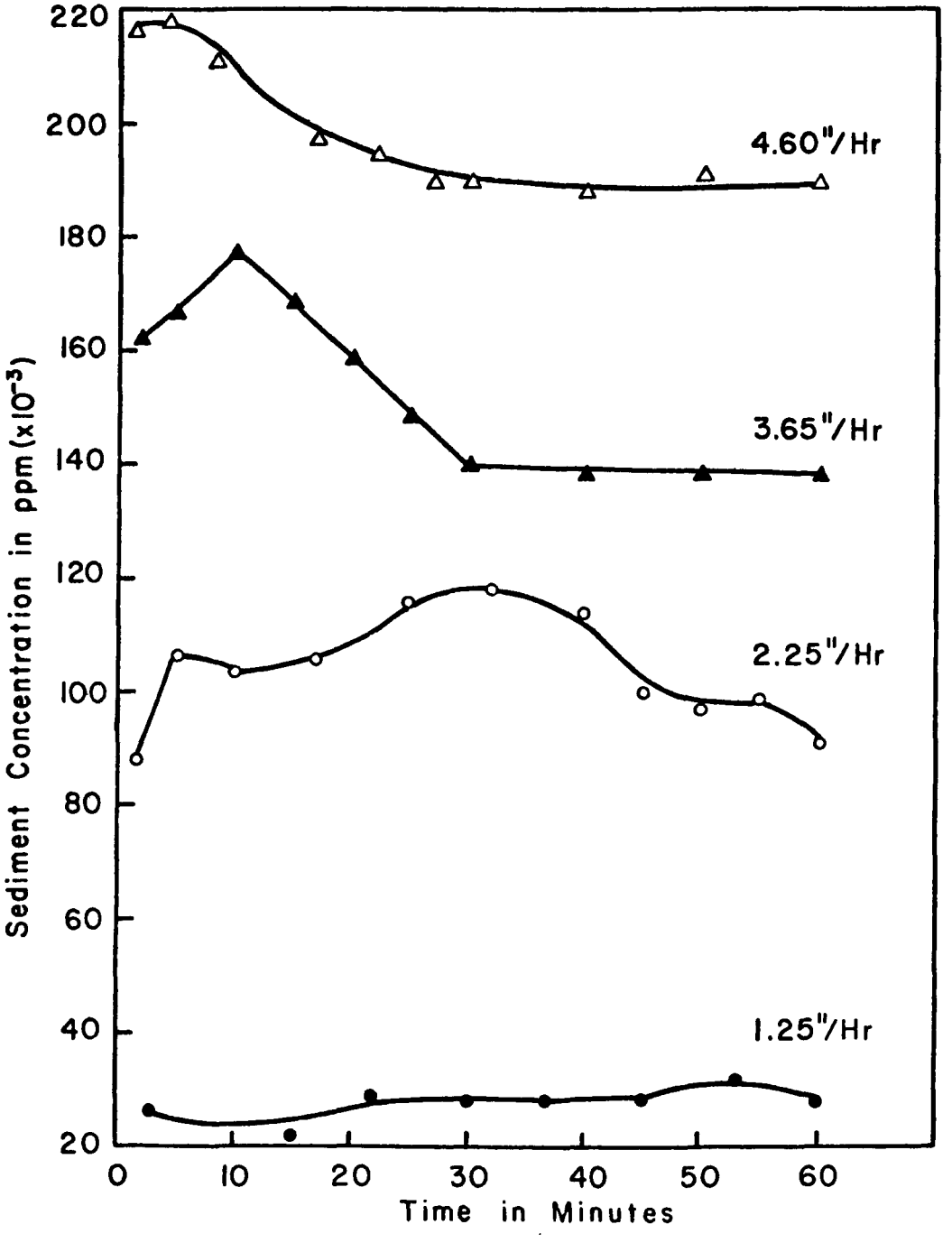

Fig. 4-4. Relationship between sediment concentration and time for given rainfall intensities on 20 percent slope.

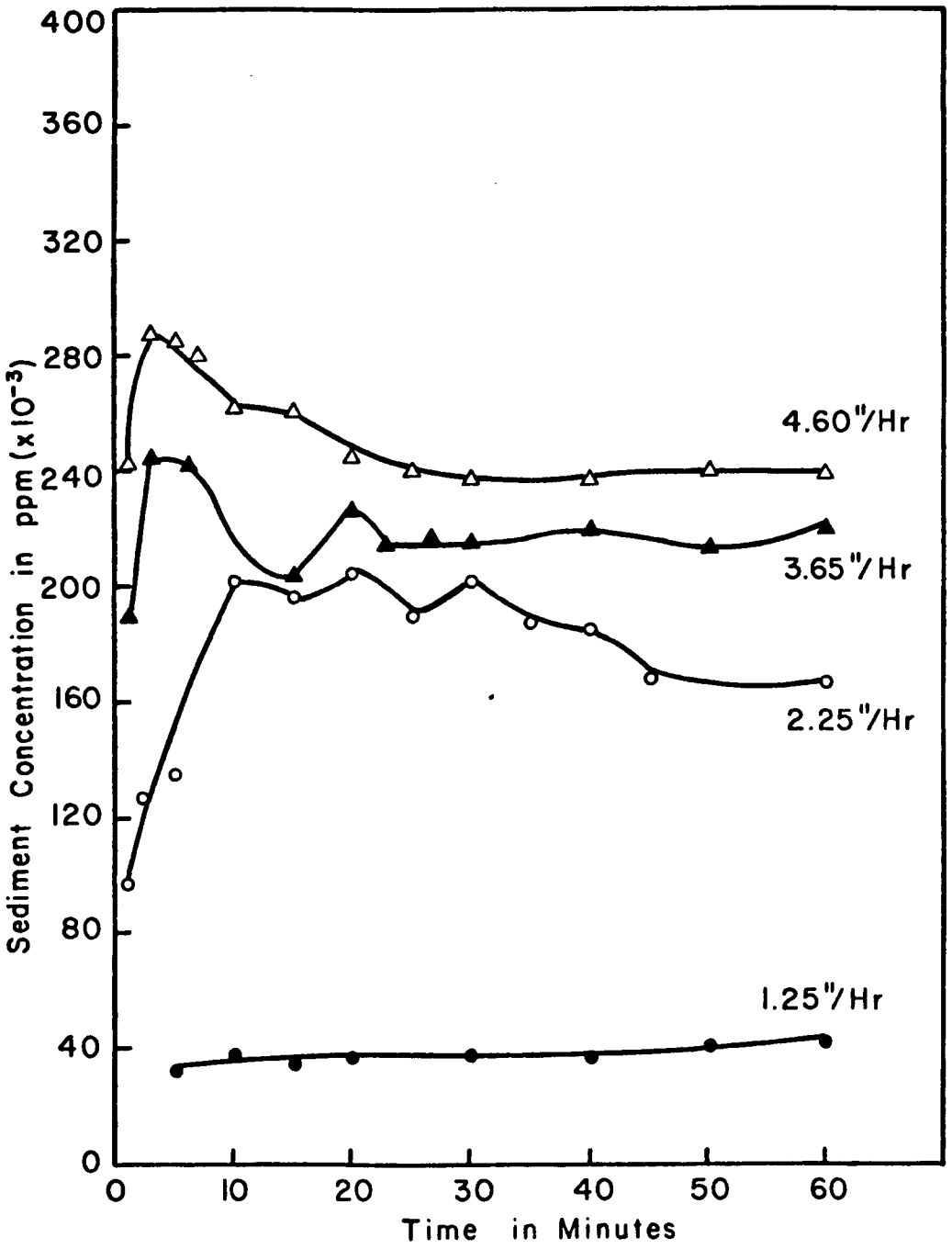

Fig. 4-5. Relationship between sediment concentration and time for given rainfall intensities on 30 percent slope.

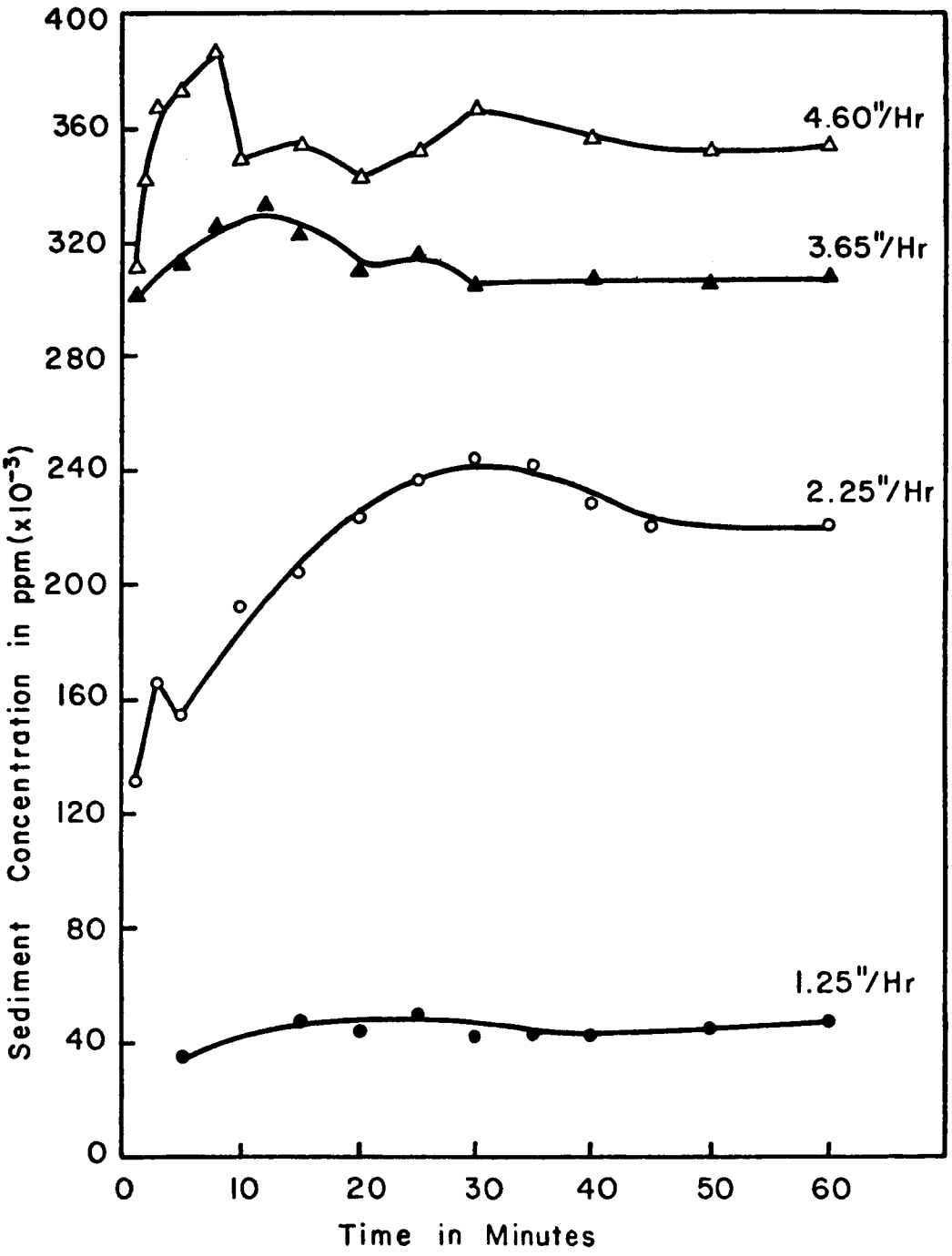

Fig. 4-6. Relationship between sediment concentration and time for given rainfall intensities on 40 percent slope.

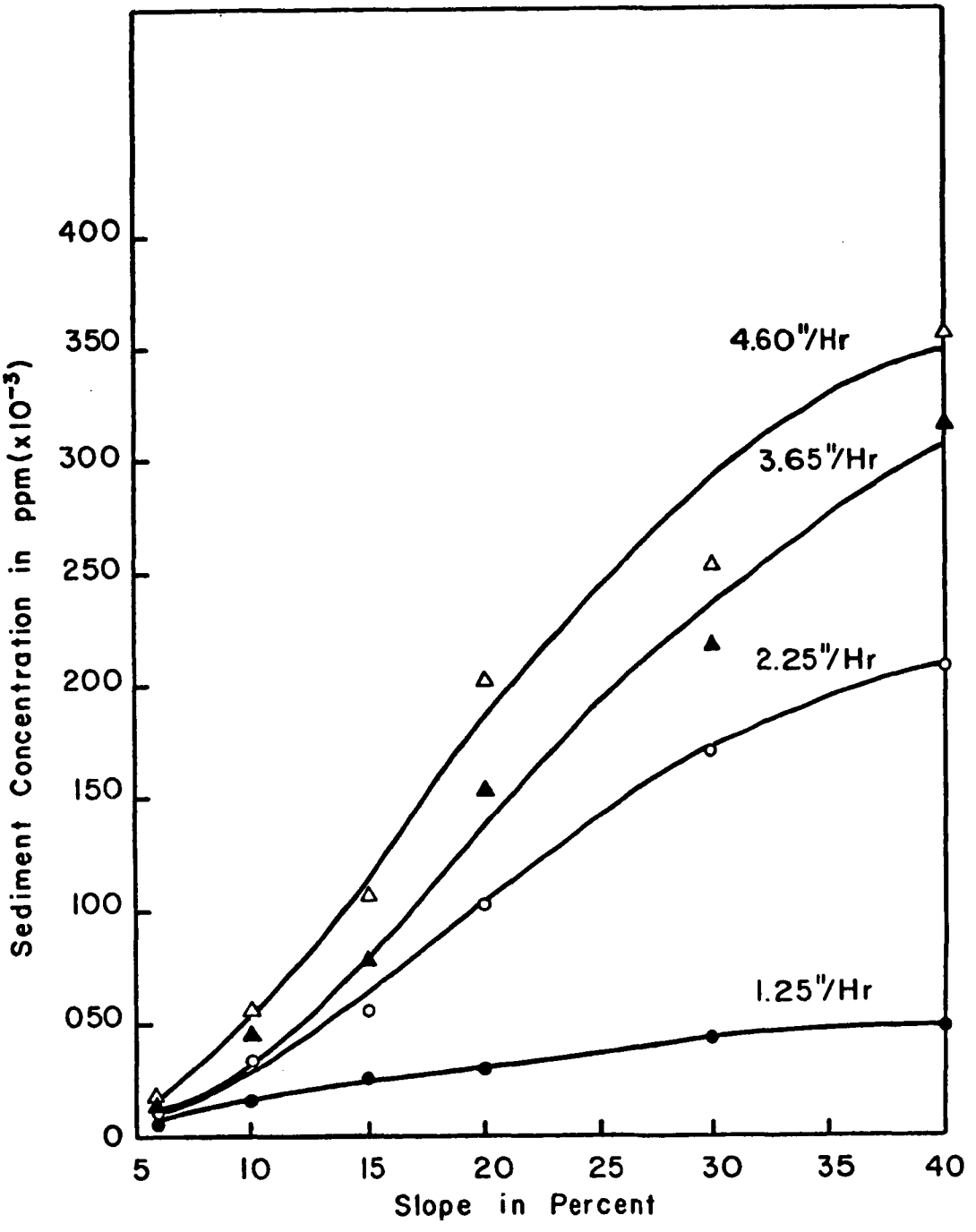

Fig. 4-7. Relationship between sediment concentration and slope for given rainfall intensities (average concentration values obtained after one hour run).

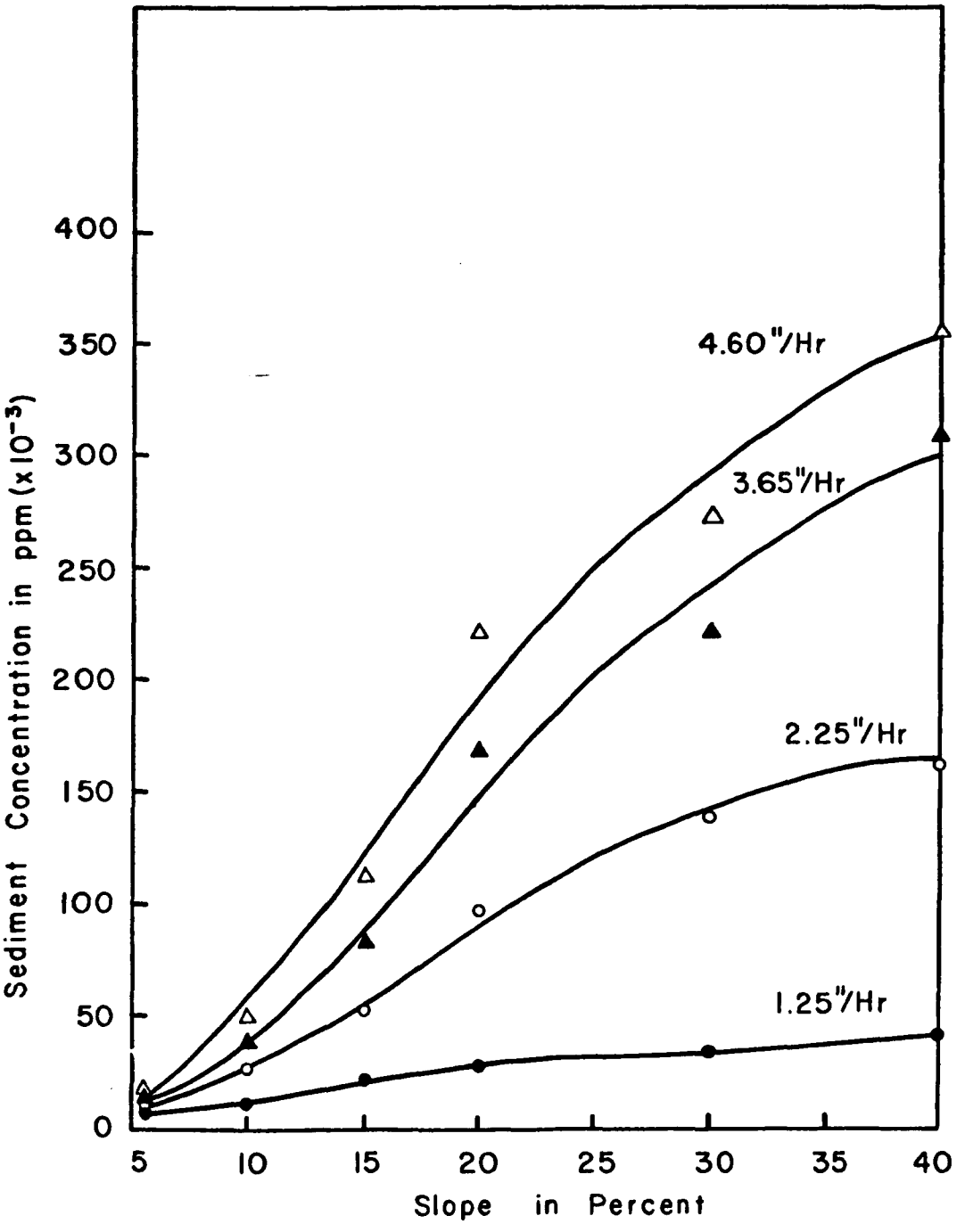

Fig. 4-8. Relationship between sediment concentration and slope for given rainfall intensities (average concentration values obtained between 0-10 minutes).

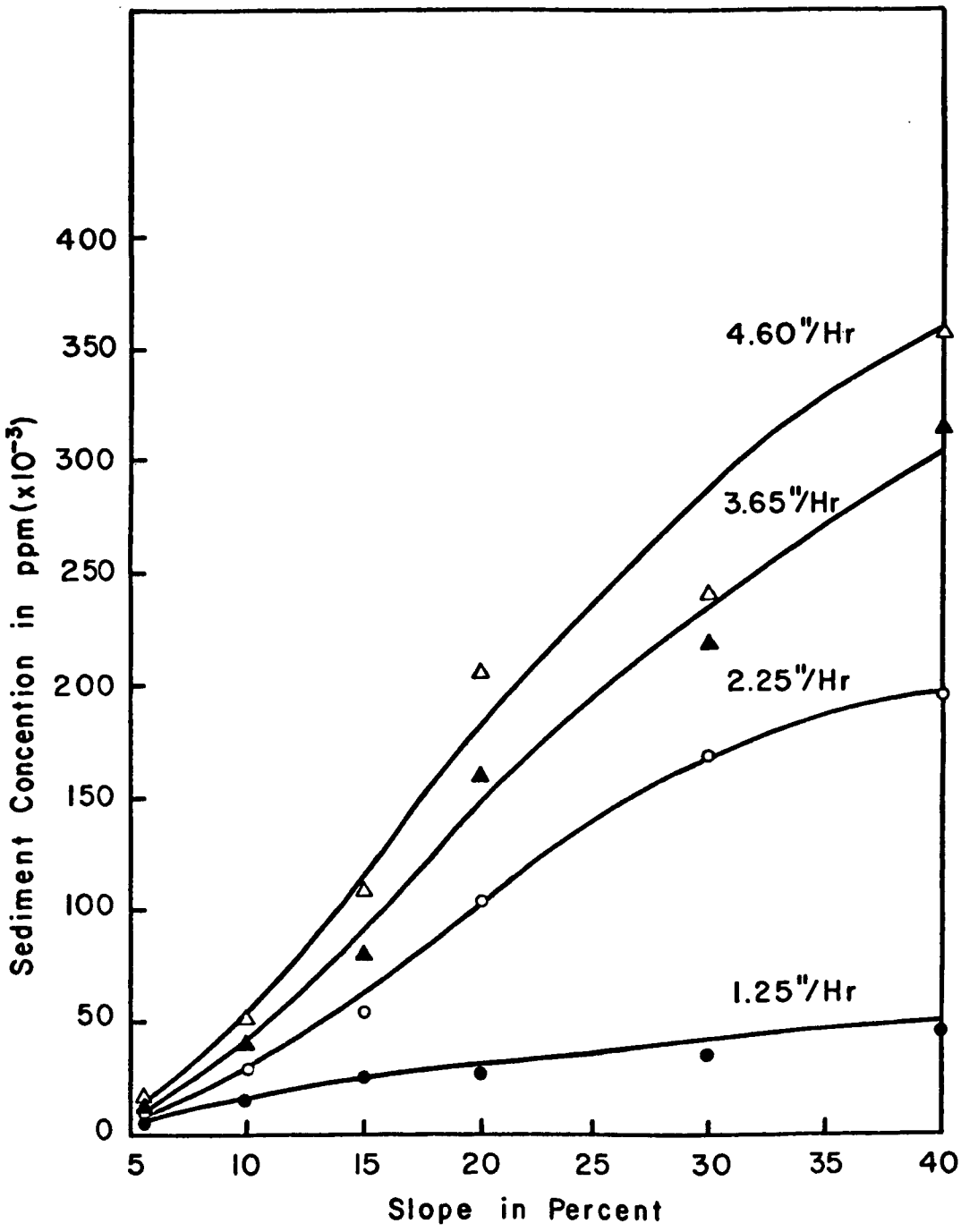

Fig. 4-9. Relationship between sediment concentration and slope for given rainfall intensities (average concentration values obtained after first 30 minutes).

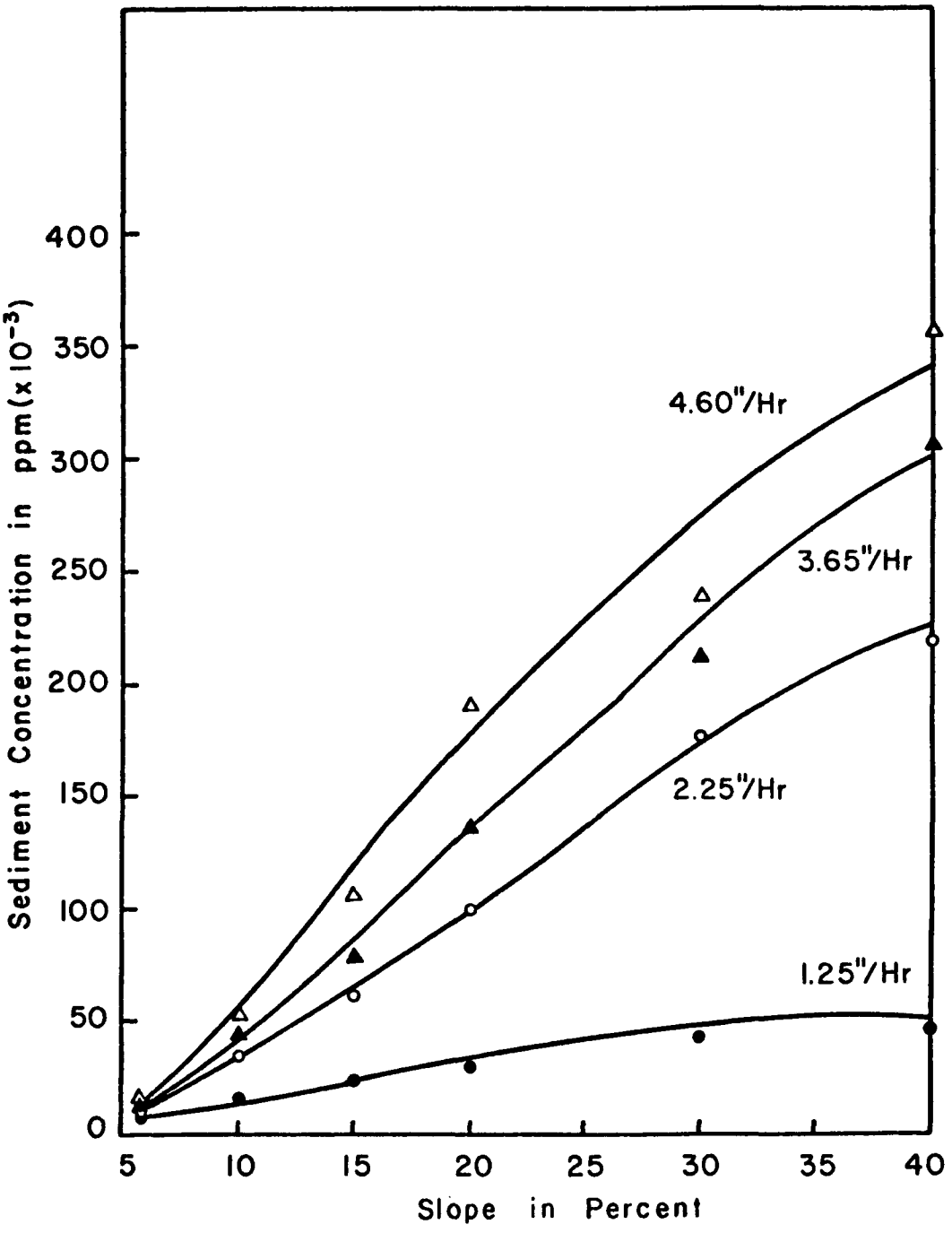

Fig. 4-10. Relationship between sediment concentration and slope for given rainfall intensities (average concentration values obtained between 30-60 minutes).

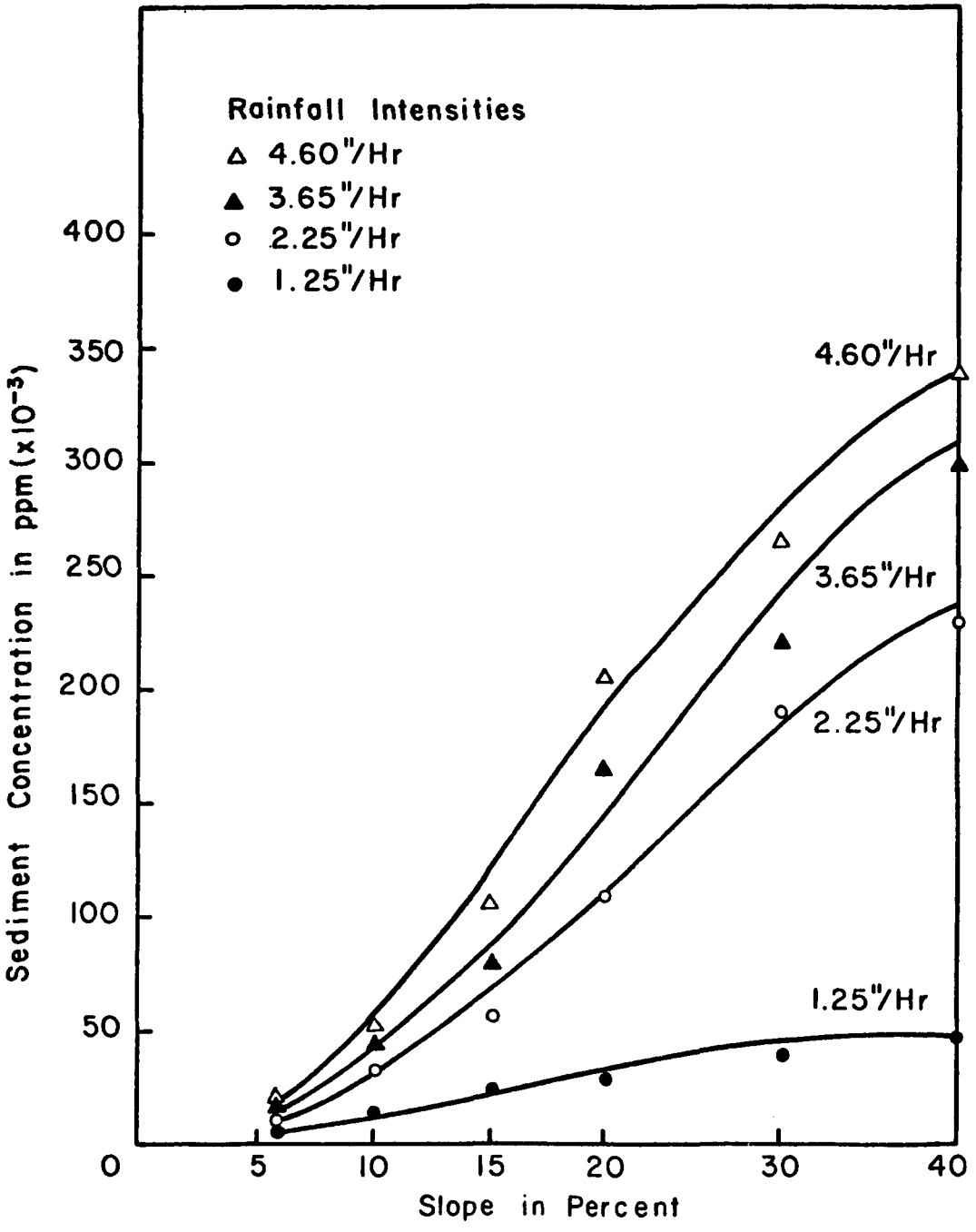

Fig. 4-11. Relationship between sediment concentration and slope for given rainfall intensities (average concentration values obtained between 30-40 minutes).

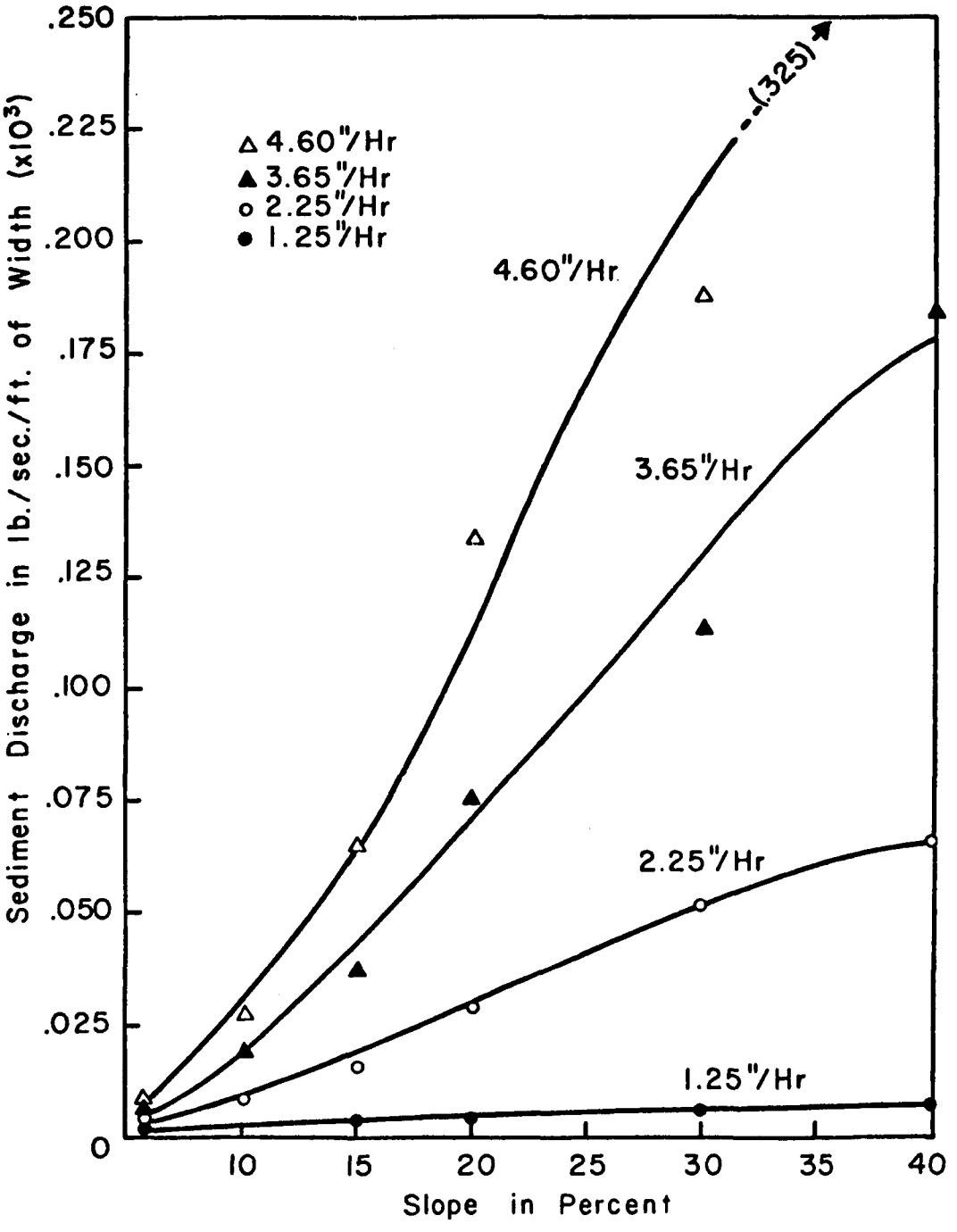

Fig. 4-12. Relationship between sediment discharge and slope for given rainfall intensities (q_s in lb/hr/ft of width).

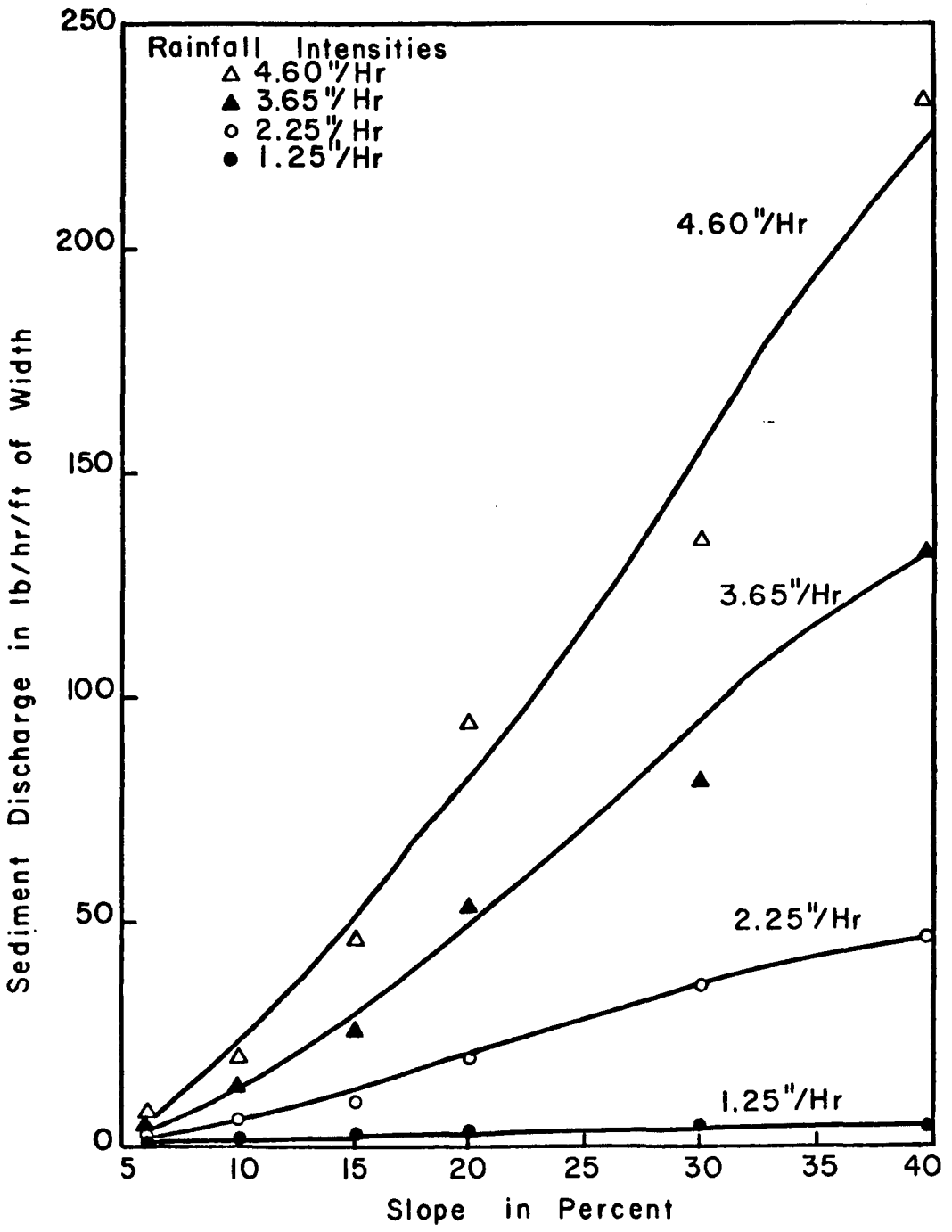

Fig. 4-13. Relationship between sediment discharge and slope for given rainfall intensities (q_s in lb/hr/ft of width).

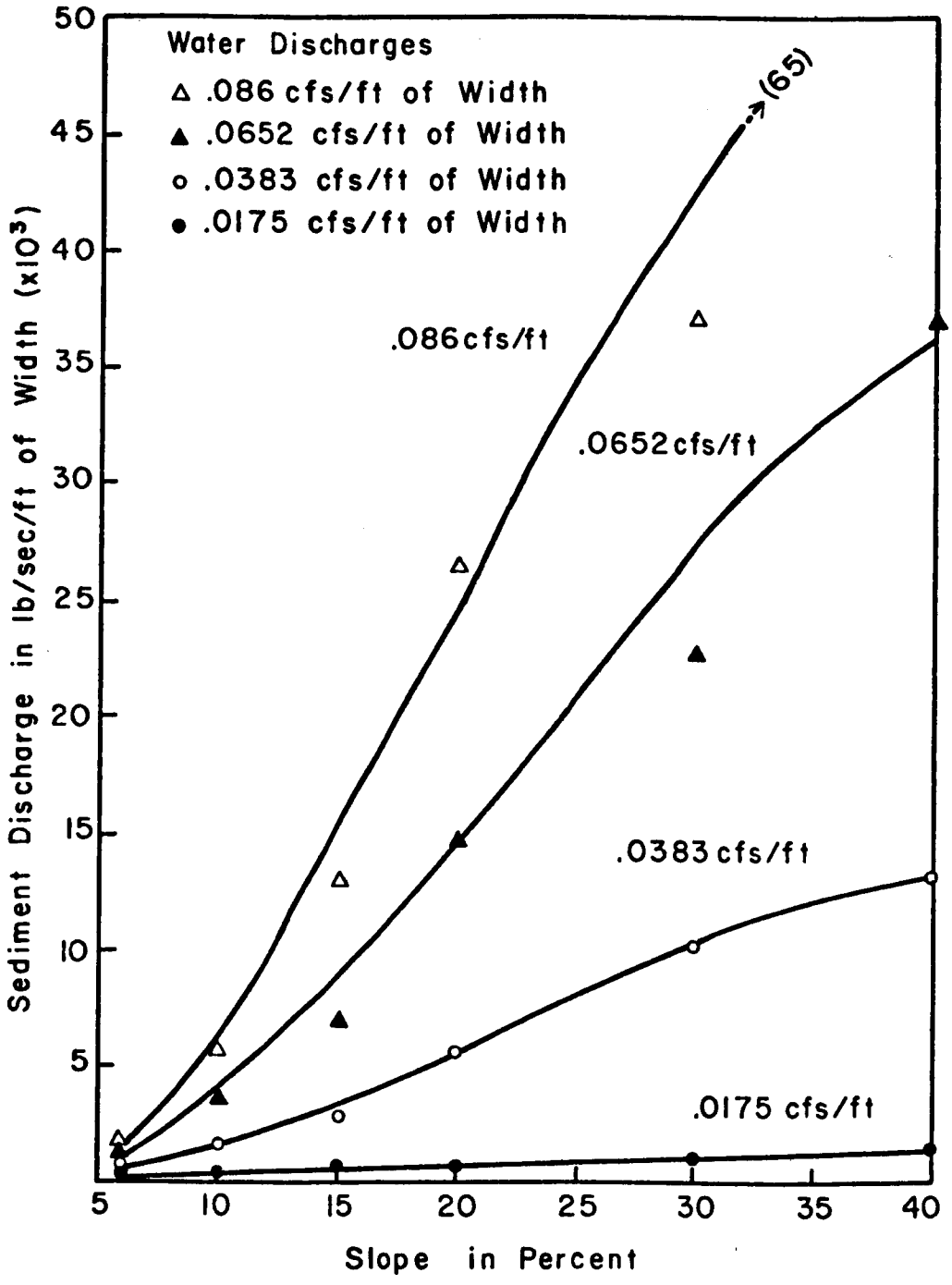

Fig. 4-14. Relationship between sediment discharge and slope for given water discharges (q in cfs/ft of width and q_s in lb/sec/ft of width).

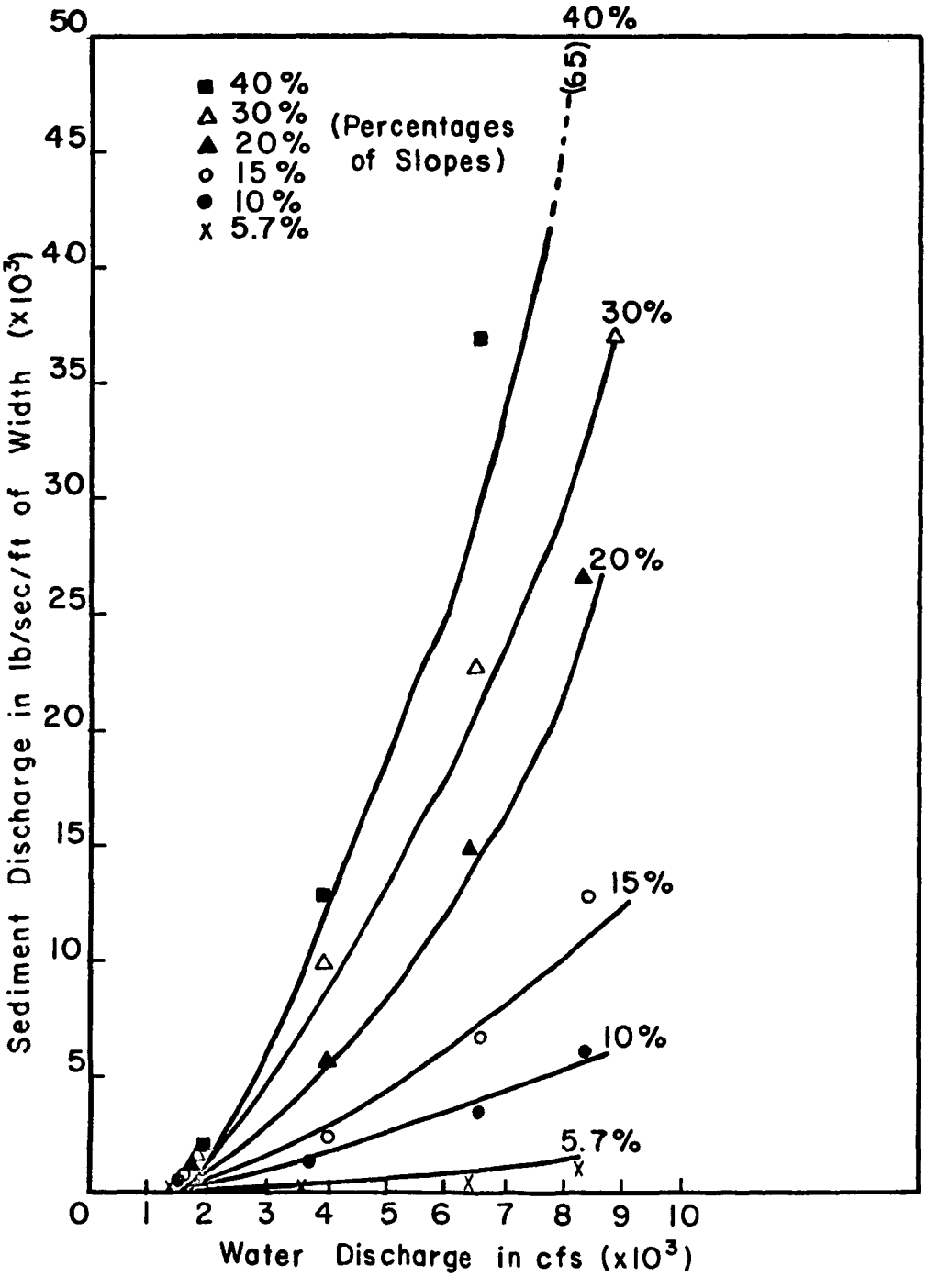

Fig. 4-15. Relationship between sediment discharge and water discharges on given slopes for one hour run.

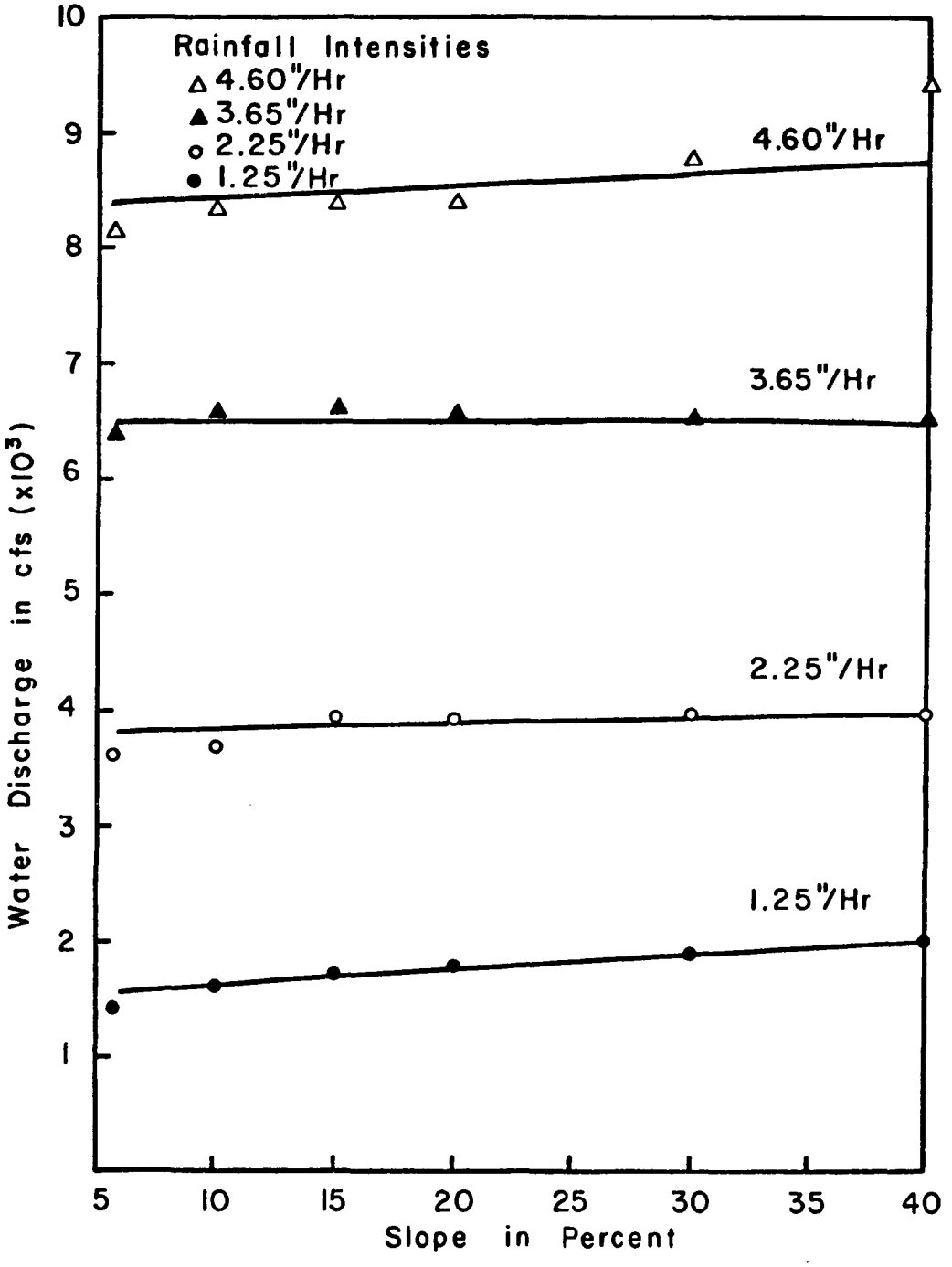

Fig. 4-16. Relationship between water discharge and slope for given rainfall intensities.

4.2.5 Local Mean Velocity and Depth Versus Overland Flow Distance, Slope and Intensity

Local mean velocity and depth versus distance were plotted in Figs. (4-17) to (4-22) for each slope and for given intensities of rainfall.

4.2.6 Friction Factor, f , Versus Reynolds Number, Re

For each given run and slope, the relationship between friction factors, f , which are calculated by Eq. (2-5), the calculated Reynolds number, and f versus distance was plotted in Figs. (4-23), and (4-24) through (4-29).

4.2.7 Effect of Vegetation on Erosion and Sediment Discharge

To show the qualitative effects of vegetation on erosion rate, the percentage-decreased erosion rate versus intensity of rainfall were plotted for four runs in Fig. (4-30). Averaged sediment concentration, C_s , from vegetated surface and bare surface at 40 percent slope versus intensity of rainfall were plotted in Fig. (4-31) to compare the vegetal effect on C_s.

4.3 ANALYSIS OF DATA

Statistical analyses of the data using nonlinear multiple regression analysis are explained and results of regression equations are shown and briefly discussed. Stepwise nonlinear multiple regression analysis was utilized transgeneration procedure to convert data into logarithmic form.

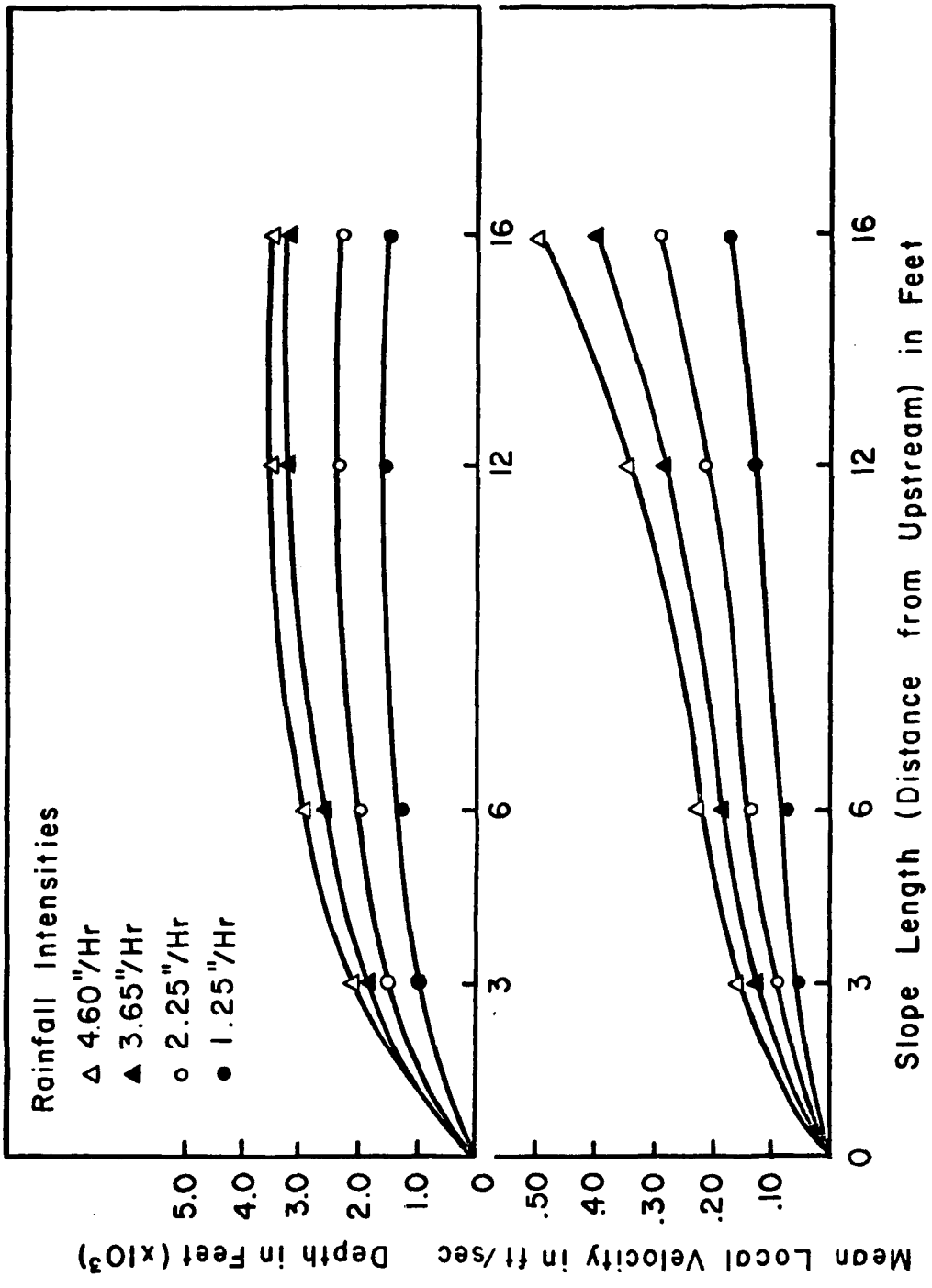

Fig. 4-17. Mean local velocity and depth related to slope length for given rainfall intensities on 5.7 percent slope.

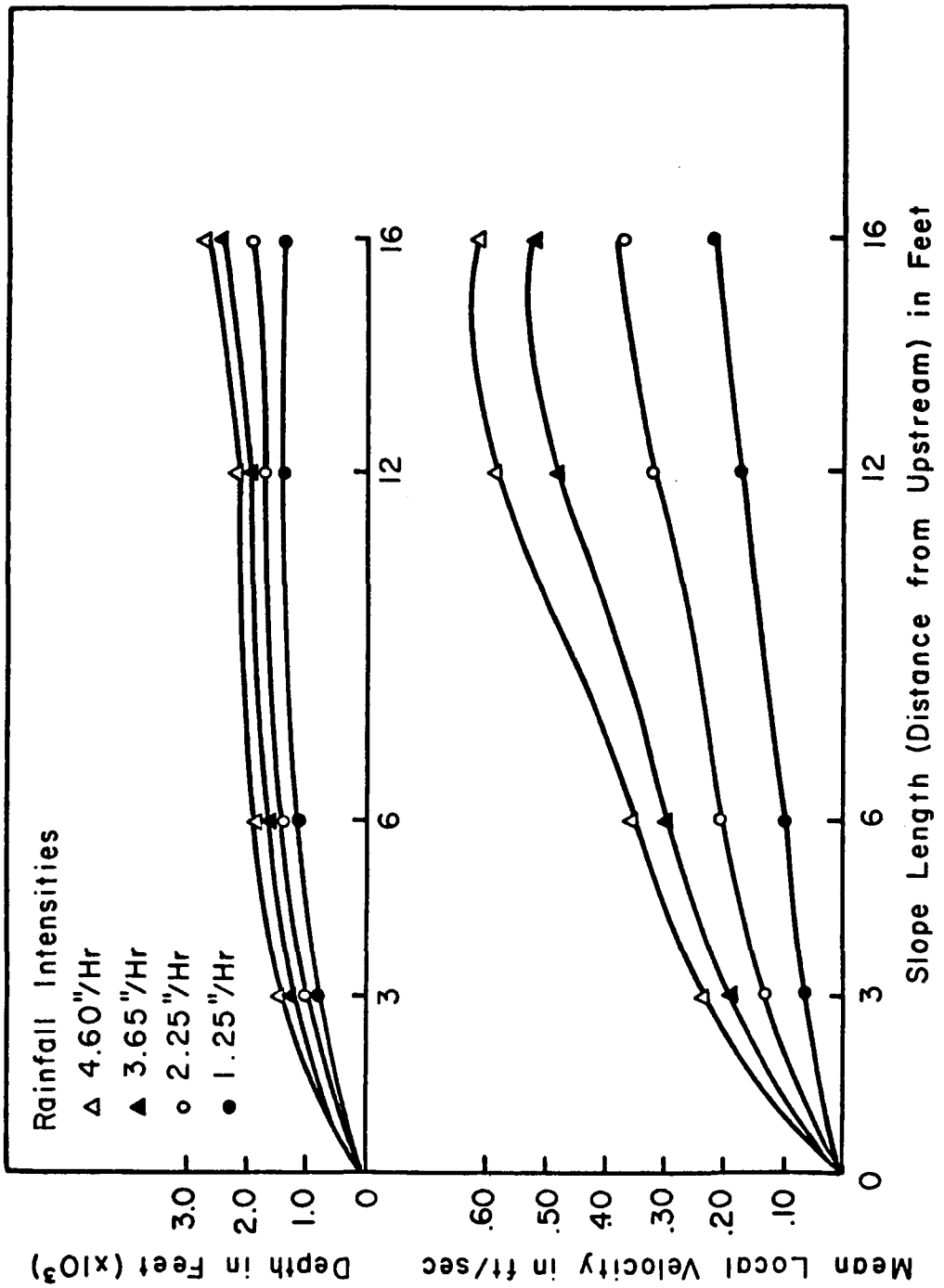

Fig. 4-18. Mean local velocity and depth related to slope length for given rainfall intensities on 10 percent slope.

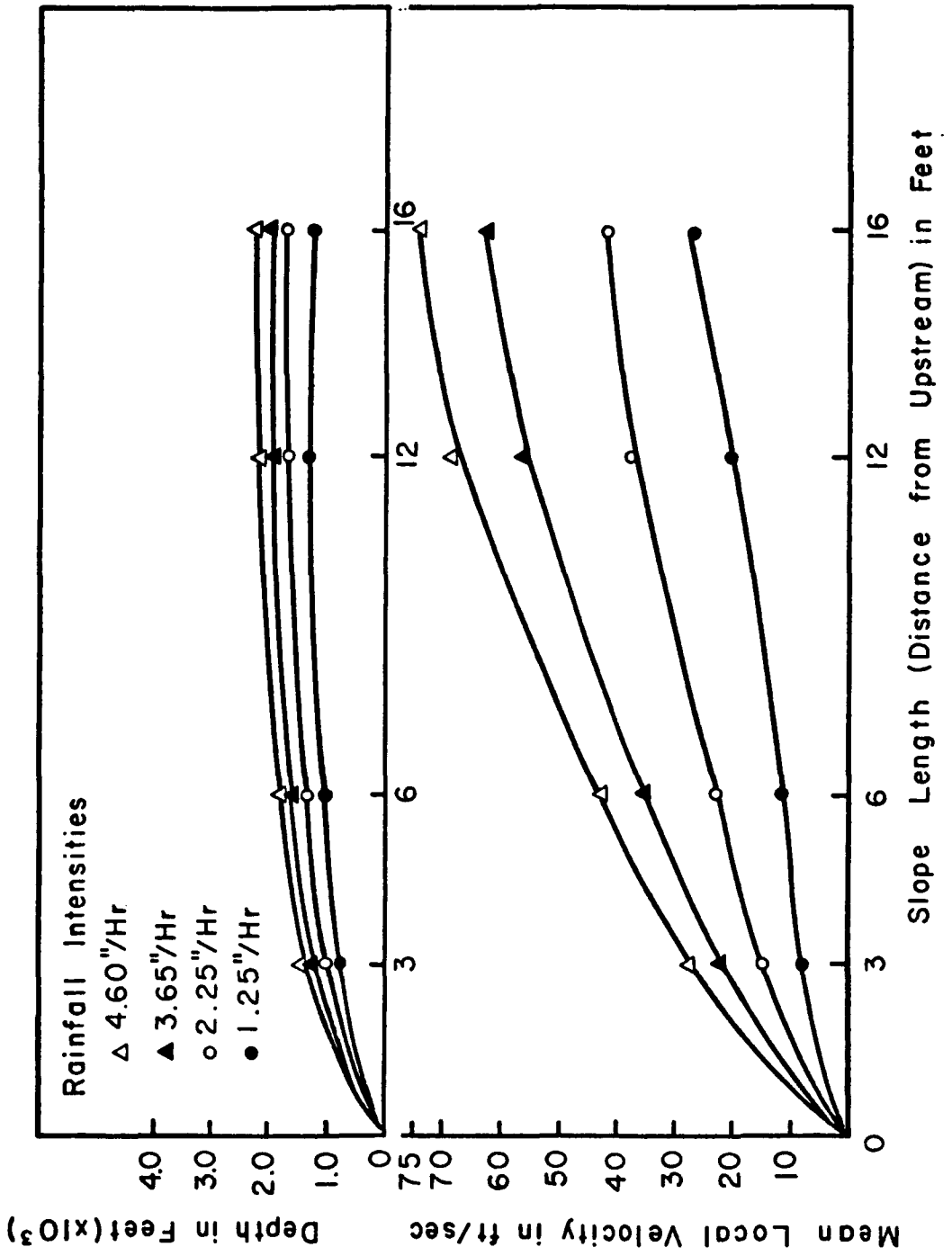

Fig. 4-19. Mean local velocity and depth related to slope length for given rainfall intensities on 15 percent slope.

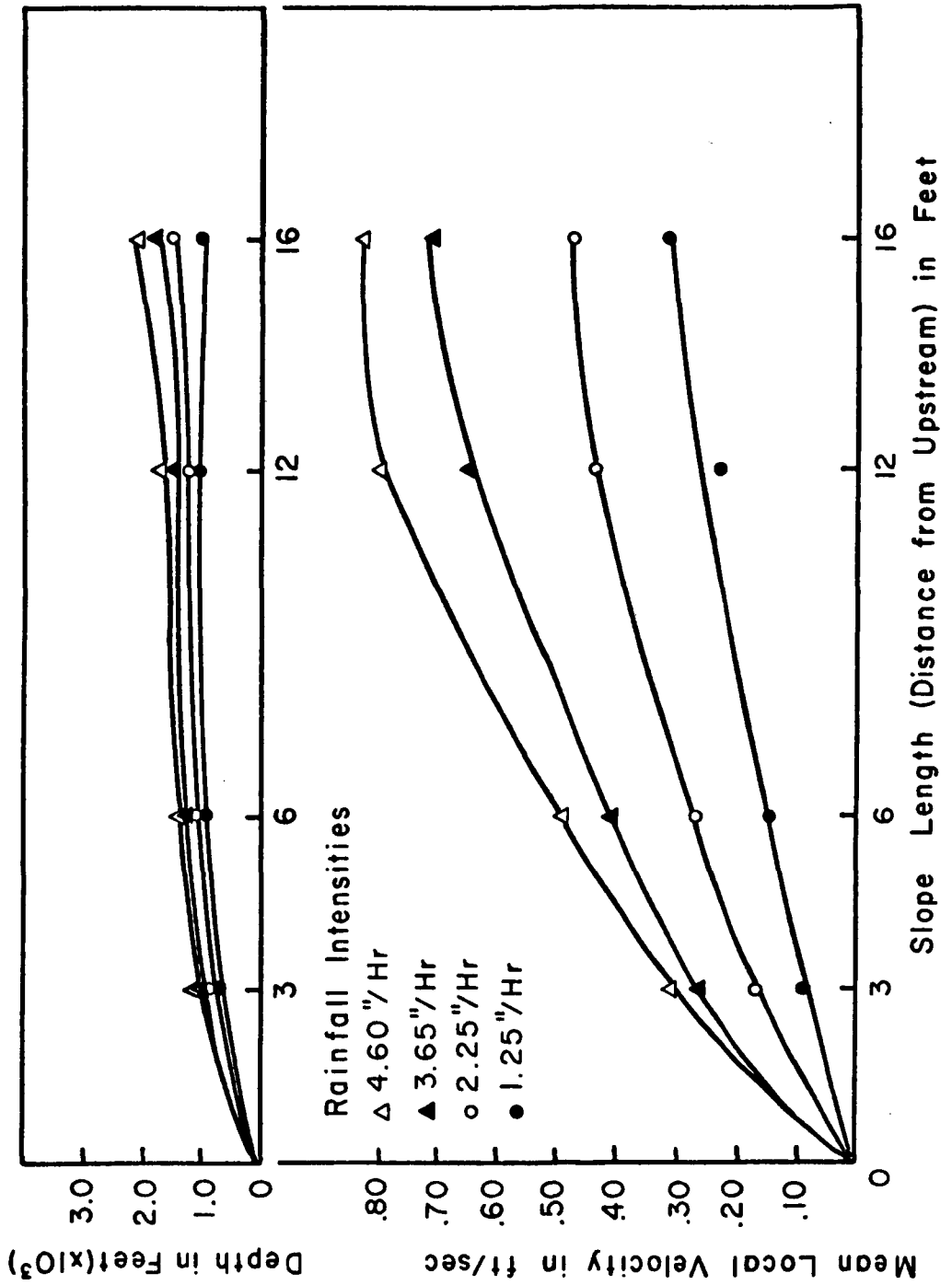

Fig. 4-20. Mean local velocity and depth related to slope length for given rainfall intensities on 20 percent slope.

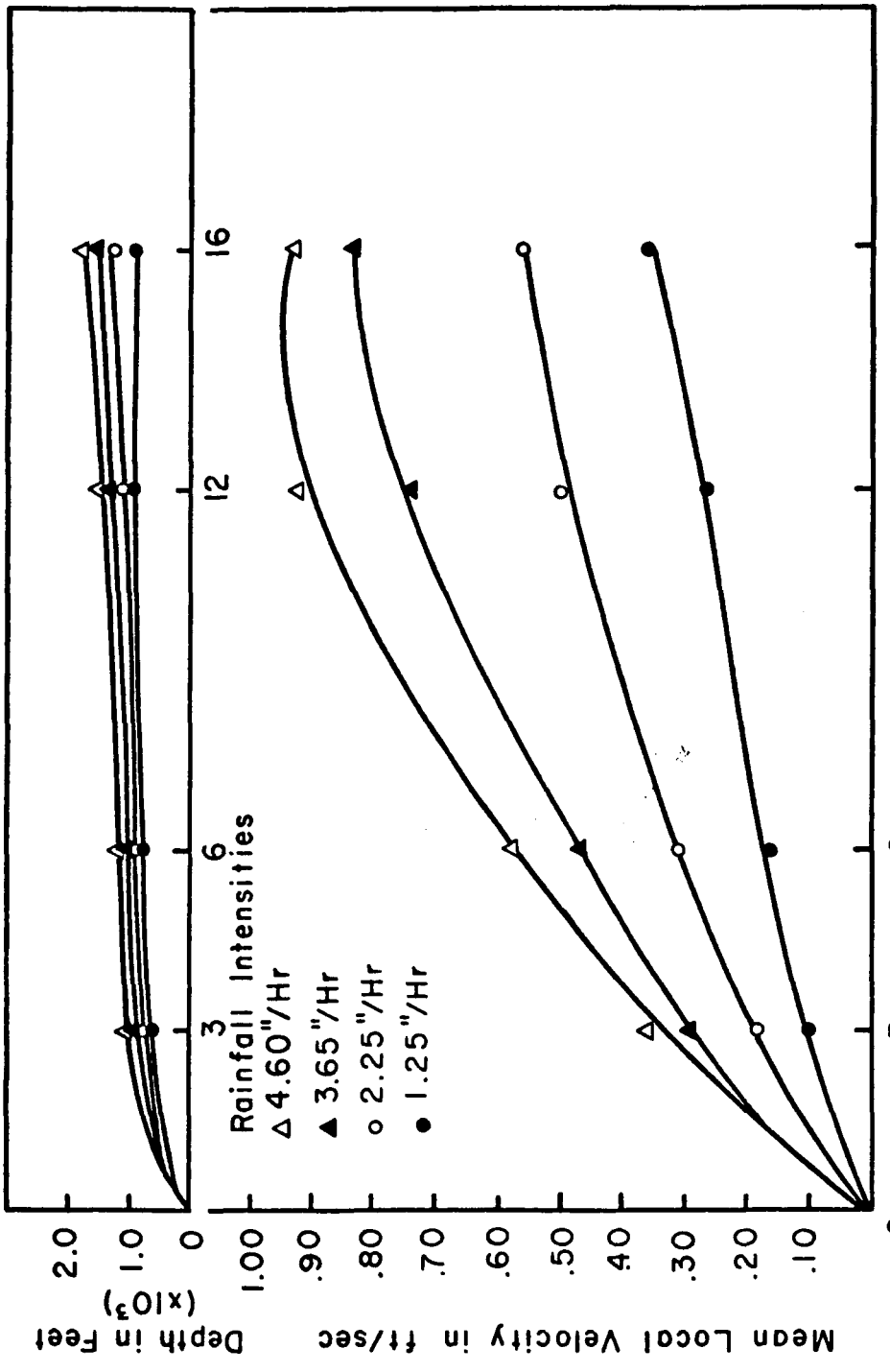

Fig. 4-21. Mean local velocity and depth related to slope length for given rainfall intensities on 30 percent slope.

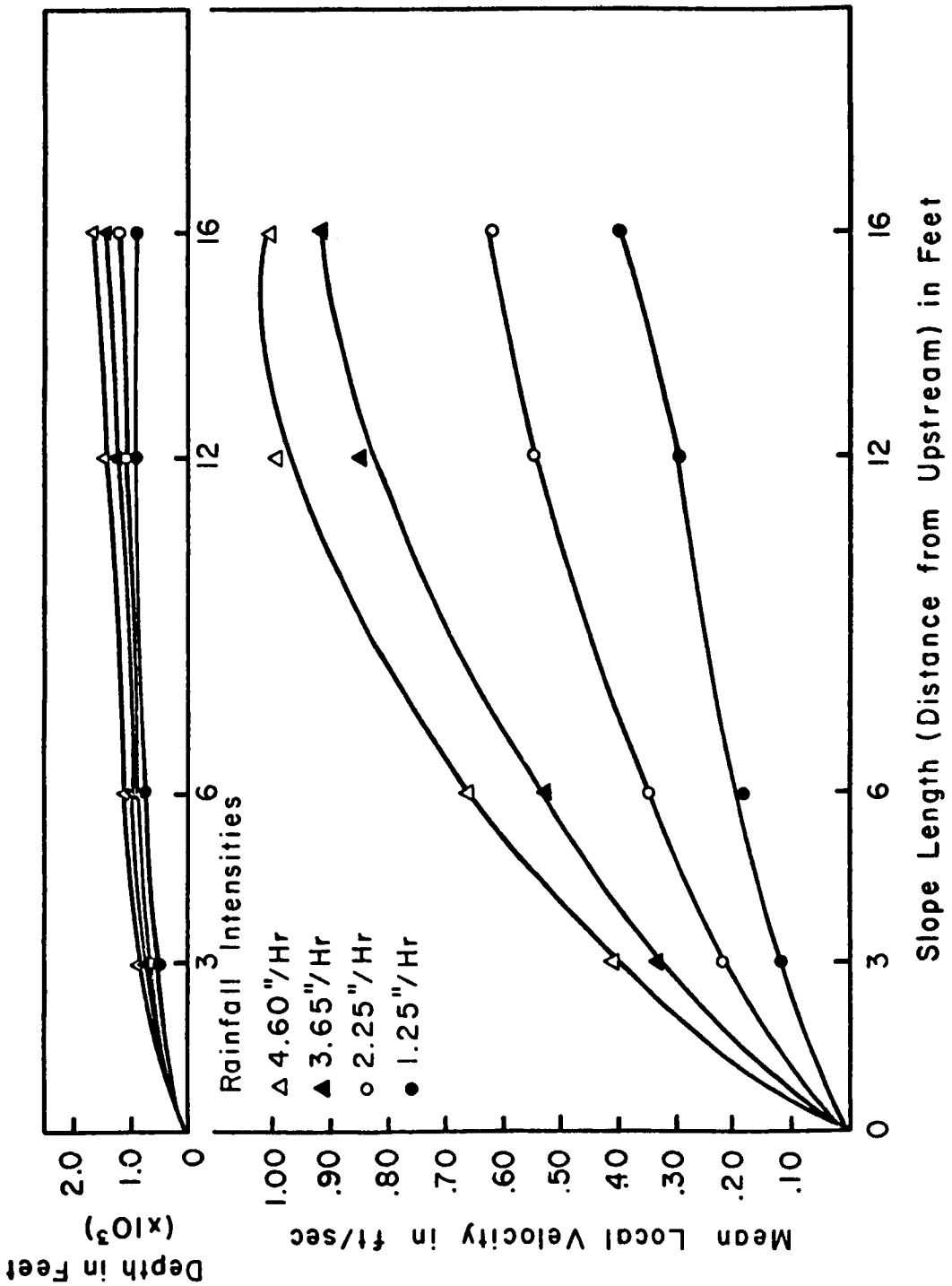

Fig. 4-22. Mean local velocity and depth related to slope length for given rainfall intensities on 40 percent slope.

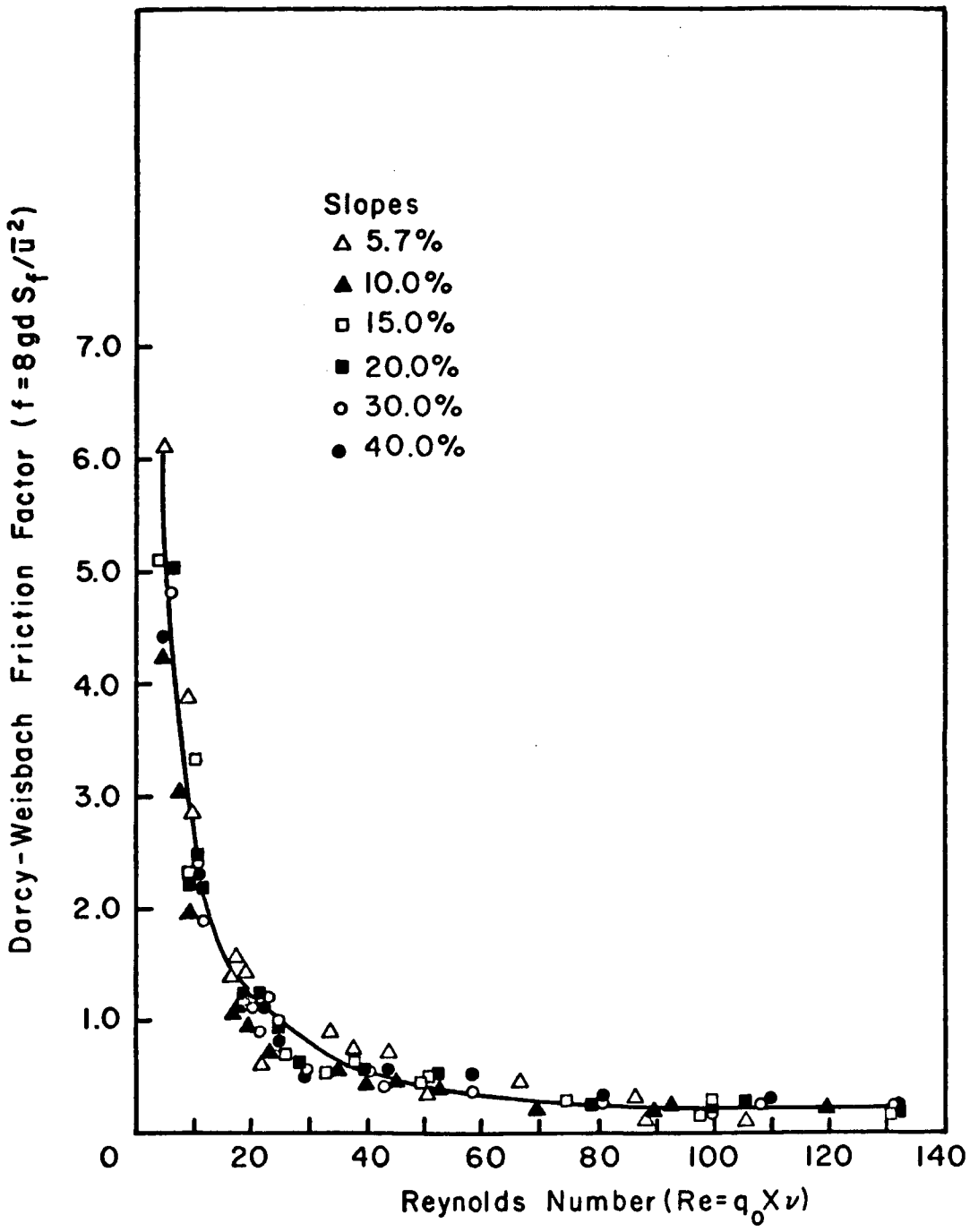

Fig. 4-23. Relationship between Darcy-Weisbach friction factor, f , and Reynolds number Re for given slopes.

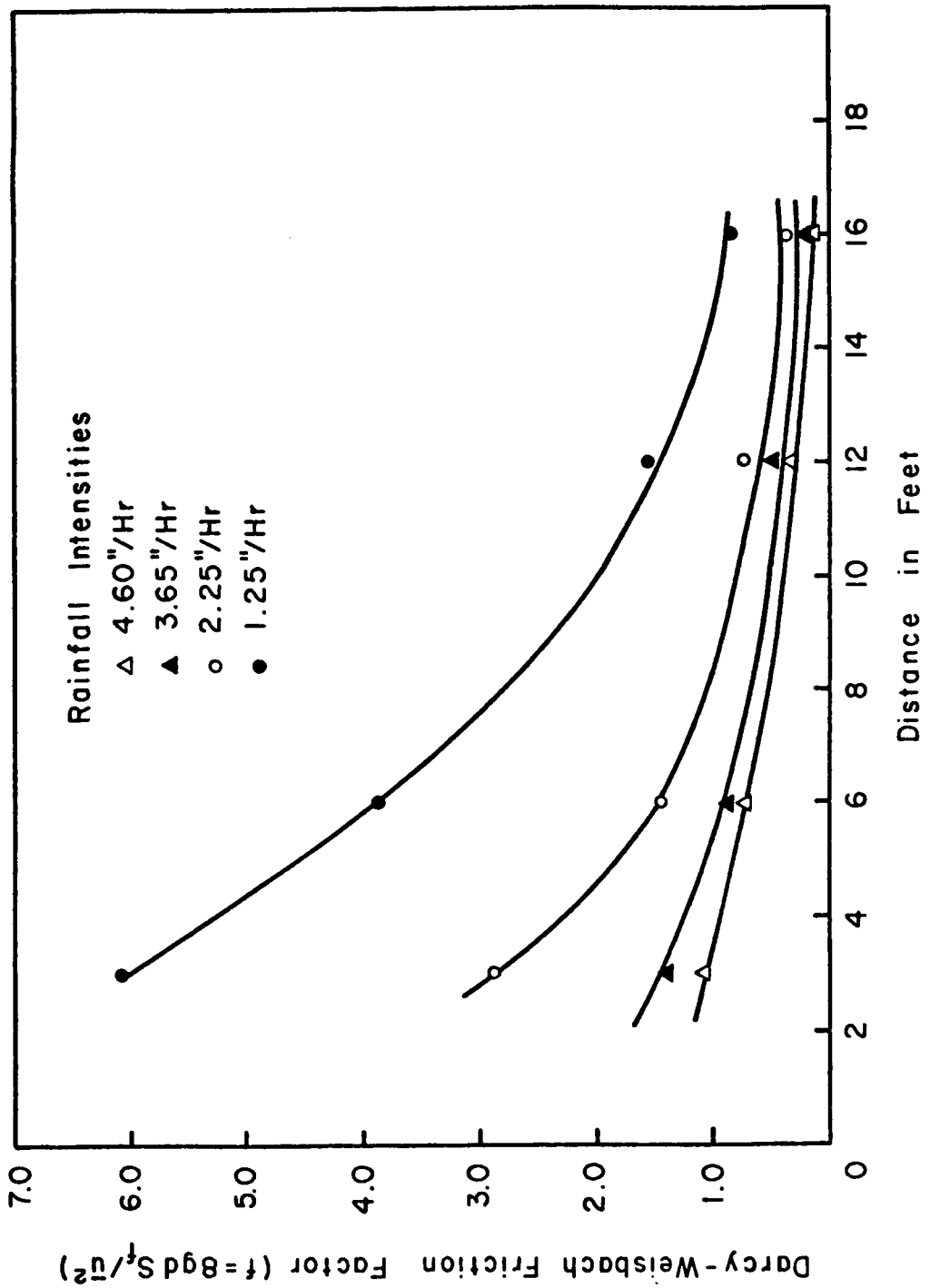

Fig. 4-24. Relationship between Darcy-Weisbach friction factor and distance for given rainfall intensities on 5.7 percent slope.

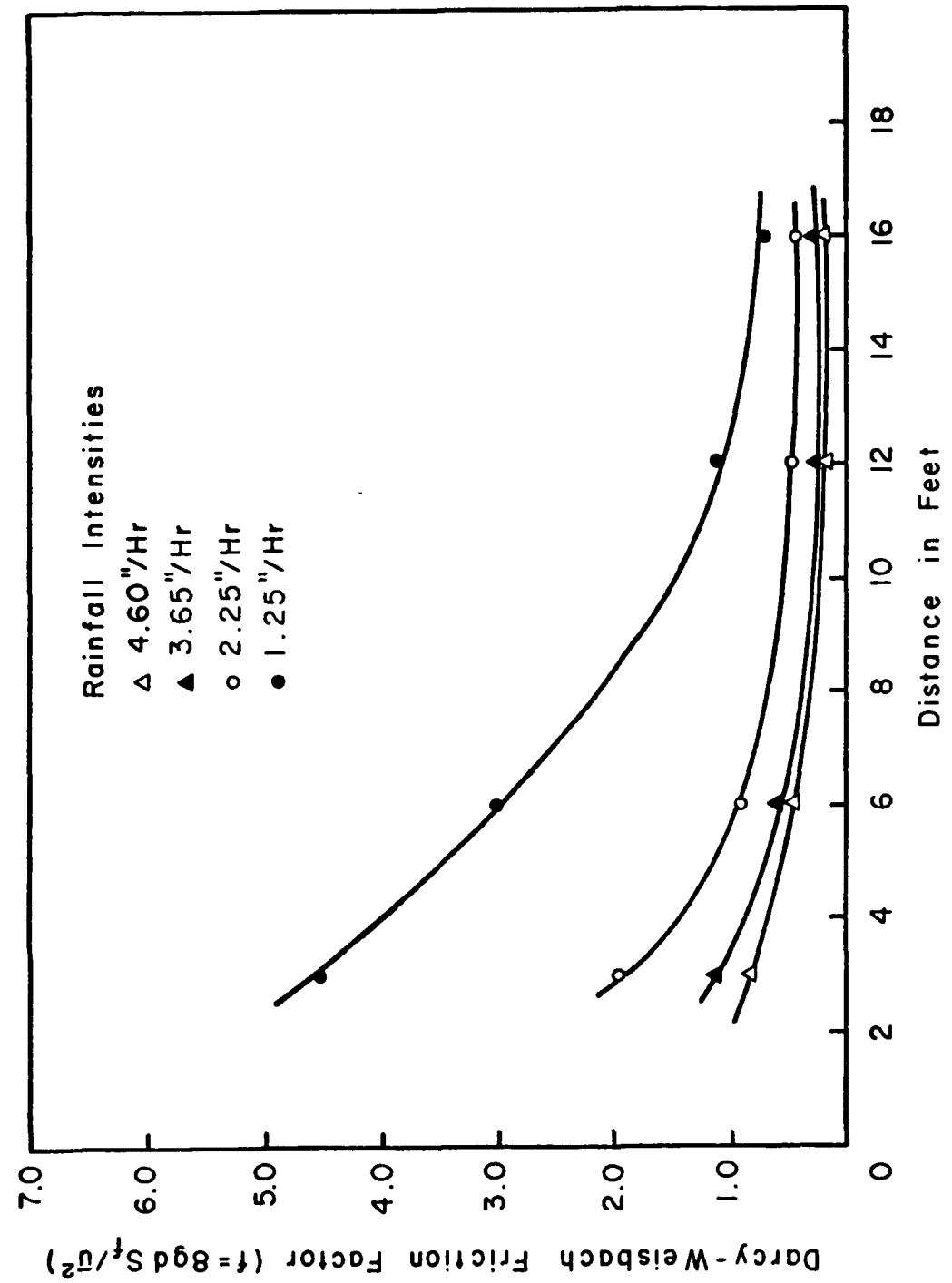

Fig. 4-25. Relationship between Darcy-Weisbach friction factor and distance for given rainfall intensities on 10 percent slope.

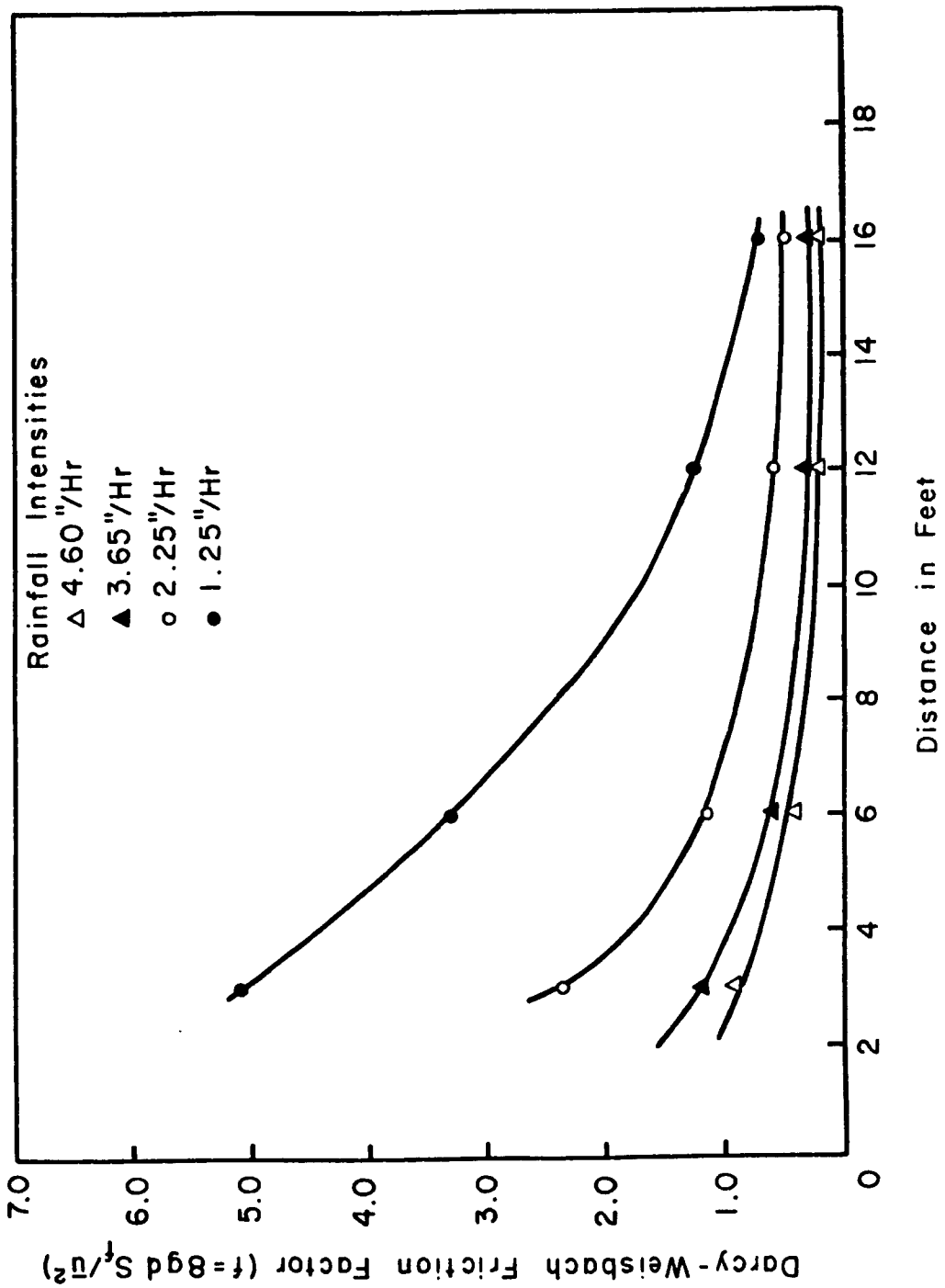

Fig. 4-26. Relationship between Darcy-Weisbach friction factor and distance for given rainfall intensities on 15 percent slope.

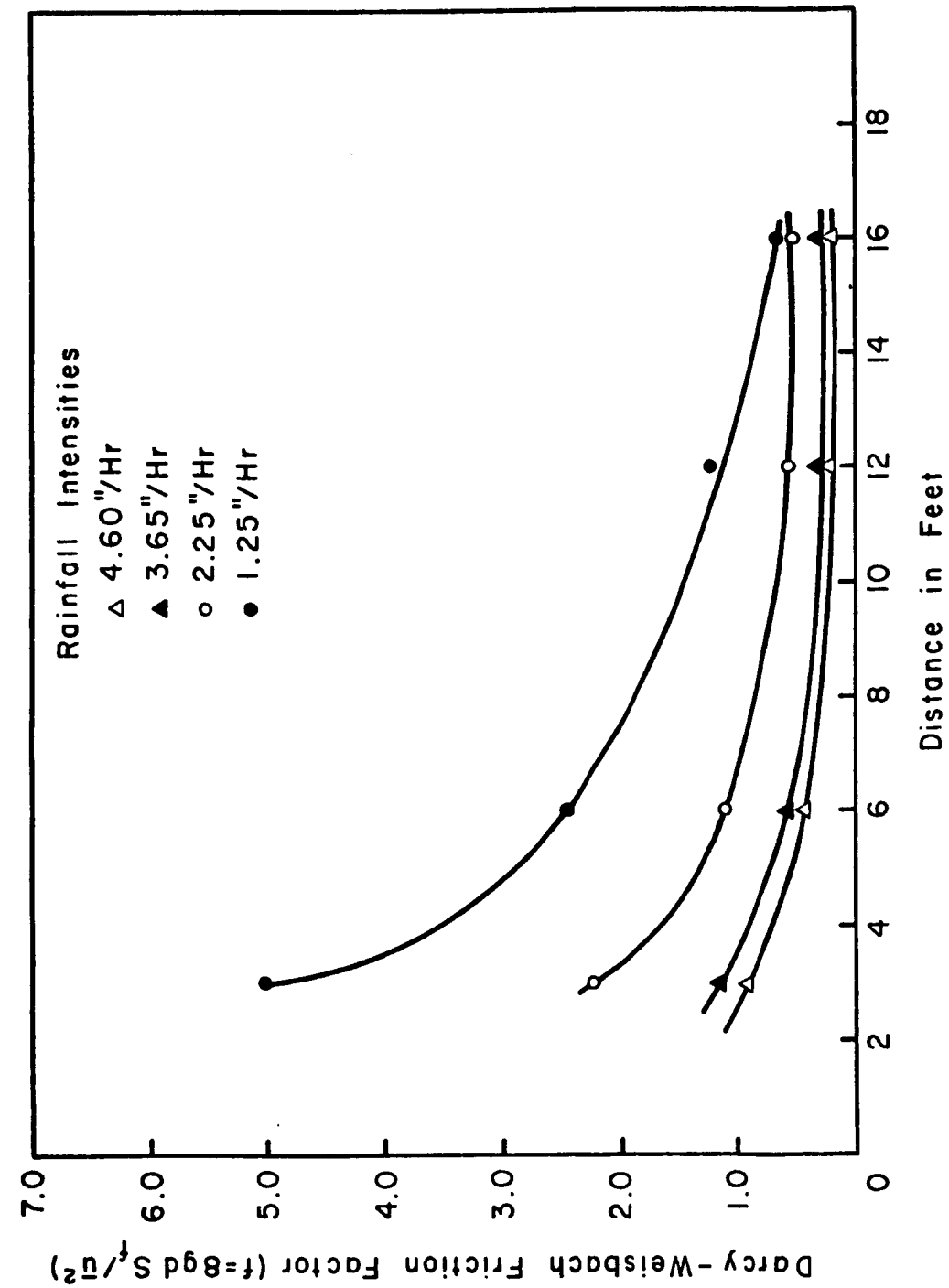

Fig. 4-27. Relationship between Darcy-Weisbach friction factor and distance for given rainfall intensities on 20 percent slope.

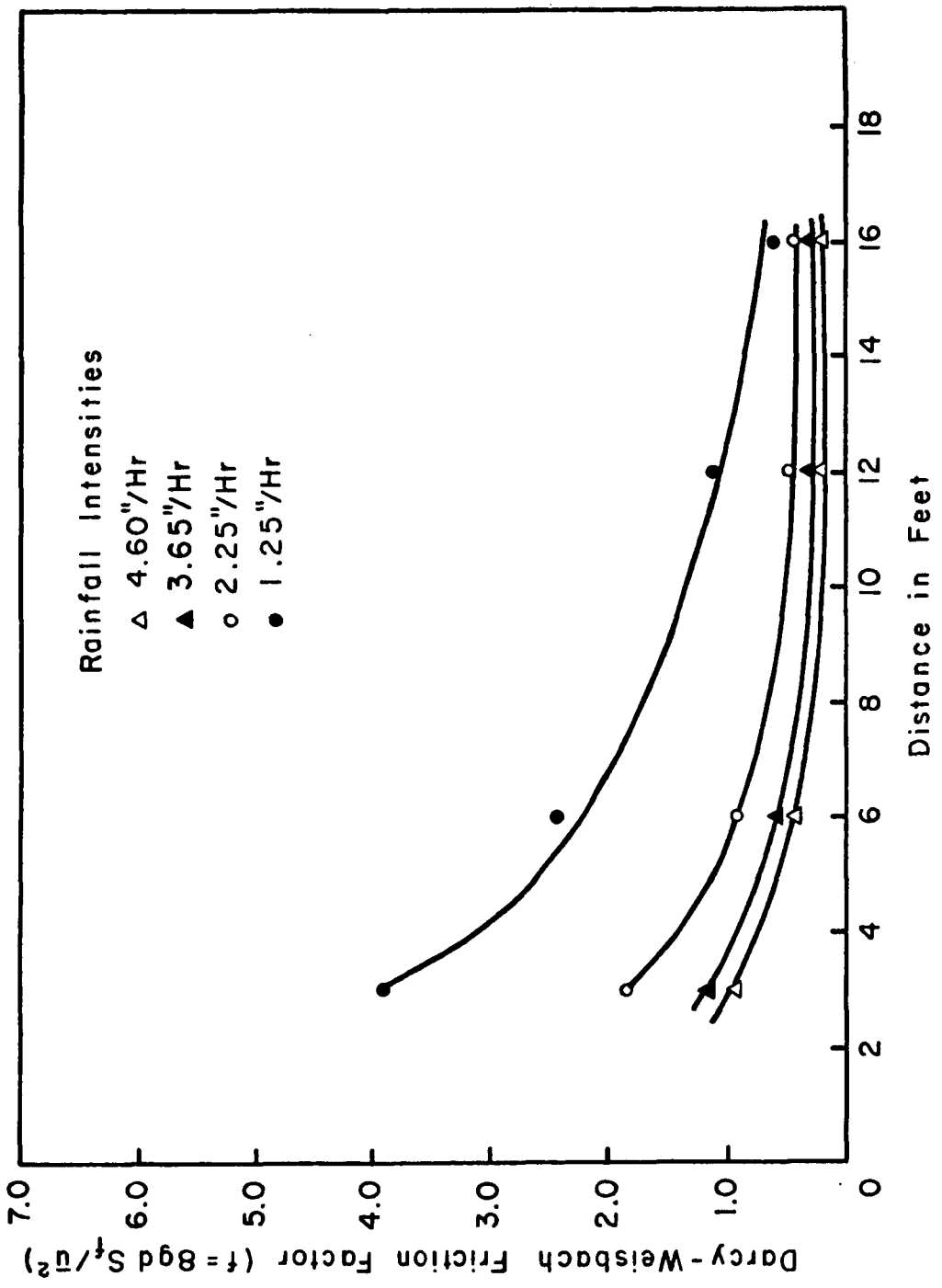

Fig. 4-28. Relationship between Darcy-Weisbach friction factor and distance for given rainfall intensities on 30 percent slope.

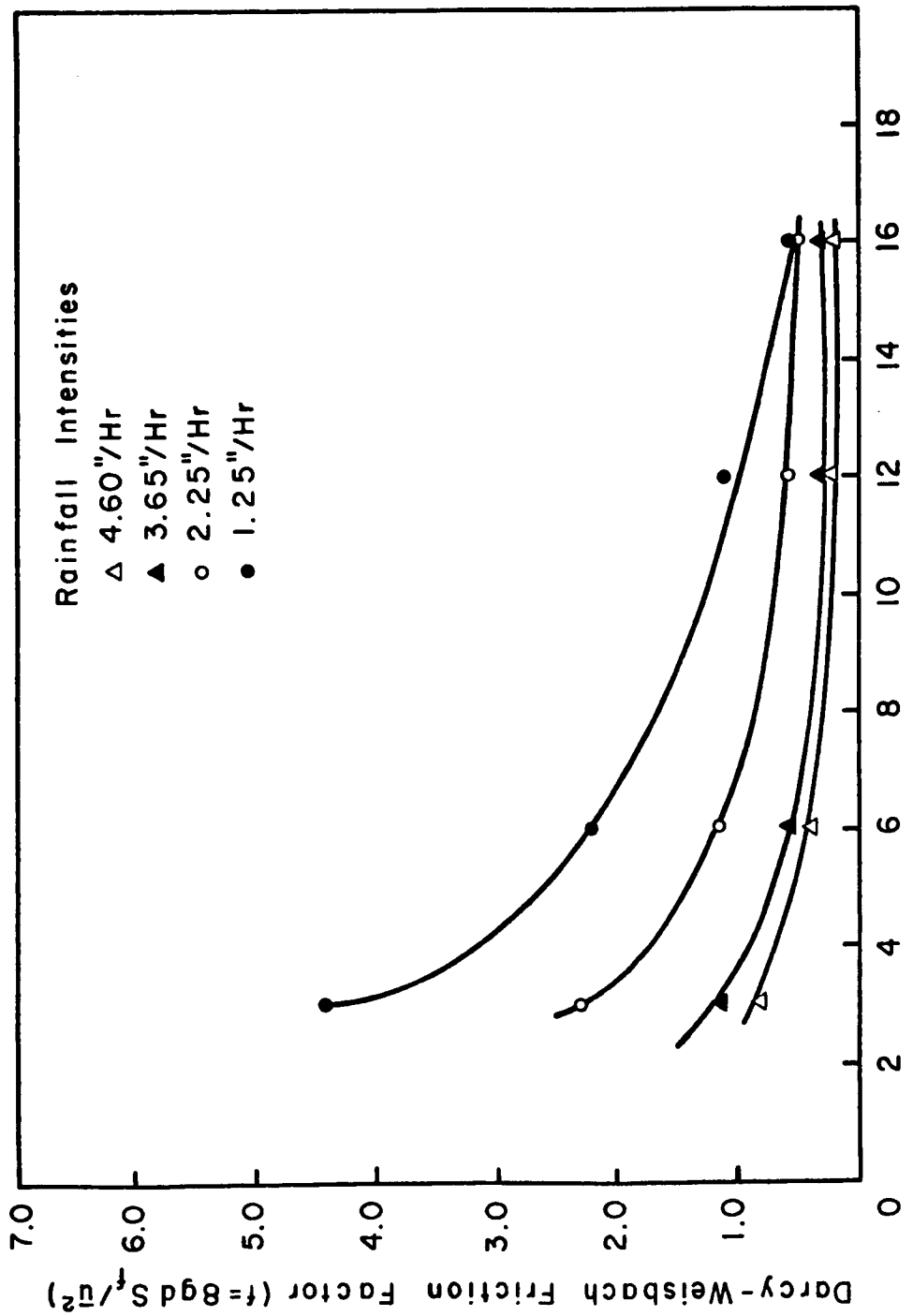

Fig. 4-29. Relationship between Darcy-Weisbach friction factor and distance for given rainfall intensities on 40 percent slope.

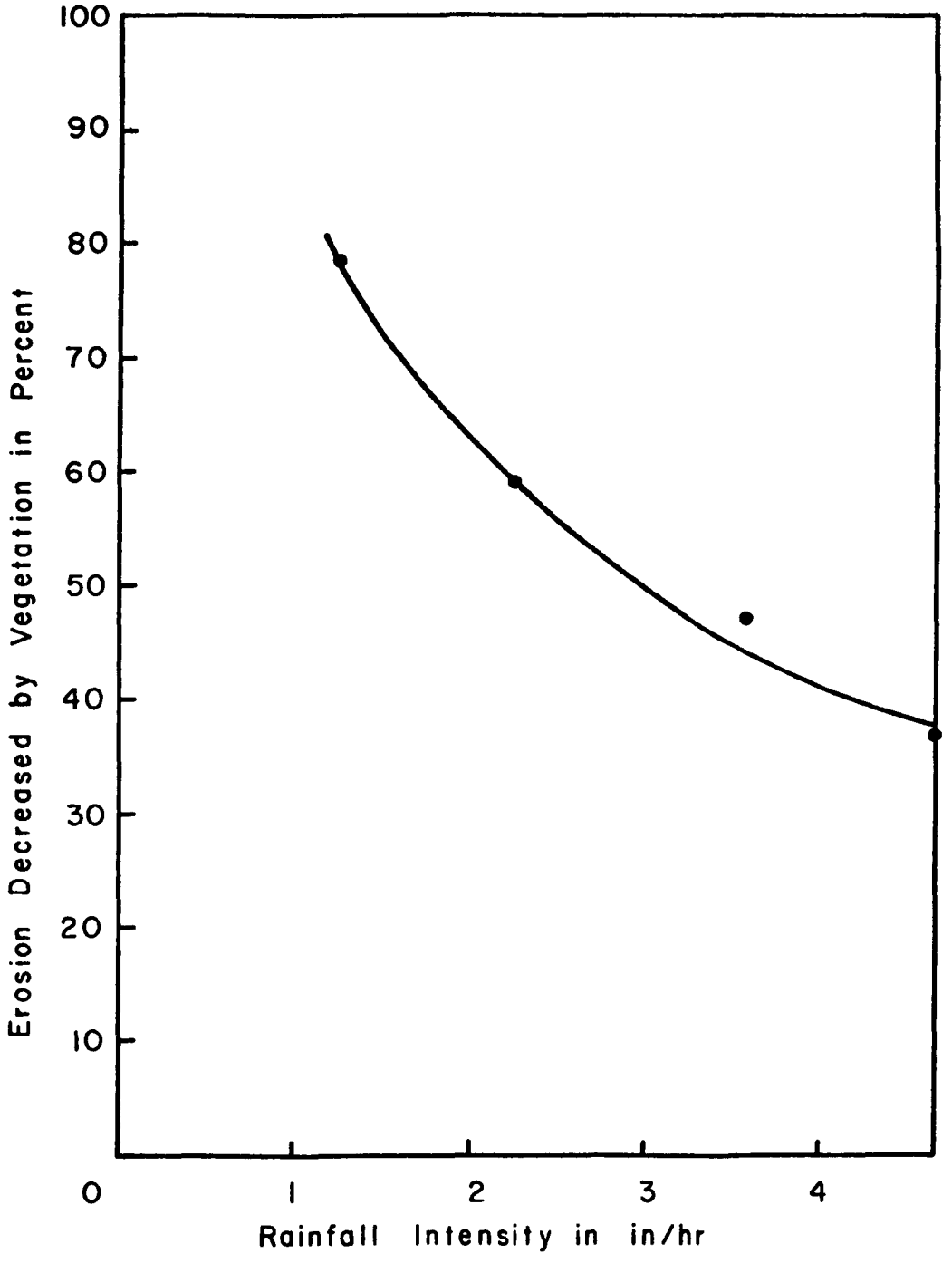

Fig. 4-30. Relationship between percentage of erosion decreased by vegetation and rainfall intensity on 40 percent slope (40 percent surface is covered with 3-4 inch high winter wheat).

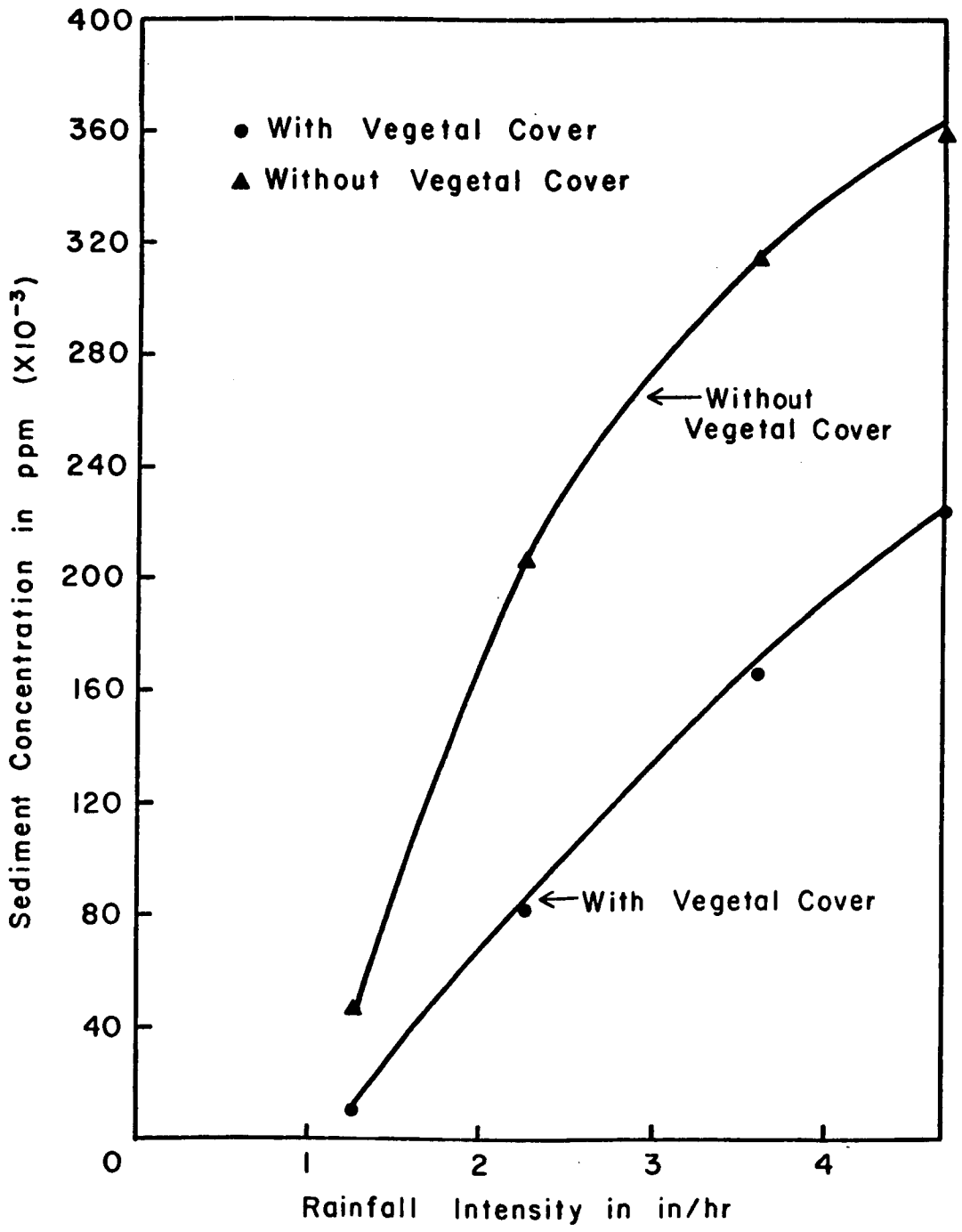

Fig. 4-31. Relationship between sediment concentration and rainfall intensity (with and without vegetal cover on 40 percent slope).

Major analyses are based on data from 24 runs without vegetation. Four runs with vegetation are used only for qualitative comparison. Data collected from vegetated surface included sediment concentration, sediment and water discharges.

Sediment transport and erosion rate correlations with independent variables show steady but nonlinear relationships. Nonlinear multiple regression anlaysis was performed on sediment discharge, sediment concentration, water discharge, rill volume and surface area, slope, rainfall intensity, rainfall excess, velocity, depth kinematic viscosity, median diameter of sand, bulk density and the Reynolds numbers.

For the purpose of analysis, sediment discharges, sediment concentration, erosion, median diameter of transported sediment, local mean velocity and depth of flow, gully volume and gully surface area were used individually as dependent variables. Slope, rainfall intensity, rainfall excess, median diameter of sediment, d_{50} , depth and mean velocity of flow, water discharge, kinematic viscosity, bulk density and length of slope (overland flow distance) were used as independent variables. Major dependent variables were erosion, sediment discharge, and concentration. Whenever these major variables were used as dependent variables, remaining variables were considered independent. When velocity, depth and median diameter of sediment were used as dependent variables, erosion, sediment discharge and concentration were not taken into account in the analysis. The single correlation matrix of variables used in this analysis, except rill volume and area, are shown in Table (4-15). Rills were analyzed separately.

TABLE 4-15. CORRELATION MATRIX OF MAJOR VARIABLES USED IN STEPWISE NONLINEAR REGRESSION ANALYSIS

Variable Number	C_s	C_s/A	q_s	E_r	S_o	q_o
Sediment concentration (C_s)	1.000	1.000	.961	.957	.816	.565
Concentration/area (C_s/A)		1.000	.963	.960	.808	.573
Sediment discharge (q_s)			1.000	1.000	.660	.758
Erosion (E_r)				1.000	.649	.766
Slope (S_o)					1.000	.054
Rainfall excess (q_o)						1.000

Variable Number	q	d_{50}	r	$\bar{u}$	d	ν
Sediment concentration (C_s)	.565	-.819	.524	.891	-.192	-.470
Concentration/area (C_s/A)	.573	-.814	.532	.893	-.181	-.463
Sediment discharge (q_s)	.758	-.685	.727	.968	.060	-.324
Erosion (E_r)	.766	-.677	.735	.969	.073	-.314
Slope (S_o)	.054	-.928	-.000	.571	-.696	-.734
Rainfall excess (q_o)	1.000	-.131	.996	.849	.676	.156
Water discharge (q)	1.000	-.131	.996	.849	.676	.156
Mean diameter of transported sediment (d_{50})		1.000	-.084	-.602	.596	.738
Rainfall intensity (r)			1.000	.819	.710	.174
Mean local velocity ($\bar{u}$)				1.000	.185	-.290
Depth of flow (d)					1.000	.696
Kinematic viscosity (ν)						1.000

The purpose of this analysis is to develop equations which would provide a means to predict sediment discharge or soil loss due to overland flow erosion for practical use in the field. It is hoped that such equations could utilize the readily available information for the soil type under consideration on slope and intensity of rainfall due to a single storm.

In the following sections, the results of computer analysis and equations, thus, derived are tabulated with brief explanations, wherever necessary. The correlations obtained from the computer are presented in the same sequence in which independent variables were first considered. Some less significant intermediate sequences are omitted. The increment, ΔR^2 , on coefficient of determination, R^2 , and change in standard error of estimate, SEE , thus can easily be seen. The standard error of estimate, SEE , is to be compared with the standard deviation of the dependent variable; the smaller the SEE , the better the equation. The coefficient of determination, R^2 , shows to what extent variations of dependent variables were explained by independent variables; the higher the R^2 , the better the equation (the range of R^2 is 0 to 1).

4.3.1 Sediment Concentration as a Dependent Variable

Computer Run Number (1): The purpose of this first run was to test whether the sediment concentration was steady or unsteady with respect to time. A one-hour run, therefore, was divided into 6 to 13 time intervals and instantaneous sediment concentration, C_i , was punched for each interval with corresponding slope, S_o , and intensities of rainfall, r . The result of the run showed that time did not

enter into the multiple regression analysis. This means that there is no significant change of concentration with respect to time. This result is very important and is used in further analysis. Because sediment concentration was steady, sediment transport was also steady. Since sediment concentration was steady, only the averaged values of sediment concentration, C_s, and discharge, q_s, for each run of a given slope and intensity were used throughout the analyses. All values were obtained at the end of 16 feet length. Moreover, the experimental data showed that water discharge, velocity, rainfall intensity and rainfall excess were steady. Consequently, flow was spatially varied with respect to distance but not time. Sediment discharge and concentration varied nonlinearly with respect to distance, water discharge varied linearly due to constant rainfall, and infiltration with respect to distance.

The first run of C_i as a function of S_o, r, and time gives:

Sequence of regression equations	R^2	SEE	ΔR^2	
$C_i = e^{13.888} S_o^{1.585}$	.6838	.6804	.6838	(4-12)
$C_i = e^{12.540} S_o^{1.225} r^{1.525}$	.9267	.3284	.2429	(4-13)

in which

C_i is in ppm,

S_o is in (ft/ft), and

e is the base of the natural logarithm.

As seen above, time did not enter the equation at all.

Computer Run Number (2): After the first run, the averaged sediment concentration, C_s, was related to S_o, q_o, $r/\bar{u}$, q, d_{50}, d_{50}/d_{50_o}, d_{50_o}, r, $\bar{u}$, d, ν. The variables which correlated most strongly with C_s were the mean velocity, $\bar{u}$, and slope, S_o. The equations obtained were:

Sequence of regression equations	R^2	SEE	ΔR^2	
$C_s = e^{6.926}\ \bar{u}^{2.258}$	.7947	.5615	.7947	(4-14)
$C_s = e^{9.600}\ \bar{u}^{.826}\ S_o^{1.600}$	.9347	.3241	.1400	(4-15)
$C_s = e^{62.323}\ \bar{u}^{.558}\ (r/\bar{u})^{3.196}$ $S_o^{2.330}\ \nu^{1.823}/d_{50}^{1.127}$	.9515	.3019	.0168	(4-16)

in which

C_s is in ppm,

$\bar{u}$ is in (ft/sec),

S_o is in (ft/ft),

ν is in (ft^2/sec) and

d_{50} is in millimeter (mm).

Computer Run Number (3): Eliminating d_{50}/d_{50_o}, $r/\bar{u}$ from the previous analysis, the equation,

$$C_s = e^{33.022}\ S_o^{.728}\ \bar{u}^{1.478}\ \nu^{2.934}/d_{50}^{1.096} \qquad (4\text{-}17)$$

was correlated with highest R^2, with R^2 equal to .9446 and SEE equal to .3188.

Computer Run Number (4): Using slope, S_o, and rainfall, r, with sediment concentration, C_s, the following equations were obtained:

Sequence of regression equations	R^2	SEE	ΔR^2	
$C_s = e^{13.660} S_o^{1.480}$	.6657	.7164	.6657	(4-18)
$C_s = e^{15.553} S_o^{1.479} r^{1.246}$	.9407	.3089	.2750	(4-19)

Computer Run Number (5): By changing the units of the variables and analyzing them, the same type of equations with the same coefficients and constants were found, as long as C_s was dimensionless.

Computer Run Number (6): Due to the constant effect of certain variables such as ν, d_{50}, d_b, and X, no significant correlation with sediment concentration could be obtianed. To enter the variables necessary for analysis, dimensionless forms were tried, and significant results were obtained. For example, X and ν did not give good results, but when they were used with a Reynolds number of $Re = q_o X/\nu$, a high correlation with sediment concentration was obtained. A similar result was obtained for sediment discharge because of the same reasons. The basis for the grouping of variables came from the results of dimensional analysis. The Reynolds number and slope were the most important parameters throughout the analysis, correlating with sediment discharge, sediment concentration and local mean velocity.

Because dimensional analysis of C_s gave, $C_s = \emptyset$ (Re, S_o, roughness), a regression analysis of C_s as a function of the Reynolds number and slope was run. The equation found was:

$$C_s = e^{9.554}\ Re^{.963}\ S_o^{1.453} \qquad (4\text{-}20)$$

with R^2 equal to .9220 and SEE equal to .3674.

Computer Run Number (7): Sediment concentration, C_s, was divided by the total area of flume, and the sediment concentration per unit area C_s/A was obtained. When C_s/A was run as a function of S_o, q_o, q, d_{50}, r, $\bar{u}$, d, a sequence of equations was obtained:

Sequence of regression equations	R^2	SEE	ΔR^2	
$C_s/A = e^{2.581}\ u^{2.231}$	.7981	.5487	.7981	(4-21)
$C_s/A = e^{5.140}\ u^{1.600}\ S_o^{.791}$	.9302	.3302	.1321	(4-22)
$C_s/A = e^{30.848}\ u^{1.548}\ S_o^{.956}\ \nu^{2.252}$	.9355	.3253	.0053	(4-23)
$C_s/A = e^{37.19}\ u^{1.475}\ S_o^{.678}\ \nu^{2.957}/d_{50}^{1.153}$	.9409	.3194	.0054	(4-24)

After $\bar{u}$ and S_o entered the Eq. (4-22), R^2 did not increase significantly by adding more variables. The variables $\bar{u}$ and S_o, therefore are of considerable importance.

If $(r/\bar{u})$ is added and q_o, q is eliminated from the independent variables, C_s/A will give the final relationship:

$$C_s/A = e^{57.669}\ S_o^{2.250}\ (r/\bar{u})^{3.136}\ u^{.572}\ \nu^{.868}/d_{50}^{1.184} \qquad (4\text{-}25)$$

with R^2 equal to .9477 and SEE equal to .3088.

If C_s/A were a function of only S_o and r, it would yield:

Sequence of regression equations	R^2	SEE	ΔR^2	
$C_s/A = e^{9.200} S_o^{1.144}$	.6532	.7192	.6532	(4-26)
$C_s/A = e^{11.095} S_o^{1.445} r^{1.246}$	.9363	.3156	.2831	(4-27)

4.3.2 Sediment Discharge as a Dependent Variable

As shown in Table (4-4), sediment discharge was first calculated in terms of pound per second per foot of width, then converted into different units, such as pound per hour, pound per hour per foot of width, pound per second, ton per hour per acre. Sediment discharge was also converted in terms of surface erosion loss in feet per hour, inches per hour, and inches per second. Surface erosion, as discussed previously, was defined as removal of soil surface layer in terms of a length unit. The following discussion will show these steps and sequences.

Computer Run Number (1): The first run of the computer was made with sediment discharge, q_s, (in terms of pound per second per foot of width) as the dependent variable and slope, S_o; rainfall intensity, r; rainfall excess, q_o; rainfall-velocity ration, $r/\bar{u}$; water discharge, q; mean diameter of transported sediment, d_{50}; transported-original sediment diameter ratio, d_{50}/d_{50_o}; mean local velocity, $\bar{u}$; depth of flow, d; and kinematic viscosity, ν, as independent variables. In Table (4-15), the correlation matrix, R, shows individual correlations between the variables. As seen in this table, the mean

velocity, $\bar{u}$, was the highest correlated variable with sediment discharge, q_s . Rainfall excess and water discharge followed the velocity with the same correlation matrix.

For the same reason as discussed previously, some variables did not correlate significantly due to constant effects. If these variables vary during the experiment, some of them will be significant for sediment discharge, such as, original median sediment diameter, d_{50} , kinematic viscosity, ν , and length of slope, X .

The following sequence of equations were obtained from stepwise regression analysis, where variables were individually selected.

Sequence of regression equations	R^2	SEE	ΔR^2	
$q_s = (1/e^{10.56})\ u^{3.625}$	.9372	.4589	.9372	(4-28)
(where $\bar{u}$ is in inches per second)				
$q_s = (1/e^{9.181})\ u^{3.284}\ S_o^{.428}$	.9544	.4000	.0172	(4-29)
$q_s = e^{72.670}\ u^{1.506}\ S_o^{3.217}$ $(r/\bar{u})^{5.644}$	.9719	.3394	.0175	(4-30)

in which

r and $\bar{u}$ are in inches per second and,

d_{50} is in mm.

Above analysis shows that mean velocity contributes almost 94 percent of variation in sediment discharge. Sediment discharge and sediment concentration analysis as dependent variables give similar results. Sediment concentration, C_s , exactly represents the sediment discharge,

q_s , because the entire overland flow was sampled at each sampling time for sediment concentration, so that total sediment discharge was covered.

Computer Run Number (2): When ratios of d_{50}/d_{50_o} and $(r/\bar{u})$ are eliminated from the first run, the results

$$q_s = e^{14.074} S_o^{2.585} u^{.695} d^{4.096}/d_{50}^{1.179} \quad , \qquad (4\text{-}31)$$

in which R^2 is equal to .9622 and SEE is equal to .3834.

Computer Run Number (3): Sediment discharge was run as a function of slope, S_o , and water discharge, q .

Sequence of regression equations	R^2	SEE	ΔR^2	
$q_s = e^{5.719} q^{2.129}$	.5747	1.1945	.5747	(4-32)
$q_s = e^{8.280} q^{2.035} S_o^{1.664}$	.9588	.3805	.3841	(4-33)

in which

q is represented in terms of inches per second of runoff,

S_o is represented in terms of percentage and,

q_s is represented in terms of pounds per second per foot of width. When q is used in terms of Cfs/ft of width, a similar equation with a different constant is obtained:

$$q_s = e^{11.727} q^{2.035} S_o^{1.664} \quad , \qquad (4\text{-}34)$$

in which R^2 is equal to .9588 and SEE is equal to .3805.

Computer Run Number (4): The following correlations were obtained where sediment discharge was related to rainfall excess, q_o, and slope, S_o.

Sequence of regression equations	R^2	SEE	ΔR^2	
$q_s = e^{7.667} q_o^{2.130}$	.5747	1.1945	.5747	(4-35)
$q_s = e^{10.504} q_o^{2.035} S_o^{1.664}$	.9588	.3805	.3841	(4-36)

in which

q_s is represented in terms of pounds per hour and,

q_o is represented in terms of feet per hour.

Rainfall excess is the exact representation of water discharge because water discharge is equal to rainfall excess times constant slope length ($q = q_o X$).

Computer Run Number (5): Sediment discharge in terms of feet per hour was related to rainfall intensity r in terms of feet per hour and slope, S_o.

Sequence of regression equation	R^2	SEE	ΔR^2	
$q_s = e^{8.04} r^{2.552}$	.5280	1.2584	.5280	(4-37)
$q_s = e^{11.226} r^{2.552} S_o^{1.770}$	.9635	.3581	.4355	(4-38)

Computer Run Number (6): Mean local velocity, $\bar{u}$, depth of flow, d, and kinematic viscosity, ν, are correlated with sediment discharge q_s:

Sequence of regression equations	R^2	SEE	ΔR^2	
$q_s = (1/e^{10.564}) \bar{u}^{3.625}$	.9372	.4589	.9372	(4-39)
$q_s = (1/e^{13.247}) \bar{u}^{3.711}/d^{.650}$	.9521	.4104	.0149	(4-40)
$q_s = (1/e^{36.018}) \bar{u}^{3.955}$ $\nu^{4.634}/d^{1.260}$	.9596	.3860	.0075	(4-41)

in which

q_s is represented in terms of pounds per second,

$\bar{u}$ is represented in terms of inches per second and,

d is represented in terms of inches per second.

Computer Run Number (7): Sediment discharge as a function of velocity, $\bar{u}$, the Reynolds number, Re, slope, S_o, depth, d, rainfall excess, q_o, and water discharge, q, was analyzed. The correlations are:

Sequence of regression equations	R^2	SEE	ΔR^2	
$q_s = (1/e^{3.166}) \bar{u}^{3.625}$	.9372	.4589	.9372	(4-42)
$q_s = e^{1.239} \bar{u}^{4.674}/Re^{.878}$	.9554	.3959	.0282	(4-43)

in which

$\bar{u}$ is represented in terms of feet per second and,

q_s is represented in terms of pounds per second per foot of width.

Computer Run Number (8): Sediment discharge as a function of $\bar{u}$ and q gives:

$$q_s = (1/e^{7.250}) \bar{u}^{4.360}/q^{.650} \quad (4\text{-}44)$$

in which R^2 is equal to .5747 and SEE is equal to 1.1945. The results are exactly the same as those for Eq. (4-32) except that they are constant due to different unit. This is always true if sediment discharge or other variables are expressed in different units for different times. Analysis gives similar correlations with different constants.

Computer Run Number (9): Sediment discharge was related to the Reynolds number, Re , and slope, S_o , due to the same reason as discussed previously under sediment concentration analysis. The results are:

Sequence of regression equations	R^2	SEE	ΔR^2	
$q_s = (1/e^{15.295}) \, Re^{2.300}$	.6625	1.0641	.6625	(4-46)
$q_s = (1/e^{11.645}) \, Re^{2.054} \, S_o^{1.460}$	.9517	.4119	.2892	(4-47)

in which q_s is represented in terms of pounds per second per foot of width. Equation (4-47) presents the most simple and practical relation. Because important factors such as, X and ν did not enter into the correlations because of this constant effect, dimensionless parameters of Re and S_o related to q_s so that X and ν entered into the equation indirectly.

Computer Run Number (10): Sediment discharge was related to tractive force and stream power under the previously assumed models of $q_s = K_n (\tau_o - \tau_c)^n$ and $q_s = K_m ((\tau_o - \tau_c) \bar{u})^m$. To find constants, K_n and K_m , and coefficients, n and m , of these models, τ_o

should be determined. As mentioned before, τ_o was calculated in three ways: by uniform flow assumption, by using Eq. (2-43) which was obtained by Li (1972), from statistical analysis, and by solving the momentum equation for τ_o (Eq. 2-55) by numerical approximation. The three-way determination of τ_o will result in a different value of constants and coefficients in models. Moreover, if m and n are assumed to be equal to unity, the models will be linear. For a linear model with τ_o of uniform flow, the relations obtained from computer analysis are:

Linear regression equations	R^2	SEE	ΔR^2	
$q_s = 1.0\ (\tau_o - \tau_c)$	.9222	.0055	.9222	(4-48)
$q_s = .71274\ (\tau_o - \tau_c)\ \bar{u}$	.9663	.0036	.0441	(4-49)

For nonlinear model, with τ_o of uniform flow, the relations are:

Nonlinear regression equations	R^2	SEE	ΔR^2	
$q_s = e^{1.513}\ (\tau_o - \tau_c)^{1.480}$	.8694	.6620	.8694	(4-50)
$q_s = (1/e^{.327})((\tau_o - \tau_c)\ \bar{u})^{1.089}$	.9598	.4189	.0904	(4-51)

Using Eq. (2-43), if τ_o is calculated and used for these models, the following linear and nonlinear model relations were obtained from computer analysis:

Linear regression equations	R^2	SEE	ΔR^2	
$q_s = .19907\ (\tau_o - \tau_c)$	.7377	.0102	.7377	(4-52)
$q_s = .28052\ (\tau_o - \tau_c)\ \bar{u}$	.9281	.0058	.1904	(4-53)

Nonlinear regression equations	R^2	SEE	ΔR^2	
$q_s = e^{2.05256} (\tau_o - \tau_c)^{2.784}$	.8659	.6339	.8659	(4-54)
$q_s = e^{.12249} ((\tau_o - \tau_c) \bar{u})^{1.667}$	.9476	.4216	.0817	(4-55)

The third way of calculating τ_o was the use of the momentum equation derived in Chapter II. Calculated τ_o from the momentum equation was used in the linear and nonlinear models. The equations obtained from computer analysis are:

Linear regression equations	R^2	SEE	ΔR^2	
$q_s = .33932 (\tau_o - \tau_c)$	.6184	.01942	.6184	(4-56)
$q_s = .5357 (\tau_o - \tau_c) \bar{u}$	.8517	.0076	.2433	(4-57)
Nonlinear regression equations	R^2	SEE	ΔR^2	
$q_s = e^{2.716} (\tau_o - \tau_c)^{2.506}$	.8094	.7997	.8094	(4-58)
$q_s = e^{.7441} ((\tau_o - \tau_c) \bar{u})^{1.584}$	.9195	.5196	.1101	(4-59)

As a result of above analysis, nonlinear models yield better correlation than linear models except for uniform flow assumption.

4.3.3 Averaged Surface Erosion Depths as Dependent Variables

Surface erosion, E_r, was expressed in terms of inches and feet of surface depth per second per hour. Surface erosion, E_r, was correlated with given independent variables in the same kind of nonlinear multiple regression analysis. Erosion, E_r, is also another way of expressing sediment discharge.

Computer Run Number (1): The erosion rate was analyzed with ten independent variables of slope, S_o, rainfall excess, q_o, rainfall intensity-mean velocity ratio, $r/\bar{u}$, water discharge, q, median diameter of transported sediment-original sediment ratio, d_{50}/d_{50_o}, rainfall intensity, r, mean velocity, $\bar{u}$, depth, d, and kinematic viscosity, ν. All the variables are in terms of feet per hour except d_{50} which is in mm; d is in inches and viscosity is in ft^2 per second. The correlations were obtained from the computer in the following sequence:

Sequence of equations	R^2	SEE	ΔR^2	
$Er = (1/e^{31.735})\ u^{3.593}$	.9388	.4488	.9388	(4-60)
$Er = e^{17.154}\ u^{3.500}\ \nu^{4.754}/d_{50}{}^{1.235}\ d^{.615}$	.9608	.3865	.0220	(4-61)

in which Er is measured in feet of eroded soil surface depth per hour. Mean velocity is the first variable entered and d_{50}, ν, and d follow the velocity in entering correlation but they did not increase R^2 significantly, only about 2 percent. Although rainfall excess, water discharge and slope are important factors in erosion, they do not enter into the correlation because velocity, which has high correlation with them, entered first; therefore, others are dropped out from analysis. This means that velocity takes care of the influence of q, q_o, and S_o on correlation.

Computer Run Number (2): When $(r/\bar{u})$ was eliminated from the above analysis and the variables were converted into units of inches

per second, except for d_{50} which is in mm, ν which is in ft^2 per second, and d which is in feet, almost the same type of relation was obtained except that q entered the equation after $\bar{u}$, d_{50} and ν instead of after d. The equation is:

$$Er = e^{31.412}\ \bar{u}^{4.115}\ \nu^{4.754}/d_{50}^{1.235}\ q^{.615} \quad , \qquad (4\text{-}62)$$

in which R^2 equals .9608 and SEE equals .3865.
If Eq. (4-61) is compared with Eq. (4-62) the only difference between the two is that q is selected by the computer instead of d, with the same coefficient as before because both have the same partial correlation coefficient. Therefore, the computer picks one of them with the same effectiveness as in the correlation of erosion. Thus, one of them may be written for the other.

Computer Run Number (3): When $(r/\bar{u})$, $\bar{u}$, d and ν were eliminated, different equations were obtained. Erosion, Er, was correlated to S_o, q_o, q, d_{50}/d_{50_o}, and r in terms of ft/hr, except that d_{50} is in mm, and S_o and d_{50}/d_{50_o} are dimensionless. Because $\bar{u}$ was not in the analysis, the first variable entered into the correlation was q_o, with following sequences:

Sequence of regression equations	R^2	SEE	ΔR^2	
$Er = (1/e^{1.254})\ q_o^{2.130}$	.5866	1.1663	.5866	(4-63)
$Er = e^{1.506}\ q_o^{2.038}\ S_o^{1.618}$	.9571	.3845	.3705	(4-64)
$Er = (1/e^{.022})\ q_o^{2.013}\ S_o^{1.338}/d_{50}^{.920}$	.9588	.3860	.0017	(4-65)

The second variable, S_o, when entered into the correlation increased the result by 37 percent. The last variable entered was, d_{50}, although it did not change R^2 significantly.

Computer Run Number (4): When the above variables were converted into units of inches per second, the same equations with same coefficients, except for the constant which was different, were obtained:

Sequence of regression equations	R^2	SEE	ΔR^2	
$Er = e^{7.429}\ q_o^{2.038}\ S_o^{1.618}$	.9571	.3845	.9571	(4-66)
$Er = e^{5.754}\ q_o^{2.013}\ S_o^{1.338}/d_{50}^{.920}$	.9588	.3860	.0017	(4-67)

Computer Run Number (5): Erosion, Er, as a function of only slope, S_o, and water discharge, q, gave the following sequence of regression equations:

Sequence of regression equations	R^2	SEE	ΔR^2	
$Er = (1/e^{1.254})\ q^{2.130}$	.5860	1.1663	.5860	(4-68)
$Er = e^{1.506}\ q^{2.038}\ S_o^{1.618}$	.9571	.3845	.3705	(4-69)

in which

Er is in feet of eroded soil surface per hour,

q is in feet per hour (depth of runoff), and

S_o is in percent.

Equations (4-64) and (4-65) are exactly the same as Eqs. (4-68) and (4-69) because q is an exact representation of q_o.

The variables although in different units give the same type of correlation, except for the constant, as follows:

$$Er = e^{1.778}\, q^{2.038}\, S_o^{1.618} \qquad (4\text{-}70)$$

in which

Er is in inches of eroded soil per second,

q is in inches per second, and

R^2 equals .9571 and SEE equals .3845.

In conclusion, sediment discharge, q_s, sediment concentration, C_s, and erosion, Er, produce similar correlations using independent variables, except for the effect of the constants used.

4.3.4 Median Transported Sediment Diameter, d_{50}, and the d_{50}/d_{50_o} Ratio as Dependent Variables

Computer Run Number (1): Median transported sediment diameter, d_{50}, for each run was related to slope, S_o, and intensity of rainfall, r. The correlations are:

Sequence of regression equations	R^2	SEE	ΔR^2	
$d_{50} = 1/e^{1.617}\, S_o^{.306}$	.8612	.0840	.8612	(4-71)
$d_{50} = 1/e^{1.673}\, S_o^{.306}\, r^{.037}$	.8683	.0838	.0071	(4-72)

in which

d_{50} is in mm, and

r is in feet per hour.

The slope was the first to enter the equation with a high negative correlation. In this run r, when entered was not significant at all. Negative correlation of d_{50} with slope could be explained by the

fact that finer sediments are washed down faster than coarser sediments on steeper slope because of the lack of cohesiveness of the particles. Different units of r only change the value of the constant, as follows:

$$d_{50} = 1/e^{1.880}\ S_o^{.306}\ r^{.037} \quad , \tag{4-73}$$

with R^2 equal to .8683 and SEE equal to .0838, with r in inches per second.

Computer Run Number (2): The ratio between d_{50} and d_{50_o} as a function of S_o and r gives:

Sequence of regression equations	R^2	SEE	ΔR^2	
$d_{50}/d_{50_o} = e^{.493}\ S_o^{.306}$	.8612	.0840	.8612	(4-74)
$d_{50}/d_{50_o} = d^{.550}\ S_o^{.306}\ r^{.0364}$	.8683	.0837	.0071	(4-75)

with r in feet per hour, and

$d_{50}/d_{50_o} = e^{.756}\ S_o^{.306}\ r^{.036}$	.8683	.0837	.0071	(4-76)

with r in inches per second.

Correlating d_{50} or d_{50}/d_{50_o} to slope and intensity of rainfall gives the same relationships, because d_{50_o} is constant for all runs.

Computer Run Number (3): This computer run also attempted to obtain relationships with d_{50} as a function of the remaining independent variables; the following result was obtained:

$$d_{50} = e^{8.148}\, r^{.045}\, \nu^{.768}/(C_s/A)^{.078}\, S_o^{.145} \qquad (4\text{-}77)$$

with R^2 equal to .8908 and SEE equal to .0812, with r in inches per second.

4.3.5 Mean Velocity of Overland Flow as a Dependent Variable

The results of statistical analysis up to this point show that velocity is one of the variables most highly correlated to sediment discharge, concentration, and erosion. Therefore, it is necessary to know what other variables are correlated with velocity itself. However, velocity was assumed to be an independent variable with regard to sedimentation, but velocity is dependent upon slope, rainfall intensity, or excess and surface roughness. This analysis will help us determine the variables significantly correlated to sediment discharge, concentration and erosion.

So far the distance, X , has not been included as a variable in the analysis. Now the distance, X , is entered into the analysis by using measured velocities at distances 3, 6, 12 and 16 feet, so that velocity appears as a function of distance as well as other independent variables. Velocity as a function of slope, S_o , rainfall excess, q_o , depth of flow, d , kinematic viscosity, ν , and distance, X , gives the following sequence of regression equations:

Sequence of regression equations	R^2	SEE	ΔR^2	
$\bar{u} = e^{5.220}\, q_o^{.663}$	.4054	.5081	.4054	(4-78)
$\bar{u} = e^{4.160}\, q_o^{.663}\, X^{.592}$	.6714	.3805	.2660	(4-79)

Sequence of regression equations (Continued)	R^2	SEE	ΔR^2	
$\bar{u} = (1/e^{5.782})\ q_o^{1.156}$ $X^{1.236}/d^{1.902}\ S_o^{.484}$	.8548	.2567	.1834	(4-80)
$\bar{u} = (1/e^{24.733})\ q_o^{1.188}$ $X^{1.238}/d^{1.910}\ S_o^{.596}\ \nu^{1.691}$	.8641	.2502	.0093	(4-81)

in which

$\bar{u}$ is in feet per second at a given distance,

q_o is in feet per second, and

d is in feet.

The most significant variables are q_o and X . The slope gives negative correlation because d enters into the equation before S_o so that slope and d are related with each other in negative correlation.

Computer Run Number (2): When d is eliminated from the above analysis, the result is:

Sequence of regression equations	R^2	SEE	ΔR^2	
$\bar{u} = e^{5.220}\ q_o^{.663}$	.4054	.5081	.4054	(4-82)
$\bar{u} = e^{4.160}\ q_o^{.663}\ X^{.592}$	.6714	.3805	.2660	(4-83)
$\bar{u} = e^{4.625}\ q_o^{.641}\ X^{.592}\ S_o^{.375}$	.8138	.3082	.1424	(4-84)
$\bar{u} = (1/e^{13.98})\ q_o^{.641}\ X^{.592}$ $S_o^{.375}/\nu^{1.664}$	.8228	.2886	.0090	(4-85)

Equations (4-84) and (4-85) are similar to Eq. (2-36), derived analytically, except for the constant and the coefficients which differ slightly. When d is removed from analysis, the slope is positively correlated with velocity.

Computer Run Number (3): Finally, as for C_s and q_s with Reynolds number, Re , and slope, S_o , velocity, $\bar{u}$, also was run through the computer as a function of Re and S_o . Reynolds number, Re , was the most highly correlated independent variable, accounting for 70.4 percent of the variation in this analysis. The correlations are:

Sequence of regression equations	R^2	SEE	ΔR^2	
$\bar{u} = (1/e^{3.37691}) \, Re^{.651}$	.7042	.3584	.7042	(4-86)
$\bar{u} = (1/e^{2.69687}) \, Re^{.627} \, S_o^{.336}$	.8177	.2834	.1135	(4-87)

The calculated velocities in Eq. (4-87) will be compared with measured velocities in the subsequent sections.

4.3.6 Depth of Flow as Dependent Variable

Computer Run Number (1): Depth as a function of X , q_o , S_o and ν gives the following equations:

Sequence of regression equations	R^2	SEE	ΔR^2	
$d = (1/e^{7.502})/S_o^{.438}$	.5395	.2683	.5395	(4-88)
$d = (1/e^{8.110}) \, X^{.340}/S_o^{.438}$	.7811	.1863	.2416	(4-89)
$d = (1/e^{5.472}) \, X^{.340} \, q_o^{.271}/S_o^{.452}$	.9685	.0712	.1874	(4-90)

Kinematic viscosity, ν , did not enter into regression. Depth of flow is related to slope in negative correlation as opposed to velocity. When slope becomes steeper, depth of flow changes from subcritical to supercritical.

Computer Run Number (2): Depth as a function of Reynolds number, Re , and slope, S_o , as opposed to the analysis of velocity, was correlated first with S_o before Re is negative correlation. The equations are:

Sequence of regression equations	R^2	SEE	ΔR^2	
$d = (1/e^{7.502})/S_o^{.438}$	.5394	.2683	.5394	(4-91)
$d = (1/e^{8.537})\ Re^{.304}/S_o^{.473}$	.9632	.0768	.4237	(4-92)

To conclude, throughout all of the analyses ν has no significance because of its constant effect during experimentation. Velocity, rainfall excess, slope, and Reynolds number are the important variables that are significantly correlated to sediment discharge, concentration, and erosion. Although length of slope, X , is an important factor affecting erosion and sediment discharge, it can not be tested in this study because X has almost a constant value during all runs except for a slight increase due to change of slope. This is one of the limitations inherent in the study; future research should eliminate the limitation.

4.4 RILL ANALYSIS

The rate of rill erosion mainly depends on rainfall intensity, slope of surfact, properties of soil and surface conditions (roughness,

vegetation, tillage, etc.). Rill erosion starts by channelizing flow through microchannels that are smaller than rills. If channels can be obliterated by tillage they are called rills, if they can not be they are called gullies. Thus gully is an advanced stage of a rill, whereas a rill is an advanced stage of sheet erosion. Evaluation and prediction of rill and gully development is not an easy task because the factors affecting rill and gully development are not well defined (Schwab, et al., 1966).

In this section the values and the ratios obtained from rill observations were analyzed by computer in terms of given independent variables. In the following analyses, rainfall intensity, r, and rainfall excess, q_o, are expressed in terms of ft/sec, water discharge, q, is expressed in terms of cfs/ft of width; Re and S_o are dimensionless; rill area/total area ratio, A_R/A_T and, total volume/rill volume ratio, V_R/V_T, are dimensionless; averaged depth of gully, D_R, is expressed in terms of ft/hr/ft of width and volume of gully, V_R, is expressed in terms of $ft^3/hr/ft$ of width.

4.4.1 Rill/Surface Area Ratio as a Dependent Variable

The surface area of rills for each run divided by the total area of flume surface gives the rill/area ratio, A_R/A_T. This ratio is analyzed in terms of surface slope, intensity of rainfall, rainfall excess, water discharge, and Reynolds number.

Computer Run Number (1): Eliminating q_o, q, and Re, the A_R/A_T ratio as a function of r and S_o gives:

Sequence of regression equations	R^2	SEE	ΔR^2	
$A_R/A_T = (1/e^{1.597})\ r^{.415}$	.7052	.1398	.7052	(4-93)
$A_R/A_T = (1/e^{1.269})\ r^{.415}\ S_o^{.183}$	.9400	.0645	.2348	(4-94)

Thus, rainfall intensity explains 70.5 percent of all variations in the rill area ratio.

Computer Run Number (2): Eliminating r , q , and Re , the ratio A_R/A_T as a function of q_o and S_o gives:

Sequence of regression equations	R^2	SEE	ΔR^2	
$A_R/A_T = e^{2.146}\ q_o^{.340}$	.7418	.1308	.7418	(4-95)
$A_R/A_T = e^{2.352}\ q_o^{.331}\ S_o^{.165}$	.9341	.0676	.1923	(4-96)

Computer Run Number (3): The ratio A_R/A_T as a function of q and S_o yields:

Sequence of regression equations	R^2	SEE	ΔR^2	
$A_R/A_T = e^{1.204}\ q^{.340}$	.7418	.1308	.7418	(4-97)
$A_R/A_T = e^{1.435}\ q^{.331}\ S_o^{.165}$	.9341	.0676	.1923	(4-98)

Computer Run Number (4): The A_R/A_T ratio as a function of slope and Reynolds number yields the following dimensionless form of correlation:

Sequence of regression equations	R^2	SEE	ΔR^2	
$A_R/A_T = (1/e^{2.686})\ Re^{.356}$	.7975	.1158	.7975	(4-99)
$A_R/A_T = (1/e^{2.345})\ Re^{.338}\ S_o^{.14357}$	.9406	.0142	.1431	(4-100)

The Reynolds number is the variable most correlated to A_R/A_T . Almost 80 percent of the variations are explained by Re . Water discharge gives the same correlation as rainfall excess with a dependent variable, excluding the constant. Therefore, q was eliminated from further analyses.

4.4.2 Rill Averaged Depth as a Dependent Variable

Measured depths of rills at the end of each run were averaged as representative of each run. These averaged values were correlated to the independent variables of rainfall intensity, slope, rainfall excess, and Reynolds number and are given in computer runs numbers (1), (2), (3) and (4) under the rill/surface area ratio. The results of the analysis of rill depth as a function of given variables have been combined and given simultaneously.

Computer Runs Numbers (1), (2), (3) and (4): Rill depth, D_R , was first related to r and S_o , then, q_o and S_o , and finally to Re and S_o . Keeping the slope in the analysis for each trial, the other independent variables were changed. The sequence of correlations obtained from these analyses are as follows:

Sequence of regression equations	R^2	SEE	ΔR^2	
$D_R = (1/e^{7.639})\ r^{2.748}$	.5179	1.3829	.5179	(4-101)
$D_R = (1/e^{4.106})\ r^{2.748}\ S_o^{1.964}$	.9720	.3414	.4541	(4-102)
$D_R = e^{17.598}\ q_o^{2.296}$	.5654	1.3131	.5654	(4-103)
$D_R = e^{19.894}\ q_o^{2.191}\ S_o^{1.850}$	.9674	.3683	.4020	(4-104)
$D_R = (1/e^{15.184})\ Re^{2.440}$	.6256	1.2187	.6256	(4-105)

Sequence of regression equations	R^2	SEE	ΔR^2	
$D_R = (1/e^{11.188}) \, Re^{2.219} \, S_o^{1.708}$	.9637	.3883	.3381	(4-106)

4.4.3 Rill Volume, V_R and Rill Volume/Total Erosion Volume Ratio, V_R/V_T, as Dependent Variables

Rill volume was then related to slope, rainfall intensity, rainfall excess, and Reynolds number. The independent variables were then correlated to the rill/erosion ratio, V_R/V_T, in the same way previously mentioned in this section. The analysis of V_R with these variables yields correlations as follows:

Sequence of regression equations	R^2	SEE	ΔR^2	
$V_R = (1/e^{6.464}) \, r^{3.163}$	.5494	1.4939	.5494	(4-107)
$V_R = (1/e^{2.602}) \, r^{3.163} \, S_o^{2.147}$	.9838	.2900	.4144	(4-108)
$V_R = e^{22.517} \, q_o^{2.636}$	.5968	1.4131	.5969	(4-109)
$V_R = e^{25.018} \, q_o^{2.522} \, S_o^{2.016}$	.9789	.3305	.3821	(4-110)
$V_R = (1/e^{15.096}) \, Re^{2.800}$	.6580	1.3015	.6580	(4-111)
$V_R = (1/e^{10.765}) \, Re^{2.557} \, S_o^{1.851}$	.9763	.3510	.3183	(4-112)

The rill/erosion ratio, V_R/V_T, as a function of given independent variables yields:

Sequence of regression equations	R^2	SEE	ΔR^2	
$V_R/V_T = (1/e^{2.015}) \, r^{.610}$	.5790	.2711	.5790	(4-113)
$V_R/V_T = (1/e^{1.337}) \, r^{.610} \, S_o^{.376}$	.9579	.0877	.3789	(4-114)

Sequence of regression equations	R^2	SEE	ΔR^2	
$V_R/V_T = e^{3.552}\ q_o^{.506}$	.6242	.2561	.6242	(4-115)
$V_R/V_T = e^{3.988}\ q_o^{.486}\ S_o^{.351}$	.9532	.0925	.3290	(4-116)
$V_R/V_T = (1/e^{3.674})\ Re^{.538}$	.6904	.2325	.6904	(4-117)
$V_R/V_T = (1/e^{2.927})\ Re^{.496}\ S_o^{.319}$	.9585	.0871	.2681	(4-118)

The Reynolds number is once again one of the most important parameters in predicting rill geometry. Rainfall intensity, or rainfall excess, or water discharge and slope are the second and third most important parameters. The dimensionless form of the correlations are important in comparing this study with another study. Therefore, special emphasis is given to the equations that are in dimensionless form, especially including Reynolds number and slope.

CHAPTER V

DISCUSSION OF RESULTS

In this chapter, important analytical and statistical results are compared and discussed. Figures are also explained and discussed briefly. Moreover, selected prediction equations are explained with application and comparison. Predicted values versus measured values are plotted and compared for sediment discharges, mean local velocity and gully geometry, and the results are discussed. Finally field application of erosion loss prediction equation is explained with its limitations and advantages.

5.1 DISCUSSION OF ANALYTICAL RESULTS

5.1.1 Longitudinal Mean Local Velocity Profile

Equation (2-36) was derived on the initial assumption that vertical velocity could be approximated by parabolic curve. This assumption comes from a simplification of Navier-Stokes equation for parallel flow. For short increment of flow section, this approximation is applicable. The result of experimental data showed that equation derived with this assumption give similar results, that is, the parabolic vertical velocity profile is good enough for overland flow under rainfall.

It was found that the derived Eq. (2-36) and regression Eq. (4-85) from data are comparable. Therefore, it is concluded that Newton's law of viscosity is applicable for spatially varied, steady overland flow under rainfall with low Reynolds number.

5.1.2 Sediment Transport Equations

Sediment transport equations developed by dimensional analysis, computer analysis of data and model assumptions are similar in general form. They are also comparable for their terms in a physical sense. Equation (2-89) is a dimensionless form of sediment transport equation as a function of Reynolds number, slope, porosity and roughness characteristics. Equation (4-47) is the prediction equation of sediment discharge developed from regression of data in terms of Reynolds number and slope. A comparison of both equations shows that terms included in the equations are identical except that porosity and roughness were entered as a constant in Eq. (4-47). Equations (2-74) and (4-59) represent a model and equation obtained from a model respectively for sediment transport in terms of stream power. Although terms of Eq. (4-47) look different from terms of Eq. (4-59), their physical significance is similar.

Equation (4-47) contains slope, viscosity and Reynolds number which includes rainfall excess and flow length or water discharge. Equation (4-59) contains mean velocity and tractive force which includes depth of flow, viscosity and slope. Thus, basically both Eqs. (4-47) and 4-59) contain water discharge, viscosity and slope. In conclusion, the results of dimensional analysis, regression analysis of data and assumed model are comparable and similar.

5.2 DISCUSSION OF FIGURES AND SIGNIFICANT RELATED VARIABLES

In this secion, the highlights of the figures and variables related to sediment transport will be discussed briefly. The significance of the figures comes from their showing a single correlation

between dependent and independent variables, showing the general trend of relationships. Data plotted in these figures was also analyzed in multiple correlation, from which regression equations were selected.

5.2.1 Sediment Concentration Versus Time

Figures (4-1) to (4-6) show the change of instantaneous sediment concentration, C_i , with time on 5.7 to 40 percent slopes with a given rainfall intensity. Averaged values of C_i were calculated for the entire 60 minutes, the first 30 minutes, and for the last 30 minutes for all runs. There were no significant differences between the three averaging methods and the average concentration as calculated from the 60 minute record was used in all computations.

A statistical analysis was also performed on the concentration versus time data. For all runs C_i was found to be independent of time. In some of the figures C_i varied with t for short periods of time. The variations of C_i from the average value were believed to be caused from the formation of rills. No comprehensive study of rills was done, but rills may become an important factor in causing the concentration to change with time. Also, in many of the runs steady state conditions were not reached during the first few minutes.

5.2.2 Slope and Intensity of Rainfall

Figures (4-7) to (4-14) show the relationship between sediment yield in different units versus slopes for given intensity of rainfall. These figures have essentially the same meaning since only sediment transport was expressed in different units; therefore, the shape of the figures are similar. Sediment yield or erosion loss was increased slightly with slope almost in a straight line on smaller intensity of

1.25 inches per hour but increased rapidly as a curve on higher intensities of 2.25, 3.65 and 4.60 inches per hour. Rainfall intensity of 1.25 inches per hour may be very near critical rainfall for this soil type for given slopes; therefore, change of slope does not increase erosion loss much under this intensity of rainfall. Critical rainfall intensity may be defined as that intensity which starts erosion. Erosion loss was increased relatively more slowly with slopes up to 15 than with slopes between 15 to 35. After slope of 35 erosion loss seems to be slower again.

Among the most important factors affecting erosion loss are steepness and length of slope. Rate of erosion changes with 1.66 power of slope steepness as found in the present study (Eq. 4-34).

5.2.3 Water Discharge

Figure (4-15) shows that sediment discharge increased slowly with increasing water discharge on slopes of 5.7 to 15 percent but increased rapidly on slopes of 20 to 40 percent. Figure (4-16) shows that water discharge was constant and steady with respect to slope.

5.2.4 Mean Local Velocity, Depth of Flow Versus Length of Slope

Figures (4-17) to (4-22) show the relation between length of slope and mean velocity or mean depth for given slope and intensity of rainfall. As seen in the figures, velocity increased with increment of slope length as a curve. Depth of flow increased more with slope length on smaller slopes than on higher slopes. Mean velocity of overland flow increases with .59 power of slope length and .375 power of slope steepness as found from data analysis and .666 power of slope length and .333 power of slope steepness as found from analytical

analysis of parabolic vertical velocity assumption. These assumptions are justified by data analysis. Because of steep but short segment of slope and very shallow depth, the flow can be said to be greatly influenced by viscosity; therefore, flow behavior will not be assumed as turbulent.

5.2.5 Flow Properties, Reynolds Number and Froude Number

As shown in Table (4-8), Reynolds numbers are very small (0-130) and Froude numbers are very high (0-5.4). According to these Froude numbers, the greater part of flow is very supercritical; it is an unusual phenomenon to find supercritical laminar flow in practice. According to the Reynolds number and critical Reynolds number given by Chen and Chow (1968), the flow of present study falls into the laminar flow region. Although this is not a laminar flow due to continuous disturbence of flow by raindrops, it is not a turbulent flow either because length of run is so short that it is not possible to develop turbulent flow. Moreover, perturbation of flow by raindrop will die out as soon as raindrop impact is diminished. Most probably this flow represents the beginning of a laminar-sublayer of an undeveloped turbulent flow. This flow will be termed in this study agitated supercritical laminar flow.

Figure (4-23) shows a relationship between Re and f . Figures (4-25) to (4-29) show a relationship between f and distance, X , for given rainfall intensities on given slopes. Friction factors which are taken from Table (4-9), are exponentially decreasing with Reynolds number and distance, especially under higher intensities of rainfall.

5.2.6 Vegetation Affecting Soil Erosion

Figures (4-30) and (4-31) show the effect of vegetation on erosion loss. As seen in the figures vegetation decreased the erosion loss. Effects of vegetation on erosion loss reduced with increasing intensity of rainfall. The effects of vegetation on erosion loss are twofold: (1) vegetation dissipates raindrop impact energy and intercepts rainfall, and (2) it reduces the area exposed to erosion. Moreover, vegetation has some other indirect effects on reduction of erosion loss, such as binding effect of roots on soil particles which are built for better structure and hiding effect of stems on eroded particles. If soil particles are uniformly distributed, hiding factor is unity, as given in Einstein's paper in 1950. Existence of vegetation will increase hiding factor even if particles are uniform.

If soil surface is covered by vegetation, raindrops will first strike the vegetation and then will start flowing in a gravitational direction; therefore, splash erosion of raindrop impact and turbulence effect of drops will be reduced significantly. When overland flow starts through or over vegetation, resistance to flow and depth of flow will increase, but boundary shear may increase as a result of depth. It appears that increasing boundary shear will increase erosion loss, but this is not the case. Even if boundary shear is increased, velocity will decrease and stream power may decrease; therefore, boundary shear alone is not a good criterion for erosion loss, velocity being a better criterion to be used simultaneously with boundary shear. Moreover, less area will be exposed to shear affect because of vegetation cover; therefore, net erosion loss from total vegetated area will be less than soil loss from total bare area.

In Fig. (4-30), the effect of vegetation on erosion loss is decreased by increasing intensity of rainfall. Increasing rainfall intensity will decrease the relative effect of vegetation on raindrop impact energy and will decrease the relative effect of vegetation on resistance to flow and velocity of flow. Therefore, relatively speaking, the higher the intensity of rainfall, the less the effect of vegetation on erosion loss. Although vegetation decreases erosion, the rate of decrease of erosion depends on type and density of erosion as well as intensity of rainfall.

5.3 PREDICTION EQUATIONS AND DISCUSSION

Following sections, prediction equations obtained from the computer analysis of data, and derived analytically, are selected for velocity, sediment discharge and concentration, and gully geometry. Selected prediction equations are listed in Table (5-1). The discussion of prediction equations is based on the comparison of theory and measured values versus predicted values. In this section one of the most important objectives is to show how to predict soil loss from overland flow; therefore, special consideration will be given for the prediction of sediment discharge. Because mean velocity of overland flow as an independent variable is one of the basic factors affecting sediment discharge, more attention is given to velocity than other independent variables, so that the phenomenon can be better understood.

Velocity is not only an important factor in sediment transport but also in boundary shear and stream power, factors which determine the rate of sediment discharge. Although tractive force, velocity,

TABLE 5-1. SELECTED PREDICTION EQUATIONS WHICH ARE OBTAINED FROM NONLINEAR REGRESSION ANALYSIS AND ANALYTICAL ANALYSIS

No.	Equations	R^2	SEE	Origin[1]	Dependent variable unit[6]
1	$\bar{u} = (\frac{g}{3\nu})^{1/3} S_f^{1/3} q_o^{2/3} X^{2/3} = (\frac{g}{3\nu})^{.333} S_f^{.333} q_o^{.666} X^{.666}$			(2-36) ANALY.[2]	ft/sec
2	$\bar{u} = (1/e^{13.98} \nu^{1.664}) S_o^{.37526} q_o^{.64132} X^{.59211}$	.8228	.2836	(4-85) REG.[3]	ft/sec
3	$\bar{u} = (1/e^{2.69687}) Re^{.627} S_o^{.33598}$	.8177	.2834	(4-87) REG.	ft/sec
4	$C_s = e^{9.59952} \bar{u}^{.82628} S_o^{1.59977}$	.9347	.3241	(4-15) REG.	ppm
5	$C_s = e^{9.55318} Re^{.96315} S_o^{1.45277}$	.9224	.3674	(4-20) REG.	ppm
6	$q_s^* = C_s = \phi(Re, S_o, P, d_{50}/d)$			(2-89) ANALY.	
7	$q_s = (1/e^{9.181}) \bar{u}^{3.28437} S_o^{.42756}$	.9544	.400	(4-29) REG.	lb/sec/ft of width
8	$q_s = S_{TF} q^{5/3} S_o^{5/3} = S_{TF} q^{1.666} S_o^{1.666}$			(2-72) MODL.[4]	lb/sec/ft of width
9	$q_s = e^{11.7269} q^{2.03475} S_o^{1.66374}$	.9588	.3805	(4-34) REG.	lb/sec/ft of width

TABLE 5-1. (continued) SELECTED PREDICTION EQUATIONS WHICH ARE OBTAINED FROM NONLINEAR REGRESSION ANALYSIS AND ANALYTICAL ANALYSIS

No.	Equations	R^2	SEE	Origin [1/]	Dependent variable unit [6/]
10	$q_s = e^{10.50448}\ q_o^{2.03475}\ S_o^{1.66374}$	.9588	.3805	(4-36) REG.	lb/sec/ft of width
11	$q_s = (1/e^{11.64517})\ Re^{2.05403}\ S_o^{1.46002}$	.9517	.4119	(4-47) REG.	lb/sec/ft of width
12	$q_s = e^{.7441}\ ((\tau_o - \tau_c)\bar{u})^{1.5836}$	.9195	.5196	(2-74)&(4-59) MODL-REG. [5/]	lb/sec/ft of width
13	$A_R/A_T = e^{2.35186}\ q_o^{.33062}\ S_o^{.16547}$	.9341	.0676	(4-96) REG.	ft^2/ft^2
14	$A_R/A_T = (1/e^{2.344968})\ Re^{.33758}\ S_o^{.14357}$	.9406	.0142	(4-100) REG.	ft^2/ft^2
15	$V_R = e^{25.01813}\ q_o^{2.52194}\ S_o^{2.01617}$	.9789	.3305	(4-110) REG.	$ft^3/hr/ft$ of width
16	$V_R = (1/e^{10.76525})\ Re^{2.55688}\ S_o^{1.85121}$	.9763	.3510	(4-112) REG.	$ft^3/hr/ft$ of width
17	$V_R/V_T = e^{3.98813}\ q_o^{48628}\ S_o^{.35128}$	.9532	.0925	(4-116) REG.	ft^3/ft^3

TABLE 5-1. (continued) SELECTED PREDICTION EQUATIONS WHICH ARE OBTAINED FROM NONLINEAR REGRESSION ANALYSIS AND ANALYTICAL ANALYSIS

No.	Equations	R^2	SEE	Origin[1/]	Dependent variable[6/] unit
18	$V_R/V_T = (1/e^{2.92708}) \, Re^{.49654} \, S_o^{.31906}$	.9585	.0871	(4-118) REG.	ft^3/ft^3

1/ Original chapter and number which equations first appear.

2/ Analytically derived equation.

3/ Regression equation.

4/ Model from literature.

5/ Assumed model which its coefficients were found by data analysis.

6/ Units which values are predicted.

Note: Units of independent variables are: S_f and S_o are in ft/ft, q_o is in ft/sec, q is in cfs/ft of width, X is in ft, e is natural logarithm base, ν is ft^2/sec, Re is dimensionless.

and stream power are very important factors, it is very difficult to measure or evaluate them from overland flow generated by rainfall. Therefore, regression equations with slope, water discharge, rainfall excess and Reynolds number, which are easier to measure, are useful for prediction of sediment discharge. Moreover, velocity and shear stress are related to those variables above. In conclusion, the slope, the Reynolds number, which includes rainfall excess, and distance have the dominant parameters for any prediction equation presented in these sections.

5.3.1 Mean Velocity Prediction of Overland Flow

First, under the assumption of $S_f = S_o$, mean velocities were calculated using analytical Eq. (2-36). Predicted values were plotted against measured mean velocities at given distances, slopes, and rainfall intensities, as shown in Table (5-2) and Figs. (5-1 and 5-2). In the figures, the difference between the perfect line (the line with a 45° axes) and actual line shows that predicted values are less than measured values. These differences come from the assumption of $S_f = S_o$, because S_f is always greater than S_o for spatially varied flow, especially under rainfall impact. According to Eq. (2-36), the greater the S_f the higher the velocity. Although there are discrepancies, predicted values show that Eq. (2-36) gives fairly good approximations. If S_f should be evaluated, much better results could be obtained. The correlation between measured values (Table 4-5) and predicted values (Table 5-2) is very high, with R^2 equal to .9885.

The second prediction equation used was regression Eq. (4-87). Using Eq. (4-87), mean local velocities of overland flow were calculated

TABLE 5-2. PREDICTED MEAN LOCAL VELOCITIES OF OVERLAND FLOW GENERATED BY RAINFALL AT A GIVEN DISTANCE FOR EACH RUN FROM ANALYTICALLY OBTAINED EQUATION

(EQUATION 2-36: $\bar{u} = (\frac{g}{3\nu})^{1/3} S_o^{1/3} q_o^{2/3} x^{2/3}$)

	Predicted velocities, $\bar{u}$ s in ft/sec			
Run No.	@ 3'	@ 6'	@ 12'	@ 16'
I	.050735	.08054	.127845	.15487
II	.091793	.145713	.231305	.280206
III	.134649	.213743	.3342	.411027
IV	.15940	.25304	.401674	.486593
V	.064719	.102735	.163082	.19756
VI	.112788	.17904	.284208	.34429
VII	.165225	.2622785	.41634	.50436
VIII	.195229	.30991	.49195	.59595
IX	.078657	.12486	.1982	.240107
X	.129392	.205397	.3260471	.394978
XI	.194136	.30817	.4891917	.5926135
XII	.232115	.368459	.584893	.708547
XIII	.090995	.144446	.229294	.27777
XIV	.143923	.22846	.362663	.43933
XV	.218144	.34628	.549689	.66590
XVI	.256789	.4076276	.6470685	.7838676
XVII	.106105	.16843	.267367	.323892
XVIII	.16986	.269638	.4280235	.5185135
XIX	.254009	.4032	.640063	.77538
XX	.2944	.46735	.74187	.8987
XXI	.1183187	.187819	.29814	.361176
XXII	.187458	.29757	.472365	.57223
XXIII	.280306	.44496	.70632	.85565
XXIV	.3242968	.514789	.8171769	.98994

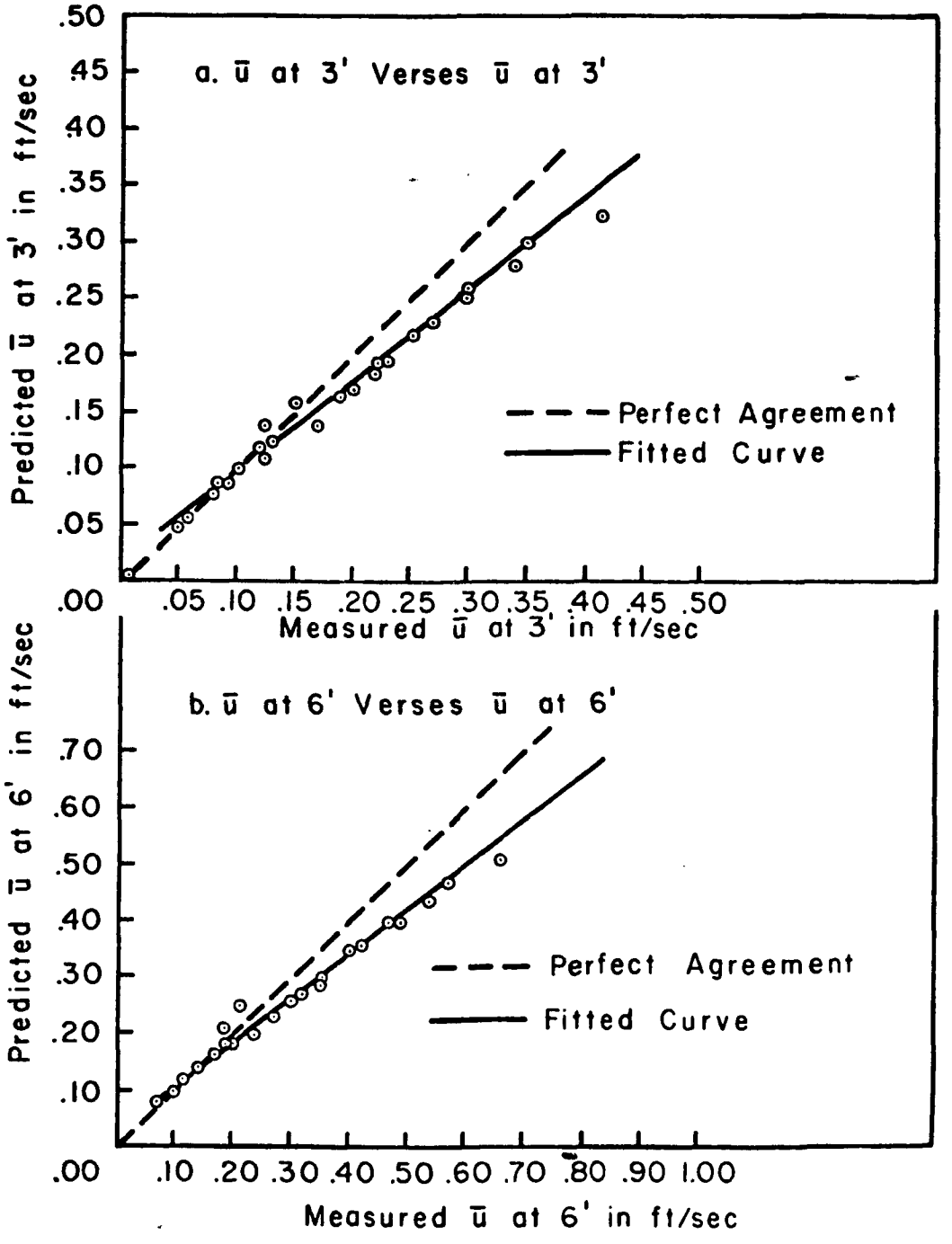

Fig. 5-1. Predicted velocity versus measured velocity at 3' and 6' ($\bar{u} = (g/3\nu)^{1/3} S_o^{1/3} q_o^{2/3} \chi^{2/3}$).

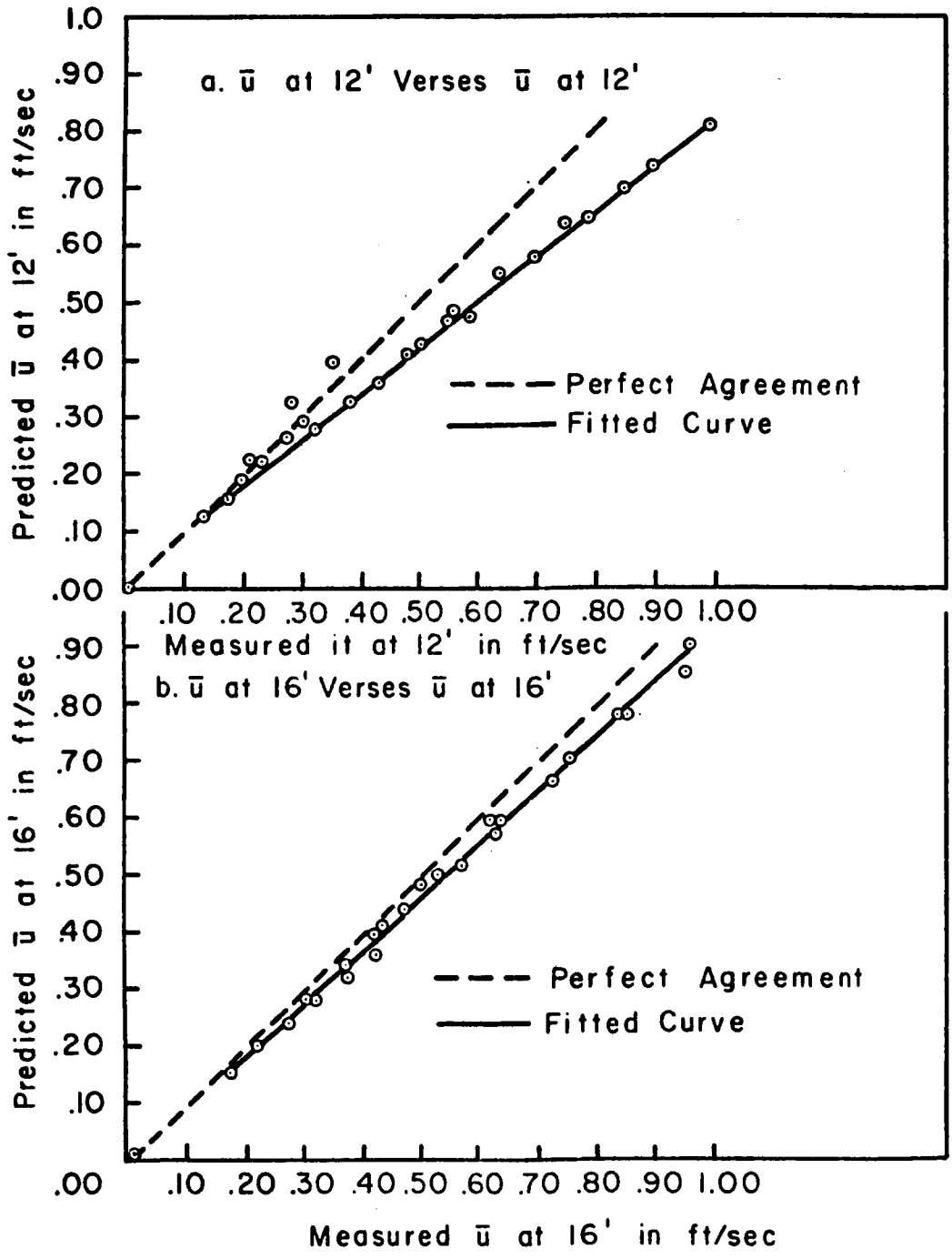

Fig. 5-2. Predicted velocity versus measured velocity at 12' and 16' ($\bar{u} = (g/3\nu)^{1/3} S_o^{1/3} q_o^{2/3} x^{2/3}$).

and plotted at given distances, slopes and intensities, as shown in Table (5-3) and Figs. (5-3 and 5-4). The comparison among the predicted values shown in Table (5-3) and the measured values shown in Table (4-5) indicates that predicted values are slightly less than the measured values except that velocities at 16 ft. are almost the same. These differences, which are shown in Figs. (5-3) and (5-4), come from regression Eq. (4-87), which could only explain 82 percent of variation of velocities, having R^2 of .8177. Thus, 18 percent of the variations related to velocities are still unexplained. Although predicted values differ from the measured values of velocities, the correlation among them, with R^2 equal to .9880, is very high.

Equation (4-85) was not used to predict velocity because of its similarity to Eq. (4-87). The purpose of selecting regression Eq. (4-85) is to show the near agreement with coefficients of Eq. (2-36), which is derived analytically, and Eq. (4-85) obtained from data analysis see Table (5-1). This comparison helps to clarify the mathematical model of overland flow velocity variation under rainfall.

Accepting Eq. (2-36) as a mathematical model of overland flow, mean velocity involves a limitation of assuming laminar and parallel flow for short increments of distance. In a future study, a mathematical model should be derived for turbulence flow as well.

5.3.2 Sediment Concentration and Erosion Depth

Sediment concentration, discharge, and erosion depth have the same physical significance in relating independent variables, because sediment concentration is a dimensionless form of sediment discharges and erosion depth is the conversion of sediment weight into depth of

TABLE 5-3. PREDICTED MEAN LOCAL VELOCITIES OF OVERLAND FLOW GENERATED BY RAINFALL AT A GIVEN DISTANCE FOR EACH RUN FROM REGRESSION EQUATION

(EQUATION 4-87: $\bar{u} = (1/e^{2.69687}) \, Re^{.6270} \, S_o^{.33598}$)

Run No.	Predicted $\bar{u}$'s in ft/sec @ 3'	@ 6'	@ 12'	@ 16'
I	.062179	.09603	.1483	.1776
II	.1052133	.162486	.25094	.2998
III	.15065	.23262	.35924	.42984
IV	.17731	.27382	.42291	.50602
V	.07756	.11978	.18499	.22048
VI	.13027	.20118	.31069	.37178
VII	.18640	.28787	.4445	.5324
VIII	.218041	.33675	.52007	.62288
IX	.09604	.14832	.22894	.2742
X	.1481	.22877	.3530	.42312
XI	.2228	.34406	.5317	.63668
XII	.2656	.41013	.6336	.75868
XIII	.11250	.1737	.2683	.32146
XIV	.16621	.25676	.39655	.4749
XV	.25483	.3935	.60777	.72784
XVI	.29397	.4540	.70112	.8397
XVII	.131126	.2021	.3127	.37483
XVIII	.20116	.31076	.47584	.5745
XIX	.29828	.6406	.7647	.85188
XX	.337365	.52103	.80463	.9637
XXI	.14676	.22576	.34895	.41752
XXII	.22209	.34298	.52968	.6344
XXIII	.32908	.50822	.78477	.94006
XXIV	.37186	.57417	.88694	1.06225

TABLE 5-4. MEASURED AND PREDICTED SEDIMENT DISCHARGES BY EQUATION 4-47 AND EQUATION 4-59 RESPECTIVELY

(EQUATION 4-47: $q_s = (1/e^{11.64517}\ Re^{2.05403}\ S_o^{1.46002})$)

(EQUATION 4-59: $q_s = e^{.7441}\ ((\tau_o - \tau_c)\ \bar{u})^{1.5836}$)

Run No.	Measured q_s (lb/sec/ft of width)	Predicted q_s by Equation 4-47 (lb/sec/ft of width)	Predicted q_s by Equation 4-59 (lb/sec/ft of width)
I	.000096	.0000748	.00002682
II	.00300	.0004177	.00028941
III	.000646	.0013523	.00091326
IV	.001482	.0023078	.0021299
V	.000294	.0001905	.000287033
VI	.001508	.001121	.00192952
VII	.00372	.003413	.00461508
VIII	.00548	.00564	.00718439
IX	.000548	.0004409	.000553332
X	.002974	.001902	.00317199
XI	.007138	.007088	.00768714
XII	.01288	.012408	.01426633
XIII	.000644	.0008189	.00128039
XIV	.005686	.0030232	.00480844
XV	.014904	.012038	.01185276
XVI	.02666	.019047	.01994071
XVII	.000922	.0015584	.00230314
XVIII	.01015	.006508	.00715895
XIX	.022648	.023032	.01677803
XX	.03752	.03476	.02376312
XXI	.00134	.0024687	.0036737
XXII	.013096	.009749	.01048956
XXIII	.0370	.035356	.0237778
XXIV	.06508	.05276	.03541768

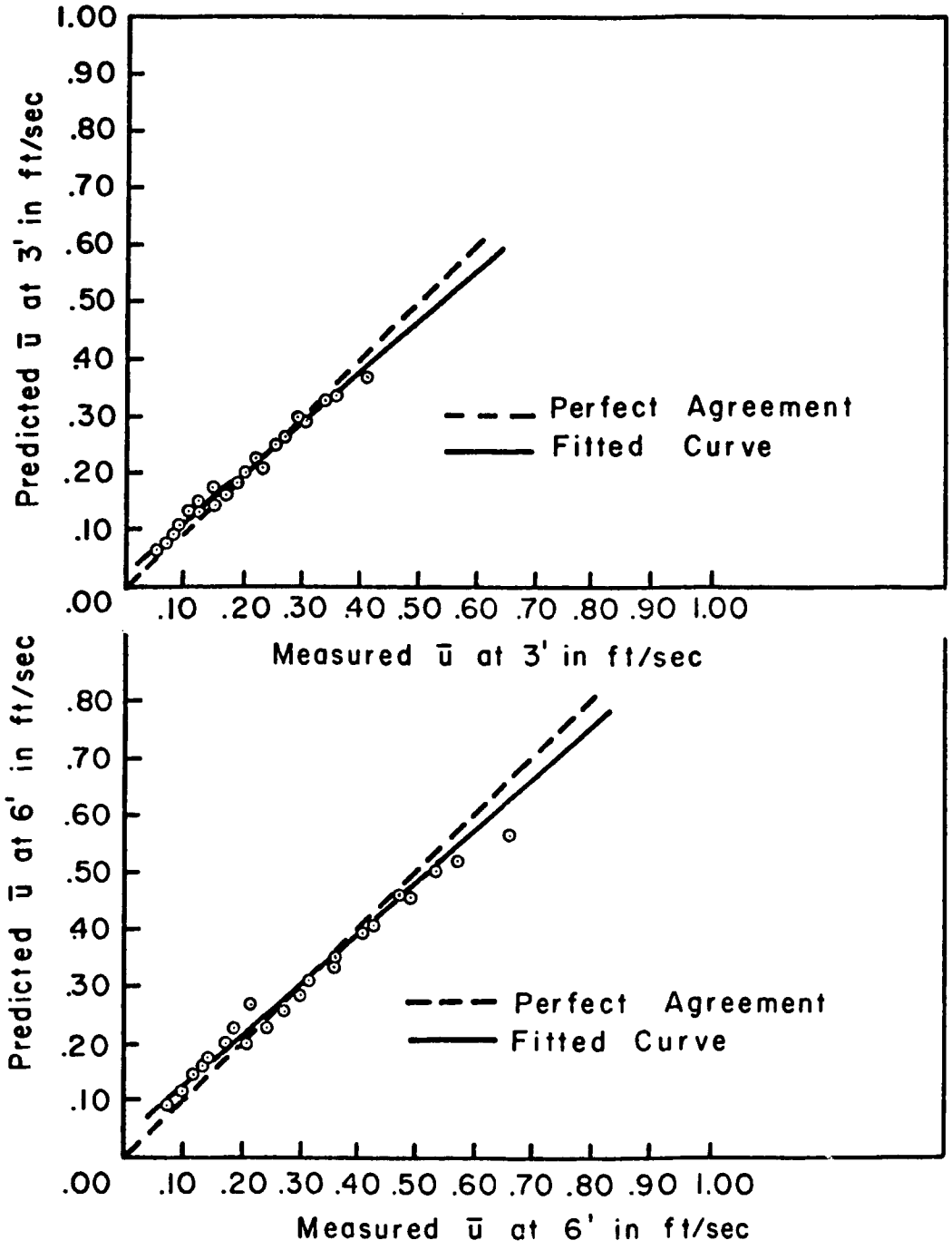

Fig. 5-3. Predicted velocity versus measured velocity at 3' and 6' ($\bar{u} = (1/e^{2.697})\ Re^{.627}\ S_o^{.336}$).

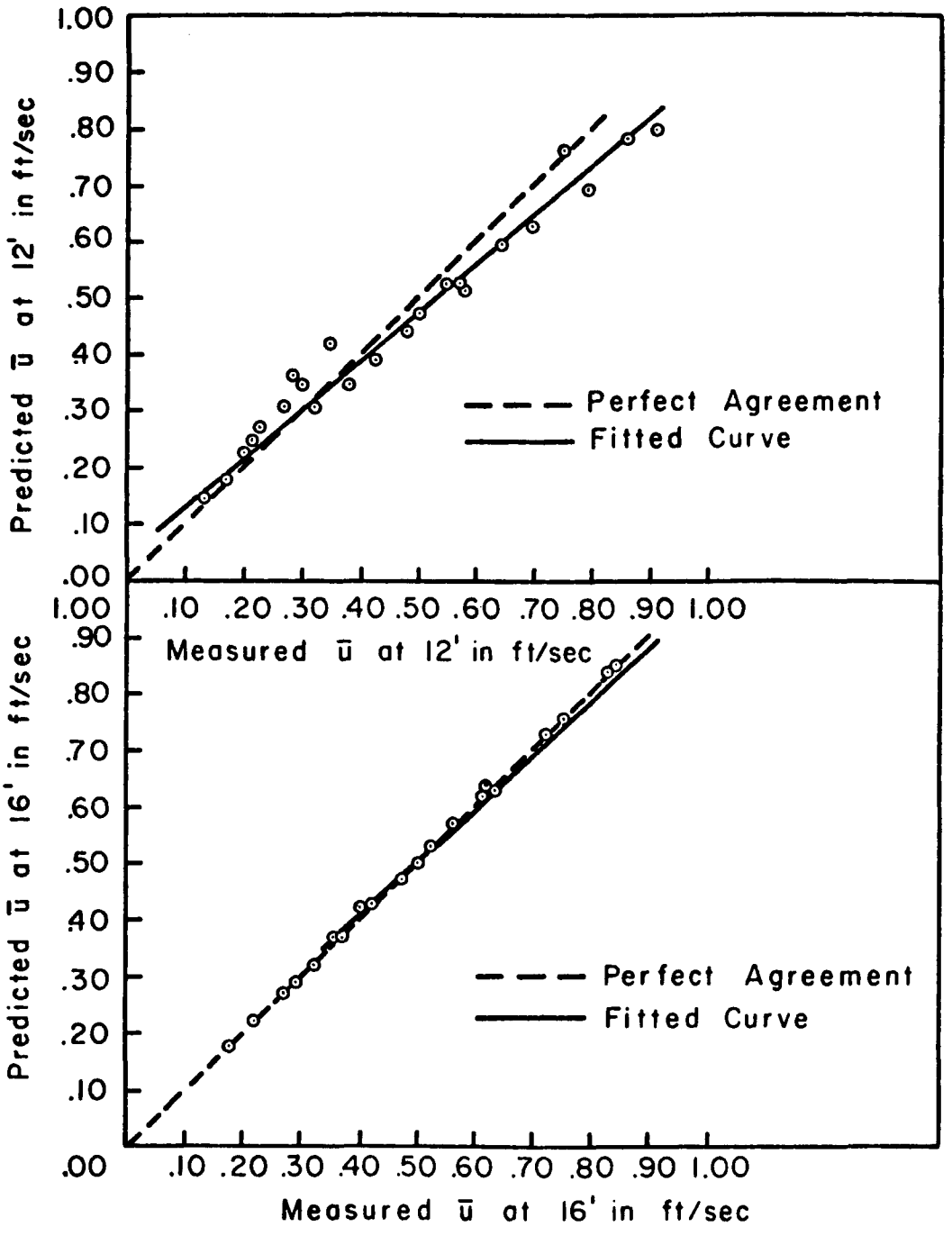

Fig. 5-4. Predicted velocity versus measured velocity at 12' and 16' ($\bar{u} = (1/e^{2.697})\ Re^{.627}\ S_o^{.336}$).

surface. Therefore, selected equations for predicting sediment concentration and erosion depth were not used here. An argument can be made similar to that discussed under sediment discharge. These are simply different ways of representing erosion loss.

5.3.3 Sediment Discharge Prediction

First, using the sediment transport model, Eq. (2-74), whose coefficients and constant were determined by data analysis (Eq. 4-59), sediment discharges for each run were predicted and plotted against measured values. Then, sediment discharges were predicted and plotted using Eq. (4-47). To compare the two methods, predicted values and measured values are listed in Table (5-4). The plots of predicted versus measured values are shown in Figs. (5-5) and (5-6) Both tables and figures show that predicted values of sediment discharges are less than the measured values. A comparison of predicted values obtained by Eqs. (4-47) and (4-59) with measured values of sediment transport gives a high correlation, having R^2 equal to .983 and R^2 equal to .97, respectively. Although correlation between predicted and measured values is very high, there are certain limitations in the use of these equations. First of all, Eq. (4-59) depends on the calculation of τ_o which is based on velocity measurements. The effect of velocity changes on τ_o is very significant. Therefore, the evaluation of τ_o is important as well as measurement of velocities. Secondly, Eq. (4-47) was obtained from data analysis; the data for this analysis were collected on the model experiment under simulated rainfall. It is not known how well simulation of rainfall represents the natural rainfall of region under study, or how much erosion due

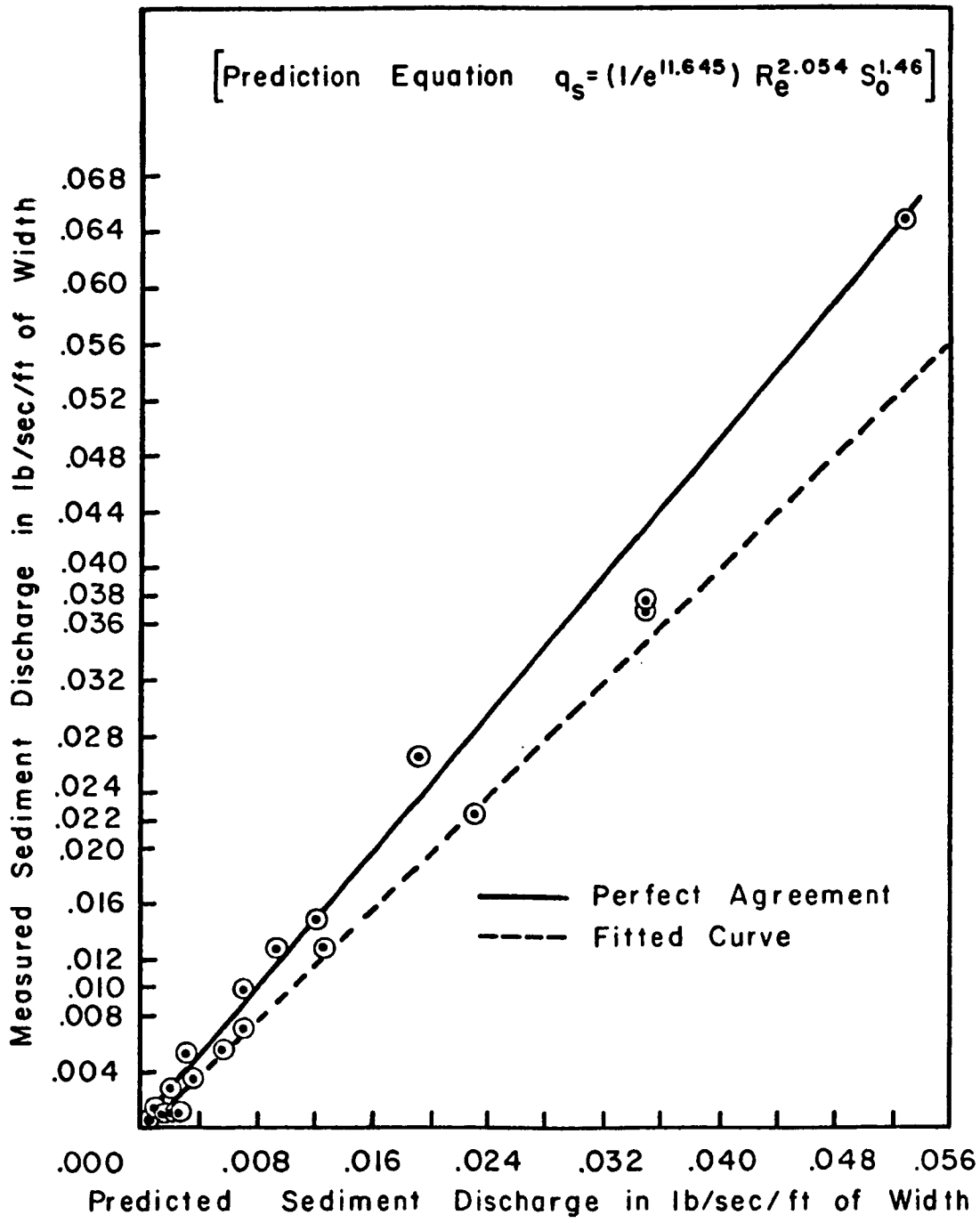

Fig. 5-5. Relationship between measured and predicted sediment discharges (prediction equation: $q_s = (1/e^{11.645}) S_o^{1.46}$).

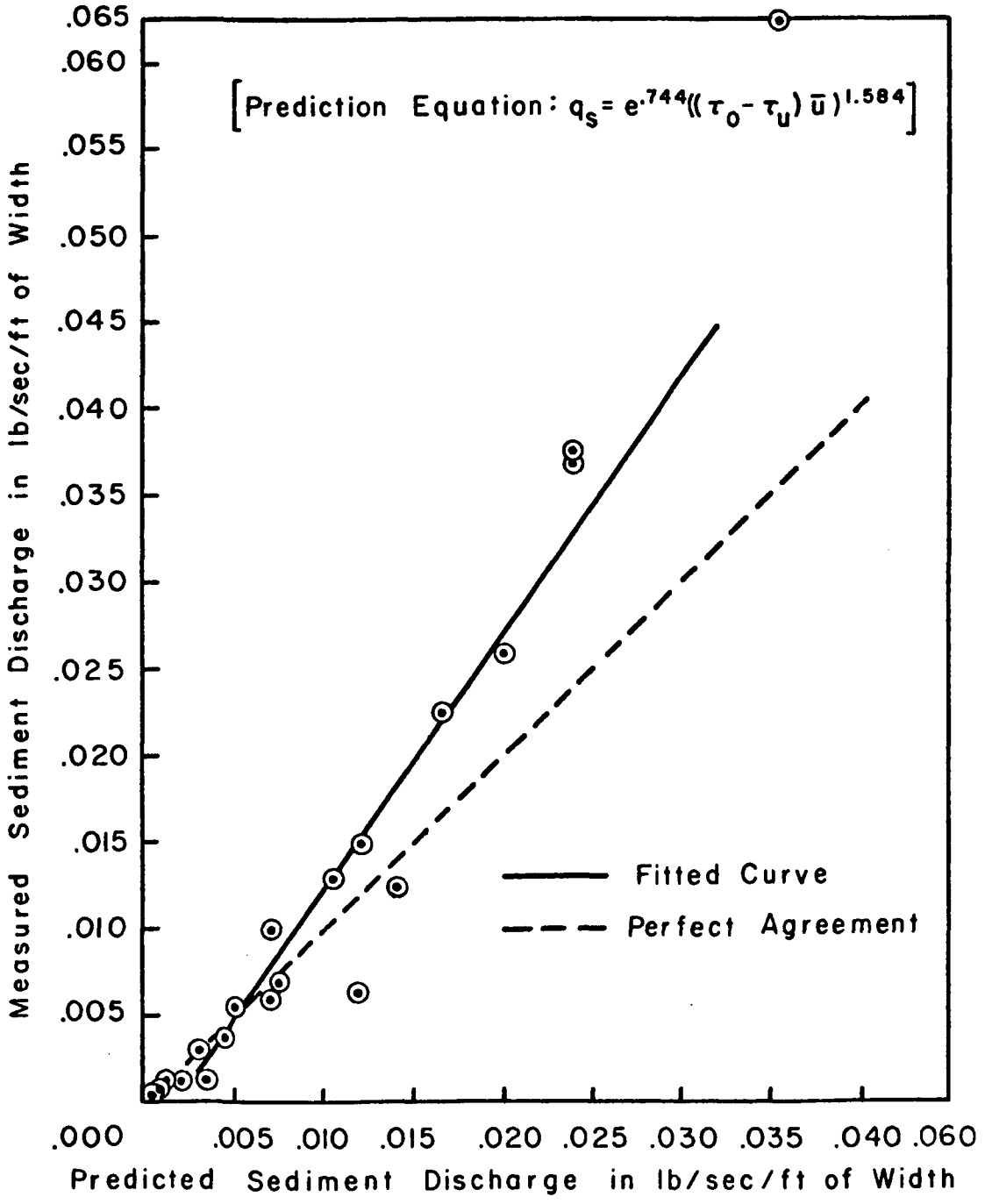

Fig. 5-6. Relationship between measured and predicted sediment discharges (prediction equation: $q_s = e^{.744}\ ((\tau_o - \tau_c)\ \bar{u})^{1.584}$).

to laminar overland flow from disturbed sandy soil over uniform slope represents erosion over undisturbed natural soil. Moreover, the length of slope did not vary during the experiment, although its effect on erosion is very significant.

In spite of the fact that limitations are important, the models are good enough to enable us to understand the mechanism of soil erosion and to approximate soil loss under similar conditions. Throughout the data analysis, the Reynolds number, slope and velocity were important factors affecting erosion and sediment discharges, especially the Reynolds number, which is defined as $Re = q_o X/\nu$ and includes rainfall excess, distance, and kinematic viscosity. As discussed before, the whole problem in sediment transport by overland flow, especially that generated by rainfall, is to find a way to determine either τ_o or S_f and f ; therefore τ_o is calculated directly from momentum equation without S_f and f. The advantage of Eq. (4-47) is that it is simple, easy and dimensionless, which makes it useful in comparing the data of other researchers.

The other equations in Table (5-1) are not tested for predicting sediment discharge, because they are similar to these two equations. The purpose of selecting them is so that they can be compared with each other. In particular the model assumed by Meyer and Wischmeier (1969), Eq. (2-72), has almost the same coefficients as Eq. (4-34), which was obtained by the regression analysis of data, except that coefficient of water discharge, q , differs, because Eq. (2-72) is in a more general form than Eq. (4-34).

5.3.4 Rill Geometry

One of the important but poorly defined subjects in erosion study is rill and gully geometry. There is very little exact theoretical basis for predicting rill and gully geometry. The study of rill and gully geometry is an art as well as a science.

Data analysis shows that rainfall and slope are the most important variables affecting rills. Because Reynolds number includes rainfall, prediction equations with Reynolds number and slope are preferred as before.

The relative rill surface area over total area for each run was predicted by using Eq. (4-100) and relative rill erosion which means volume of rill over total volume of erosion was predicted by Eq. (4-118). The predicted values are listed in Table (5-5) for each run. The remaining selected equations in Table (5-1) are given as possible prediction equations for different forms of rill geometry. They can be used in the same manner and purpose as others which have been explained. They differ from each other only slightly.

Comparison of measured values in Table (4-12) with predicted values in Table (5-5) shows very close agreement. Correlation between predicted and measured values is very high with R^2 equal to .985. Both tables show that erosion loss from gullies ranges from between 10 percent to 48 percent, and similarly, relative rill surface area ranges from 18 percent to 45 percent for our experiment.

5.4 FIELD APPLICATION OF RESULT

The main objective of this study was to seek a way and method for developing a soil loss prediction equation that could be used in the

TABLE 5-5. PREDICTION OF RILL GEOMETRY

(EQUATION 4-100: $A_R/A_T = (1/e^{2.344968}) \, Re^{.33759} \, S_o^{.14357}$)

(EQUATION 4-118: $V_R/V_T = (1/e^{2.92708}) \, Re^{.49654} \, S_o^{.31906}$)

Run No.	A_R/A_T (predicted by Equation 4-100)	V_R/V_T (predicted by Equation 4-118)
I	.17887	.0991
II	.23709	.14999
III	.287852	.19953
IV	.3143	.227046
V	.19678	.12116
VI	.26069	.18325
VII	.3163	.243522
VIII	.34418	.27575
IX	.21795	.14711
X	.2753	.20743
XI	.34304	.286675
XII	.3770	.329365
XIII	.2349	.16942
XIV	.28983	.23078
XV	.36473	.32362
XVI	.393904	.36241
XVII	.25132	.1955
XVIII	.3163	.27415
XIX	.3910	.3745
XX	.41785	.4129
XXI	.26365	.216377
XXII	.33006	.3011
XXIII	.4080	.411122
XXIV	.43564	.45291

field for a single storm. The equation sought was to be simple, accurate, and supported by basic concepts of hydraulics and theory. Therefore, any of the selected equations in Table (5-1) could serve for these purposes.

Equation (4-47) can be used as a first approximation of soil loss due to overland flow generated by a single storm. The equation can be used anywhere else if conditions are similar or if certain modifications of the constants are made. The reasons why this equation is selected are because (1) the terms in the equation can be determined easily and without any major errors or they can be obtained easily from meteorological stations, (2) anyone with a basic idea of hydraulics can use this equation to estimate soil loss, (3) the equation is not time-consuming, and (4) as an overall result it is economical to use. Moreover, this equation is comparable with the models accepted in the literature, and with the dimensional analysis. Once the Reynolds number, including discharge and at the same time rainfall and length of slope, are known the problem of determining S_f , f , or τ_o decreases the possibility of major error. The limitations, as discussed previously, are sandy disturbed soil, simulated rainfall with limited range of rainfall intensities, short distance of slope and bare leveled surface from which the equation for predicting sediment discharge was obtained.

CHAPTER VI

SUMMARY AND CONCLUSIONS

6.1 SUMMARY

The main objectives of this research were to study the mechanics of soil erosion from overland flow generated by simulated rainfall, to study the most important factors affecting soil erosion, and to develop a soil loss prediction equation. To achieve these objectives, experiments were conducted at Colorado State University, Foothills Engineering Research Center, using a plywood flume with disturbed sandy soil under simulated rainfall and CSU's rainfall-runoff facilities.

A flume with 16 foot x 5 foot x 4 foot dimensions was placed between rows of rainfall risers. Four different intensities of rainfall, 1.25 in., 2.25 in., 3.65 in. and 4.60 in. per hour, over six different slopes, 5.7, 10, 15, 20, 30 and 40 percent, were used to study erosion processes. Finally, winter wheat was seeded over 40 percent of the slope and four more runs were made to study the qualitative effect of vegetation.

Data were collected for sediment concentration, surface velocity of overland flow, water discharge, water temperature, infiltration rate, bulk density of surface soil, slope, intensity of rainfall, and rill geometry. The eroded sediments collected were dried, weighed, and sieved for grain size distribution.

The results and conclusions of this study involve the limitations of (1) sandy disturbed soil, (2) Reynolds number from 0 to 130, (3)

intensity of simulated rainfall ranging from 1.25 in. to 4.60 in. per hour, (4) slopes ranging from 5.7 to 40 percent, (5) flume dimensions of 4'x5'x16', and, (6) steady, spatially varied flow under constant uniform rainfall and infiltration.

6.2 CONCLUSIONS

The major conclusions and results of this study are summarized below:

1. Longitudinal mean local velocity of spatially varied, steady overland flow can be predicted in terms of viscosity, gravitational acceleration, friction slope, rainfall excess, and length of run. The derived equation is:

$$\bar{u} = \left(\frac{g}{3\nu}\right)^{.333} S_f^{.333} q_o^{.666} \chi^{.666} \quad .$$

The regression equation obtained from data analysis is:

$$\bar{u} = \left(1/e^{13.98} \nu^{1.664}\right) S_o^{.375} q_o^{.64} \chi^{.59} \quad .$$

It was found that the derived and regression equations were comparable. Hence, laminar flow equations were found to be used for flow under rainfall. As a result of similarity between the two equations, it was concluded that a parabolic vertical velocity profile and Newton's law of viscosity were applicable for spatially varied, steady overland flow under rainfall with low Reynolds number.

2. The boundary shear stress, τ_o, can be approximated from the momentum equation of overland flow under rainfall by the numerical method.

3. The dimensionless form of the sediment transport equation was found to be a function of Reynolds number, slope, porosity, and roughness characteristics, as follows:

$$q_s^* = C_s = \phi \left(Re,\ S_o,\ P,\ \frac{d_{50}}{d} \right) \quad .$$

4. It was found that Reynolds number and slope were the most important parameters to be used in sediment transport. The prediction equation developed from the regression of data is:

$$q_s = \left(1/e^{11.65} \right) Re^{2.05}\ S_o^{1.46} \quad .$$

Sediment discharge increased with the square of Reynolds number, Re, and an almost 3/2 power of the slope.

5. It was concluded that stream power, $\tau_o\ \bar{u}$, gives better predition of sediment discharge than boundary shear, τ_o, alone. The model derived from regression analysis of the data is:

$$q_s = e^{.744} \left(\left(\tau_o - \tau_c \right) \bar{u} \right)^{1.584} \quad .$$

6. Analysis indicates that sediment discharge increased the square of water discharge, q, and 5/3 power of the slope. This model was comparable to the model used by Meyer and Wischmeier (1969).

The regression equation is:

$$q_s = e^{11.727}\ q^{2.035}\ S_o^{1.664} \quad .$$

Meyer and Wischmeier's model is:

$$q_s = S_{TF}\ q^{5/3}\ S_o^{5/3} = S_{TF}\ q^{1.666}\ S_o^{1.666} \quad .$$

7. Thus, it was concluded that velocity, slope and rainfall intensity were the most important factors affecting soil erosion and sediment transport. Velocity was not only found to be important in sediment transport, but it also determined the boundary shear and the stream power of the flow. Although tractive force and stream power are very important factors in the overland flow phenomena, it was very difficult to measure them in the field or in the laboratory. Therefore, regression equations with easily measurable quantities such as slope, water discharge, rainfall excess, and fluid viscosity were preferred for predicting sediment discharge. In conclusion, slope and Reynolds number, $Re = \frac{q_o X}{\nu}$, became the dominant parameters for the sediment transport prediction equations.

8. Sediment discharge was found to be increased by 3.625 (7/2) the power of the mean local velocity of overland flow and almost the square of rainfall excess (2.13). Velocity increased with 2/3 power of the Reynolds number, rainfall excess, and water discharge.

9. Reynolds number, rainfall excess, and water discharge were found to have the same significance and influence on mean velocity of overland flow and on sediment transport from overland flow.

10. Sediment yield from overland flow could be predicted for both laboratory and field conditions, with modifications, by the prediction equations developed in this study, in terms of Reynolds number and slope or discharge and slope or stream power.

11. It was found that 40 percent vegetal cover (winter wheat) on 40 percent slope reduced erosion between 37-78 percent with rainfall

intensities of 4.60 in. to 1.25 in. per hour. The effect of vegetation as a retarding agent on erosion decreased by increasing rainfall intensity.

12. The relative surface area of rills was changed by approximately 1/e power of rainfall excess, water discharge, and Reynolds number, and .16 power of slope.

13. The relative volume of rills was changed by 1/2 power of rainfall excess and water discharge, .54 power of Reynolds number, and approximately 1/3 power of slope.

14. In this study the volume of rills was increased by 2.52 power of rainfall excess and water discharge, and 2.64 power of Reynolds number and square of slope.

6.3 FUTURE STUDY

In the future, similar research should be carried on different types of undisturbed soil with varying length of slope and higher intensities of simulated rainfall representing natural rainfall more closely. Roughness properties of different soil types and the resistance to overland flow under rainfall should be studied more comprehensively. For this purpose, using better facilities, conditions and methods, an attempt should be made to measure all τ_o and velocities with respect to distance. Also, S_f and f should be evaluated from τ_o and the velocity change; then S_f and f should be related to rainfall intensity, slope, and roughness characteristics of the soil. Roughness of soil surface should be defined and a representative index of roughness should be found.

Better criteria for defining the laminar and turbulence flow under rainfall over mobile bed should be found. Analytical analysis should be done based on turbulence flow. The result of analytical analysis from turbulence flow should be compared with data analysis and laminar flow results. The overall result should be checked by field study or field data. The final developed erosion loss prediction equation should be applied to situations in the field.

A theoretical framework and equations should be developed for most general conditions of overland flow erosion under rainfall. Besides concepts from hydraulics and fluid mechanics, wherever necessary, concepts from stochastic statistics should be used.

To test the effect of vegetation on soil erosion, a different type and density of vegetation should be used on various slopes under varying rainfall. Hydraulic properties of vegetation on roughness and velocity should be studied. The prediction equation should include the roughness characteristics of soil and the effects of vegetation.

Because it is impossible to have sheet erosion alone, rill and gully erosion should also be studied simultaneously. After flow concentration, small micro channels, rills, start developing, and these rills start developing gullies. The mechanics of rill and gully formation and all associated erosion should be studied and understood.

REFERENCES

Albertson, M. L., Barton, J. R., and Simons, D. B., 1965, Fluid mechanics for engineers, Fifth Printing: Prentice-Hall, Inc., N. J., 564 p.

Bagnold, R. A., 1966, An approach to the sediment transport problem from general physics: Geological Survey Professional Paper 422-I, 37 p.

Baver, L. D., 1965, Soil physics, Third Ed., Fifth Printing: John Wiley and Sons, Inc., New York, London, Sydney, 489 p.

Behlke, C. E., 1957, The mechanics of overland flow: Ph.D. dissertation, Stanford University.

Borst, H. L., and Woolburn, R., 1940, Rain simulator studies of effect of slope on erosion and runoff: U.S.D.A. Soil Conservation Service, SCS-TP-36, 30 p.

Chen, C. L., 1962, An analysis of overland flow: Ph.D. dissertation, Mich. State Univ., East Lansing, Mich.

Chen, C. L., and Chow, V. T., 1968, Hydrodynamics of mathematically simulated surface runoff: Civil Engineering Studies, Hydraulic Engineering Series No. 18, Dept. of Civil Engr., University of Ill., Urbana, Ill., 132 p.

Chen, C. L., and Hansen, V. E., 1966, Theory and characteristics of overland flow: Trans. Am. Soc. of Agr. Engr., Vol. 9, No. 1, p. 20-26.

Chow, V. T., and Harbaugh, T. E., 1965, Raindrop production for laboratory watershed experimentation: J. Geophysical Research, Vol. 70, No. 24, p. 6111-6119.

Colby, B. R., 1964, Discharge of sands and mean-velocity relationships in sand-bed streams: U.S. Geol. Survey Prof. Paper 462-A.

Du Boys, P., 1879, Étudeş du régime du Rhône et l'action exercee' par les eaux sur un lit a fond de graviers indefiniment affouillable: Annales des ponts et Chaussees, Ser. 5, 18, 141-95 (Cited by Raudkivi, A. J., 1967, Loose boundary hydraulics: Pergamon Press, New York, London, Sydney, 330 p.).

Duley, F. L., and Hays, O. E., 1932, The effect of the degree of slope on runoff and soil erosion: J. Agricultural Research, Vol. 45, No. 6, p. 349-360.

Einstein, H. A., 1950, The bed-load function for sediment transportation in open channel flows: U.S. Dept. of Agriculture, Soil Conservation Service, Washington, D.C., Tech. Bulletin No. 1026.

REFERENCES - (Continued)

Ellison, W. D., 1944, Studies of raindrop erosion: Agricultural Engineering, Vol. 25, No. 4, P. 131-136, and Vol. 25, No. 5, p. 181-182.

Ellison, W. D., 1945, Some effects of raindrops and surface-flow on soil erosion and infiltration: Trans., Am. Geophys. Union, Vol. 26, No. 3, p. 415-429.

Ellison, W. D., 1947, Soil erosion studies: Agricultural Engineering, Vol. 28, p. 145-146, 197-201, 245-248, 297-300, 349-351, 402-405, 442-444.

Emmett, W. W., 1970, The hydraulics of overland flow on hillslopes: U.S. Geol. Survey Prof. Paper 662-A, 68 p.

Favre, H., 1933, Contribution à l'étude des courants liquides (Contribution to the study of flow of liquid), Dunod, Paris, (Cited by Ven Te Chow, Open Channel Hydraulics: McGraw-Hill Book Company, Inc., New York, 1959, p. 327).

Grace, R. A., and Eagleson, P. S., 1965, Similarity criteria in the surface runoff process: M.I.T. Dept. Civil Engr., Hydrodynamics Lab. Rept. 77.

Grace, R. A., and Eagleson, P. S., 1966, The modeling of overland flow: J. Water Resources Research, Vol. 2, No. 3, p. 393-403.

Graf, Walter Hans, 1971, Hydraulics of sediment transport: McGraw-Hill Book Co., Inc., New York, 513 p.

Henderson, F. M., and Wooding, R. A., 1964, Overland flow and groundwater flow from a steady rainfall of finite duration: J. Geophys. Res., Vol. 69, No. 8, p. 1531-1540.

Hinds, J., 1926, Side channel spillways; Hydraulic theory, economic factors, and experimental determination of losses: Trans., Am. Soc. of Civil Engineers, Vol. 89, p. 881-927.

Holland, M. E., 1969, Colorado State University experimental rainfall-runoff facility: Colorado State University Experiment Station, Ft. Collins, Colorado, CER 69-70 MEH 21, 81 p.

Horner, W. W., and Jens, S. W., 1942, Surface runoff determination from rainfall without using coefficients: Trans., Am. Soc. of Civil Engineers, Vol. 107, p. 1039-1117.

Horton, R. E., 1938, Interpretation and application of runoff plot experiments with reference to soil erosion problems: Proceedings, Soil Science Society of America, Vol. 3, p. 340-349.

REFERENCES - (Continued)

Huff, D. D., and Kruger, P., 1967, The chemical and physical parameters in a hydrologic transport model for radioactive aerosol: Proceedings, The International Hydrology Symposium, Ft. Collins, Colorado, Vol. 1, Paper No. 17, p. 128-135.

Izzard, C. F., and Augustine, M. T., 1943, Preliminary report on analysis of runoff resulting from simulated rainfall on a paved plot: Trans., Am. Geophys. Union, Vol. 24, p. 500-509.

Izzard, C. F., 1944, The surface-profile of overland flow: Trans. Am. Geophys. Union, Pt. VI, p. 559. 968.

Kalinske, A. A., 1947, Movement of sediment as bed in rivers: Trans. Am. Geophys. Union, Vol. 28, p. 615-620.

Keulegan, G. H., 1944, Spatially variable discharge over a sloping plane: Trans. Am. Geophys. Union, Pt. VI, p. 956-959.

Kisisel, I. T., 1971, An experimental investigation of the effect of rainfall on the turbulence characteristics of shallow flow: Ph.D. dissertation, Purdue University, Lafayette, Ind.

Langhaar, H. L., 1967, Dimensional analysis and theory of models: 8th Printing, John Wiley and Sons, Inc., New York, London, Sydney, 166 p.

Laursen, E. M., 1958, The total sediment load of stream: J. Hydraulics Division, Proceedings of the Am. Soc. of Civil Engineers, Vol. 84, No. HY1.

Laws, J. O., 1941, Measurements of the fall velocity of waterdrops and raindrops: Trans. Am. Geophys. Union, V. 22, p. 709-721.

Laws, J. O., and Parsons, D. A., 1943, Relation of raindrop-size to intensity: Trans. Am. Geophys. Union, V. 24, p. 452-460.

Li, R. M., 1972, Effect of rainfall on sheet flow: M.S. Thesis, Colorado State University, Ft. Collins, Colorado.

Liggett, J. A., 1959, Unsteady open channel flow with lateral inflow: Tech, Rept. 2, Dept. Civil Engineering, Stanford University.

MacDougall, C. H., 1934, Bed-sediment transportation in open channels: Trans. Am. Geophys. Union, Vol. 15, p. 491-495.

Meyer. L. D., and Monke, E. J., 1965, Mechanics of soil erosion by rainfall and overland flow: Trans. of the Am. Soc. of Agr. Engr., Vol. 8, No. 4, p. 572-577, 580.

REFERENCES - (Continued)

Meyer, L. D., 1971, Soil erosion by water on upland areas: River Mechanics, Vol. 2, Edited and published by H. W. Shen, P. O. Box 606, Fort Collins, Colorado, USA, 80521, Chap. 27, 25 p.

Meyer, L. D., and Wischmeier, W. H., 1969, Mathematical simulation of the process of soil erosion by water: Trans. Am. Soc. of Agr. Engr., Vol. 12, p. 754-758, 762.

Meyer-Peter, E., and Muller, R., 1948, Formulae for bed-load transport: Proc. 2nd Meeting IAHR, Stockholm, p. 39-64.

Morgali, J. R., 1963, Hydraulic behavior of small drainage basins: Dept. of Civil Engineering, Stanford Univ., Stanford, Calif., Technical Report No. 3.

Musgrave, G. W., 1947, The quantitative evaluation of factors in water erosion, a first approximation: J. Soil and Water Conservation, Vol. 2, p. 133-138.

Neal, J. H., 1937, The effect of the degree of slope and rainfall characteristics on runoff and soil erosion: Missouri Agr. Exp. Sta. Research Bull. 280.

Nordin, C. F., and Richardson, E. V., 1971, Instrumentation and measuring techniques: River Mechanics, Vol. 1, Edited and published by H. W. Shen, P. O. Box 606, Fort Collins, Colorado, USA, 80521, Chap. 14, 38 p.

Parson, D. A., 1949, Depths of overland flow: Soil Conservation Service, Technical Paper 82.

Ree, W. O., 1939, Some experiments on shallow flows over a grassed slope: Trans. Am. Geophys. Union, Vol. 20, p. 653-656.

Ree, W. O., 1949, Hydraulic characteristics of vegetation for vegetated waterways: Agricultural engineering, Vol. 31, p. 184-187, 189.

Robertson, A. F., et al., 1964, Runoff from impervious surfaces under conditions of simulated rainfall: Trans. Am. Soc. of Agr. Engr., Vol. 9, No. 3, p.343-346.

Schoklitsch, A., 1934, Der Geschiebetrieb und Geschiebefracht: Wasserkraft und Wasserwirtschaft, p. 37, (Cited by Raudkivi, A. J., 1967, Loose boundary hydraulics: Pergamon Press, New York, London, Sydney, 330 p.).

Schwab, G. O., et al., 1966, Soil and water conservation engineering: Second Ed., John Wiley and Sons, Inc., New York, London, Sydney, 683 p.

REFERENCES - (Continued)

Smerdon, E. T., and Beasley, R. P., 1961, Critical tractive forces in cohesive soils: Agricultural Engineering, Vol. 42, No. 1, p. 26-29.

Smith, D. D., and Wischmeier, W. H., 1962, Rainfall erosion: Advances in Agronomy, Academic Press, Inc., New York, Vol. 14, p. 109-148.

Soil Conservation Society of America, 1952, Soil and water conservation glossary: J. Soil and Water Conservation, Vol. 7, No. 3, p. 144-146.

Task Committee on Preparation of Sedimentation Manual, Committee on Sedimentation, 1965, Sediment transportation mechanics; Nature of sedimentation problems: J. Hydraulics Division, Proceedings of the Am. Soc. of Civil Engineers, Vol. 91, No. HY2, p. 251-266.

Wischmeier, Walter H., 1959, A rainfall erosion index for a universal soil loss equation: Soil Sci. Soc. of Am. Proceedings, Vol. 23, p. 246-249.

Woo, D. C., 1956, Study of overland flow: Ph.D. dissertation, University of Michigan, Mich.

Wooding, R. A., 1965, A hydraulic model for the catchment-stream, problem I. Kinematic wave theory: J. Hydrology, Vol. 3, p. 254-267.

Woolhiser, D. A., and Liggett, J. A., 1967, Unsteady, one-dimensional flow over a plane - the rising hydrograph: J. Water Resources Research, Vol. 3, No. 3, p. 753-771.

Woolhiser, D. A., 1969, Overland flow on a converging surface: Trans. Am. Soc. of Agr. Engr., Vol. 12, No. 4, p. 460-462.

Yoon, Y. N., and Wenzel, H. G., 1971, Mechanics of sheet flow under simulated rainfall: J. Hydraulics Division, Proceedings of the American Society of Civil Engineers, Vol. 97, No. HY9, p. 1367-1401.

Yu, Y. S., and McNown, J. S., 1963, Runoff from impervious surfaces: U.S. Army Engineer Waterways Experiment Station, Corps of Engineers, Contract Rept. No. 2-66.

Zingg, A. W., 1940, Degree and length of land slope as it affects soil loss in runoff: Agricultural Engineering, Vol. 21, p. 59-64.